BRITISH COLUMBIA
The Best Place on Earth

Ministry of Energy, Mines & Petroleum Resources
Mining & Minerals Division
BC Geological Survey

BC Geological Survey Assessment Report 42881

Assessment Report Title Page and Summary

TYPE OF REPORT [type of survey(s)]: Geophysical

TOTAL COST: $11,100.00

AUTHOR(S): David G Mark **SIGNATURE(S):** David Mark

NOTICE OF WORK PERMIT NUMBER(S)/DATE(S): n/a **YEAR OF WORK:** 2023

STATEMENT OF WORK - CASH PAYMENTS EVENT NUMBER(S)/DATE(S): SOW # 5978368 dated March 28, 2023

PROPERTY NAME: Lara

CLAIM NAME(S) (on which the work was done): 1094248, 1094386

COMMODITIES SOUGHT: copper, gold, silver, lead, zinc

MINERAL INVENTORY MINFILE NUMBER(S), IF KNOWN: 092B 129

MINING DIVISION: Victoria **NTS/BCGS:** 92B/08 /// 092B.081

LATITUDE: 48 ° 52 '47.9 " **LONGITUDE:** 123 ° 53 '45.0 " **(at centre of work)**

OWNER(S):

1) David Mark
2) Kelly Funk

MAILING ADDRESS:

132 Saddlehorn Drive
Kaleden BC, V0H 1K0

301 - Mount Royal Place
Nanaimo, BC, V9R 6A4

OPERATOR(S) [who paid for the work]:

1) Geotronics Consultng Inc.
2)

MAILING ADDRESS:

132 Saddlehorn Drive
Kaleden BC, V0H 1K0

PROPERTY GEOLOGY KEYWORDS (lithology, age, stratigraphy, structure, alteration, mineralization, size and attitude):

Sicker Group, Nanaimo Group, Kuroko-type exhalite massive sulphide deposits, VMS deposits, polymetallic mineralization

REFERENCES TO PREVIOUS ASSESSMENT WORK AND ASSESSMENT REPORT NUMBERS:

#' 32888

Next Page

TYPE OF WORK IN THIS REPORT	EXTENT OF WORK (IN METRIC UNITS)	ON WHICH CLAIMS	PROJECT COSTS APPORTIONED (incl. support)
GEOLOGICAL (scale, area)			
Ground, mapping			
Photo interpretation			
GEOPHYSICAL (line-kilometres)			
Ground			
Magnetic			
Electromagnetic			
Induced Polarization			
Radiometric			
Seismic			
Other			
Airborne	3D Magnetic Interprettion	1094248, 1094386	$11,100.00
GEOCHEMICAL (number of samples analysed for...)			
Soil			
Silt			
Rock			
Other			
DRILLING (total metres; number of holes, size)			
Core			
Non-core			
RELATED TECHNICAL			
Sampling/assaying			
Petrographic			
Mineralographic			
Metallurgic			
PROSPECTING (scale, area)			
PREPARATORY / PHYSICAL			
Line/grid (kilometres)			
Topographic/Photogrammetric (scale, area)			
Legal surveys (scale, area)			
Road, local access (kilometres)/trail			
Trench (metres)			
Underground dev. (metres)			
Other			
		TOTAL COST:	$11,100.00

3D INTERPRETATION

AN

AIRBORNE MAGNETIC SURVEY

ON THE

LARA PROPERTY

CHEMAINUS RIVER, DUNCAN AREA, SOUTHWEST REGION, BC

LOCATED: 17 Km northwest of town of Duncan, BC on Solly Creek

Center of property:
- 434315 E and 5414797 N (UTM Zone 10, NAD 83)
- 48˚ 52' 47.9" N Latitude, and 123˚ 53' 45.0" W Longitude

NTS: 92B/13
BCGS: 92B.081

WRITTEN FOR: **BC MINING PROPERTIES**
301 Mount Royal Place
Nanaimo, BC, V9R 6A4
and
GEOTRONICS CONSULTING INC.
132 Saddlehorn Drive
Kaleden, British Columbia, V0H 1K0

WRITTEN BY: David G. Mark, P.Geo.
GEOTRONICS CONSULTING INC.
132 – Saddlehorn Drive
Kaleden, British Columbia V0H 1K0

DATED: May 31, 2024

TABLE OF CONTENTS

LIST OF ILLUSTRATIONS ..... *iii*

1 SUMMARY *1*

2 INTRODUCTION and GENERAL REMARKS *2*

3 PROPERTY and OWNERSHIP *2*

4 LOCATION and ACCESS *3*

5 PHYSIOGRAPHY and CLIMATE *3*

5.1 Physiography **3**

5.2 Climate **3**

6 HISTORY *4*

6.1 Underground Exploration **5**

7 GEOLOGY *5*

7.1 Regional Geology **5**

7.2 Property Geology **7**

7.3 Mineralization and Alteration **8**

7.3.1 Coronation Trend 9

7.3.2 "126" Zone 12

7.3.3 "262" Zone 12

8 airborne MAGNETIC DATA interpretation *12*

8.1 Airborne Magnetic Survey Parameters **12**

8.2 Regional Magnetic Data Over the Project Area **13**

8.3 Magnetic Data 2D Filtering **13**

8.4 3D Magnetic Modelling Methodology **14**

10 DISCUSSION OF RESULTS *19*

11 SELECTED BIBLIOGRAHY *21*

12 GEOSCIENTIST'S CERTIFICATE *25*

13 AFFIDAVIT OF EXPENSES *26*

14 APPENDIX I – MAGNETIC CONTOUR PLAN MAPS *27*

15 APPENDIX II – AIRBORNE REPORT BY AEROQUEST *28*

LIST OF ILLUSTRATIONS

MAPS	FIG /MAP #	PAGE
SUPPORT MAPS (within report)		
BC Location Map	1	After 2
Regional Location Map	2	After 3
Claim Map	3	After 3
Geology of Vancouver Island showing major geological features	4	6
Historical Geology Map of Property Showing Mineral Zones	5	10
AIRBORNE 3D MAGNETIC SURVEY MAPS		
Airborne Flight Line Map Showing Lara Claims	GP-3D1	15
3D Plan View Susceptibility Map with Overlying Magnetic TMI Map	GP-3D2	16
3D Susceptibility Map with Overlying Magnetic TMI Map – View from Northwest	GP-3D3	17
3D View of Magnetic Bodies - from Southwest	GP-3D4	18
3D Susceptibility Map with Overlying Magnetic TMI Map – View from West	GP-3D5	18
3D Susceptibility Map with Overlying Magnetic TMI Map – View from Southwest	GP-3D6	19
AIRBORNE 2D MAGNETIC CONTOUR PLAN MAPS (Appendix I)		
Total Magnetic Intensity	GP-1	
Reduce to the Pole Magnetic Field	GP-2	
Downward Continuation (100 m)	GP-3	
1st Vertical Derivative	GP-4	
2nd Vertical Derivative	GP-5	
Horizontal Derivative - East	GP-6	
Horizontal Derivative - North	GP-7	
General Derivative	GP-8	
Tilt Derivative	GP-9	
Analytic Signal	GP-10	

1 SUMMARY

A 2D and 3D interpretation was carried out on the airborne magnetic survey that was flown in 2008 over the Lara Property.

The Lara Property area is situated in the Chemainus River area of the Victoria Mining Division within southwest British Columbia 17 kilometers northwest of Duncan on Highway 1. The property consists of two mineral claims totaling 1656 hectares. Access to the property is by well-maintained logging roads from Chemainus on Hwy 1. The purpose for exploration on the property is to understand the geological controls of the volcanic massive sulphide mineralization.

The Lara Project is a high-grade volcanogenic gold and base metal deposit. The Property is underlain by the McLaughlin Ridge Formation (Horne Lake-Cowichan uplift) which is correlative with the Myra Formation (Buttle Lake uplift) sequence of felsic volcanic rocks that hosts the Zn-Pb-Cu-Ag-Au Volcanogenic Massive Sulphide (VMS) deposit of Myra Falls (~300 km to the north). The past-producing Cu-Pb-Zn mine and mineralized zones at Mt. Sicker, ~2 km southeast of the Property, are also hosted by the felsic volcanic rocks of the McLaughlin Ridge Formation (Belik, 1981; MINFILE, 1990a).

Reported diamond drilling on the Property totals some 101,730 metres in 490 drill holes. The most recent exploration work on the Property was a carried out in 1998 by Nucanolan Resources Ltd. who completed a diamond drilling program of 12 drill holes (2,559 metres) with their best reported intersection of 3.16 m @ 2.48% Cu, 1.19% Pb, 12.3% Zn, 49.80 g/t Ag, 2.30 g/t Au. A historic resource (**not compliant with NI43-101 standards**) was reported in 1998 by Nucanolan Resources Ltd. to be 580,000 tonnes grading 5.87% Zn, 1.22% Pb, 1.01% Cu, 0.138 opt Au (4.3 g/t Au) and 2.92 opt Ag (90 g/t Ag) over and average thickness of 8.3 feet or 2.53 metres (Archibald, 1999).

The magnetic maps show a west-northwesterly trend to the data which corresponds to the known geology. The 3D interpretation reveals a magnetic body at an 1800-meter depth below the southern part of the property which is indicated to be a gabbro intrusive. The 2D plan maps also show lineations striking primarily west-northwesterly and secondarily, north-northwesterly. These are indicative of geologic structure such as faults, shear zones, and contacts. One of these correlates directly with the Coronation mineralization.

BC MINING PROPERTIES

LARA PROPERTY

CHEMAINUS RIVER, DUNCAN AREA, VICTORIA MD, BC

BC LOCATION MAP

DRAWN BY:	JOB NO.:	NTS: 92B/13 BCGS: 92B .081	DATE:	FIG NO.:
DGM	23-04		May '24	1

Geotronics Consulting Inc
Exploration done right

3D INTERPRETATION

OF AN

AIRBORNE MAGNETIC SURVEY

ON THE

LARA PROPERTY

CHEMAINUS RIVER, DUNCAN AREA, SOUTHWEST REGION, BC

---

2 INTRODUCTION AND GENERAL REMARKS

This is a report on 3D modelling and 2D filter interpreting of an airborne magnetic survey carried out over the Lara Property located in the Chemainus area on the east side of Vancouver Island within British Columbia.

The work was carried out from May 05th, 2022 to March 27th, 2023.

The operator for this project was Geotronics Consulting Inc of Kaleden, BC.

3 PROPERTY AND OWNERSHIP

The Lara Property presently consists of 2 claims totaling 1,656 hectares, of which the names and tenure numbers are given in the table below.

NICKEL CREEK MINERAL CLAIMS

Tenure Number	Issue Date	Claim Name	Expiry Date	Area (ha)
1094386	2022-03-29	Lara – Coronation	2026-05-21	1571.96
1094248	2022-03-29	LA	2026-05-21	84.99
			TOTAL AREA	1656.95

The registered owners of the claims are Kelly Funk of Nanaimo, BC as to 75% and David Mark of Kaleden, BC as to 25 %. The expiry date assumes that the work being discussed within this report will be accepted for assessment credits.

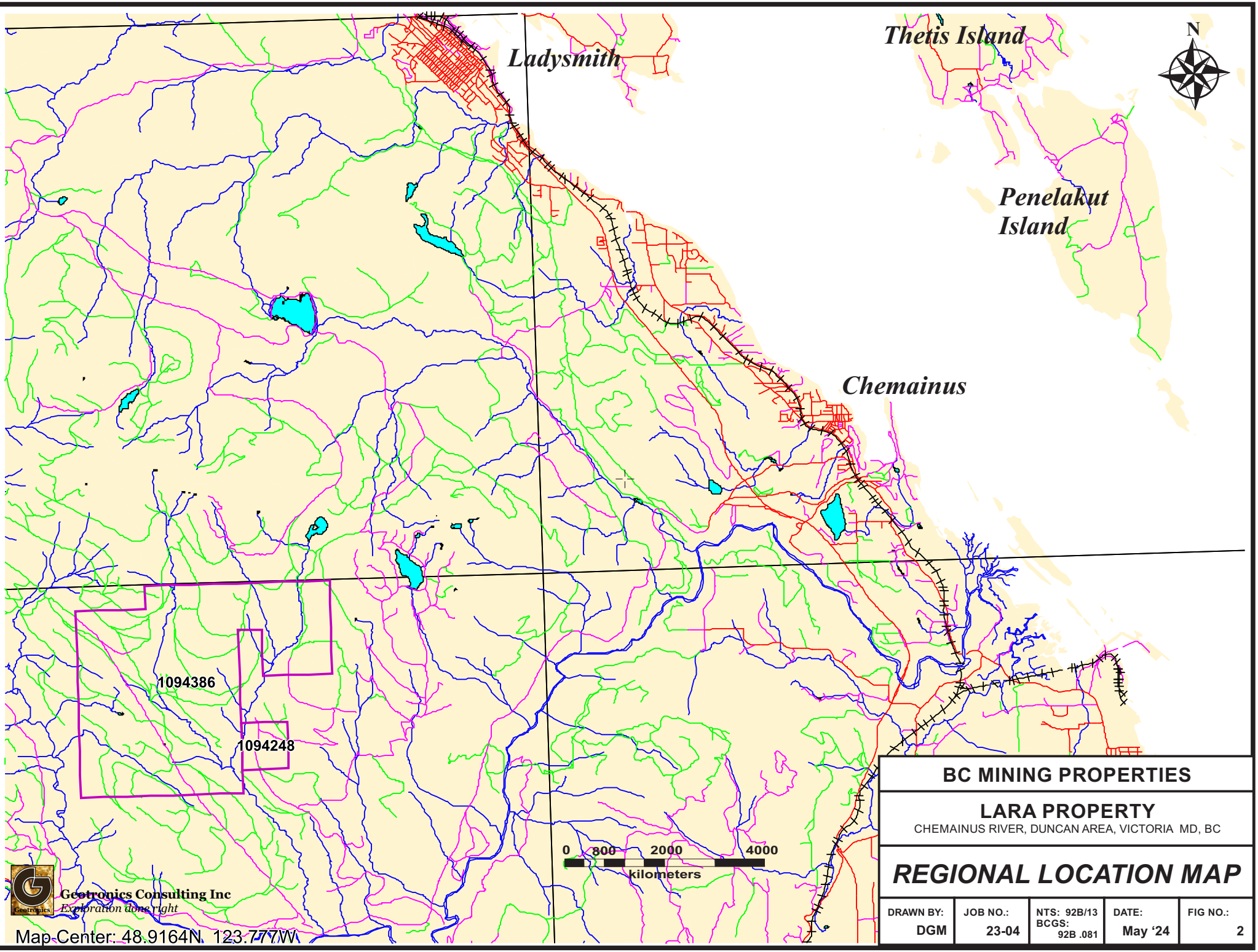

BC MINING PROPERTIES

LARA PROPERTY

CHEMAINUS RIVER, DUNCAN AREA, VICTORIA MD, BC

REGIONAL LOCATION MAP

DRAWN BY:	JOB NO.:	NTS: 92B/13 BCGS: 92B .081	DATE:	FIG NO.:
DGM	23-04		May '24	2

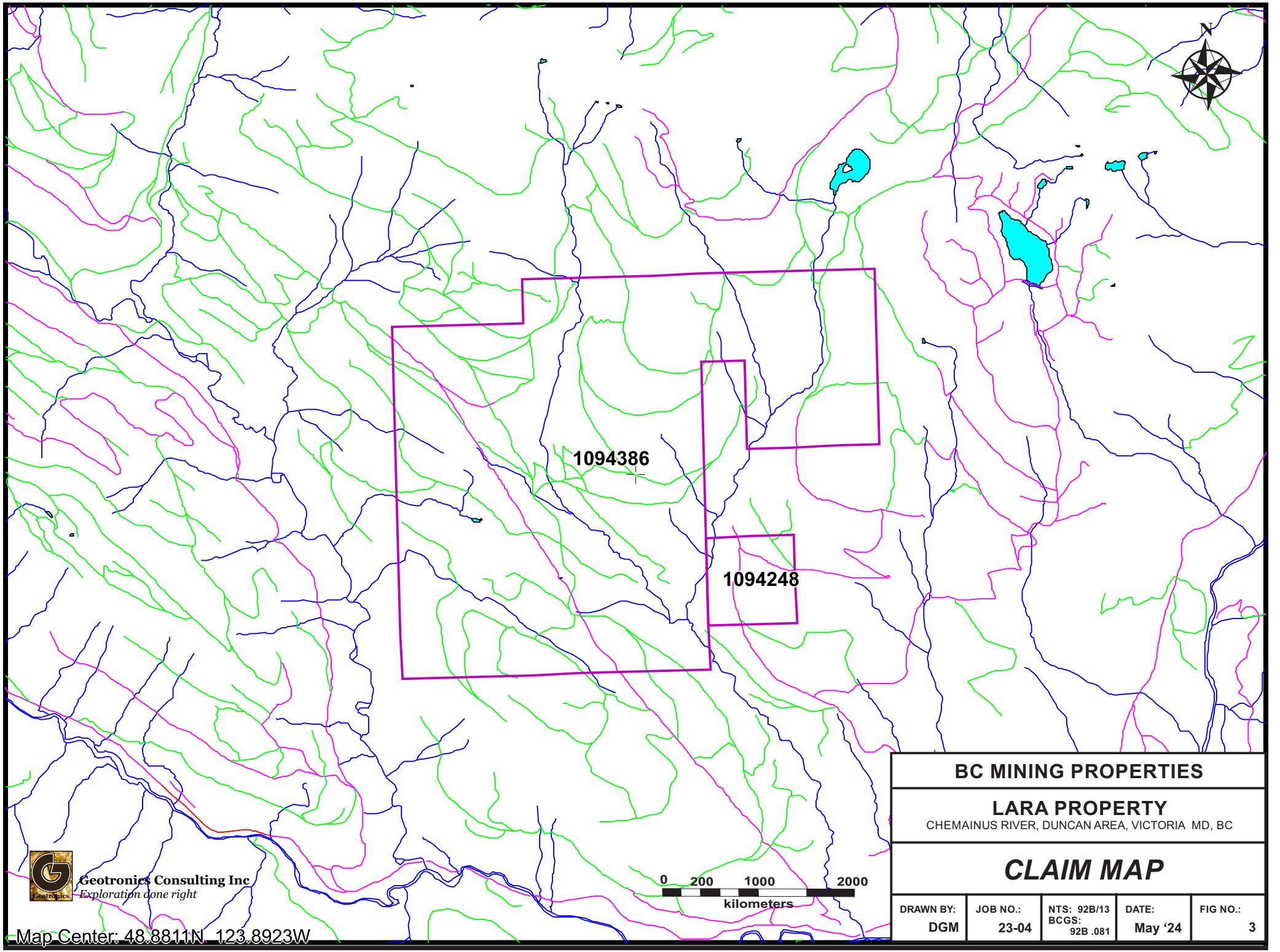

Geotronics Consulting Inc
Exploration done right

Map Center: 48.8811N 123.8923W

BC MINING PROPERTIES

LARA PROPERTY
CHEMAINUS RIVER, DUNCAN AREA, VICTORIA MD, BC

CLAIM MAP

DRAWN BY:	JOB NO.:	NTS: 92B/13 BCGS: 92B .081	DATE:	FIG NO.:
DGM	23-04		May '24	3

4 LOCATION AND ACCESS

The Lara Property area is situated on Solly Creek in the Chemainus River area of the Victoria Mining Division within southwest British Columbia 10 kilometers west-southwest of the village of Chemainus, 17 km northwest of the town of Duncan, and 60 km northwest of the city of Victoria.

The geographical coordinates for the center of the property are 48° 52' 47.9" north latitude and 123° 53' 46.0" west longitude. The equivalent in UTM NAD 83 coordinates are 434300 easting and 5414500 northing within zone 10. The property is located within NTS map # 92B/13 and BCGS map # 092B.081.

Access to the property is by well-maintained logging roads from Chemainus on Hwy 1. A network of logging roads and rough drill trails extend to most areas on the Property. Vehicle access to the Property is via the Chemainus River Logging Trunk Road (MacMillan Bloedel) for12 km from Highway No. 1 at Chemainus. From the Chemainus River Road, the Property is accessed by a network of secondary logging and forestry roads, at Mile 10, Mile 12 and C-7 to the power line service road to reach the different parts of the claim group. The B.C. Hydro Right of Way (a cleared power line right-of-way) cuts across the Property (northwest to southeast). Although these roads provide access, they go through rough terrain and steep grades. The northern and northeastern sections of the Property in particular are difficult because the terrain is steep and broken by numerous gullies: access to these areas is limited to an existing grid between the access roads. The Trans-Canada Highway (Highway No.1) provides access to these roads from Chemainus and Victoria. This route also provides the best access for heavy equipment to the Property

5 PHYSIOGRAPHY AND CLIMATE

5.1 PHYSIOGRAPHY

The Lara Property is located at the southeastern end of the Vancouver Island Mountains which is a physiographic division of the Insular Mountains. It straddles the southern flank of the Coronation Mountains. However, total relief on the property is only 520 metres ranging from 420 m above sea level ("ASL") on Solly Creek at the southeast border of the claims to about 937 m on the hill at the northwest border. The elevation on the Property increases from southeast to northwest . The topography is gentle to steep where creeks have deeply incised the terrain. Outcrop is abundant along creek valleys and roads, but in general there exists extensive thick deposits of glacial overburden and little outcrop.

The entire Property lies in a heavily forested area, although there has been extensive logging activity for the past 50 years and most of the tree cover is second or even third growth. Much of the Property has been logged by clear-cutting methods over the past 40 years with present vegetation consisting of secondary growths of spruce, balsam, fir and cedar with thick undergrowth cover (Archibald, 1999; Peatfield and Walker, 1994; Roscoe, 1988).

5.2 CLIMATE

The climate in the Duncan – Port Alberni area is a typical continental climate with moderating influences of the Pacific air throughout the year. The area lies within a rain

shadow leeward of the coastal mountains. In summer there is intense surface heating and convective showers, and in the winter, there are frequent outbreaks of Arctic air. The mean annual temperature and precipitation vary to some extent within the region, depending on the location's elevation and proximity to salt water. At sea level snow fall is infrequent, although it increases with elevation. The January mean temperatures are also moderated

with an average temperature of 2.7°C (37˚F). Duncan has a July mean maximum of 25.2°C (77.4˚F) and a July mean minimum of 11.6°C (52.9˚F). However, precipitation (with the most falling between October and March) varies from 96.1 cm (37.85 in) in Cowichan Bay, 109.2 cm (41.04 in) in Duncan, and 117.6 cm (46.28 in) in Chemainus. Vegetation is dominated by dense mixed forest of pine, spruce, cedar, alder, poplar and local low-lying swamps and marshes.

6 HISTORY

This section excerpted from report by Kelso and Wetherup, 2008

The original claims on the Lara Property were staked by Laramide Resources Inc. in 1981. The original Lara Property encompassed the Coronation Zone, Coronation Extension, Randy North and the "262" mineralized zones (see Figure 9-1). The Property boundaries were expanded in 1992 when Laramide acquired claims within the northwest and northeast blocks of Chemainus claims from Falconbridge. The new group of claims includes the northernmost mineralized zones; Anita, Silver Creek, "126" and Sharon zones (see Figure 9-1). The Chemainus Property option agreement between Falconbridge and Laramide executed in June 1992 resulted in the addition of approximately 3,725 ha. Exploration of the two properties prior to their amalgamation was carried out separately with different operators, the Chemainus Property having the longer history of exploration work. Several operators were involved in the exploration of these properties. For clarity, the historic group names will be retained for much of this report: the Lara Property, makes up the central portion of the final Property boundary comprising mostly of mineral legacy claims (Figure 4–3) and the Chemainus Property is made up of mineral cell claims to the northeast and west.

Abermin Resources Ltd. carried out the exploration programs after the first claims on the Lara Property were staked in 1981. Minnova Inc. purchased the Abermin interests in 1988 and took over as operator of the exploration programs. Nucanolan Resources Ltd. entered into an option agreement with Laramide in 1998 to conduct exploration programs on the Lara Property. Interest in the area of the Chemainus Property, in particular west of the Chemainus River began when rights to the Esquimalt and Nanaimo Railway Land Grant were surrendered back to the Crown and became available for staking. In 1903, an adit was excavated near a copper showing in the area of the Sharon Zone – it was dominated by pyrite with minor chalcopyrite. In 1915, a 50-foot shaft was sunk near the Anita Zone and revealed a chalcopyrite-bearing pyrrhotite lens in schist. In the 1960's, exploration accelerated with increasing number of geological mapping and geophysical surveys with Cominco working in the west and Imperial Oil Resources working in the east.

6.1 UNDERGROUND EXPLORATION

In 1988, an underground exploration program tested the continuity of the Coronation Zone, evaluated rock conditions for mining cost estimates and provided a bulk sample for metallurgical tests (see Section 16.0). The program included ramping (from the footwall side) and crosscutting to access the high-grade mineralized zone and was followed by geological mapping (1:100 and 1:50 scales) and sampling (muck; test hole, diamond drilling (NQ size) and chip-channel) (Harris, 1988).

The results of the program confirm the presence of several potentially economic, continuous pods of zinc and gold rich mineralization along the Coronation Trend. Zinc and gold provide the gross metal value of the deposit with lesser silver, copper and lead. The dominant mineralization style is not massive but consists of a structurally complicated mixture of sulphide bands, laminae, stringers and isolated massive pods in a siliceous, somewhat fragmental rhyolitic host rock. Reverse and normal faulting has juxtaposed the differing mineralization modes within this zone. Remobilization of primary sulphide into new modes of occurrence appears to determine the final morphology of the deposit. The presence of gold and silver not tied to any particular mineralization type or host rock also indicates secondary mineralization.

The underground mapping program delineated four major structural-mineralogical domains in the Coronation Zone that differ with respect to grade, structural setting, mineralization styles and implications for future mine design. The eastern section showed the discontinuous and poddy character of the high-grade mineralization and therefore the disadvantages to widely spaced drilling. This complex high-grade mineralized and multi-directionally faulted zone transitions to a thinner structurally simpler low- to medium-grade section to the west. The mineralization was a mixed sequence of banded, to poddy semi-massive material containing impersistent boudinaged pods and bands of massive pyrite. The western section contained mineralization that approached significant grades and widths. It consisted mainly of pyrite (85%) with locally enriched sphalerite and chalcopyrite banded and brecciated zones. The entire zone was strongly sericitized and appeared shattered and brecciated (Harris, 1988).

7 GEOLOGY

7.1 REGIONAL GEOLOGY

This section excerpted from report by Kelso and Wetherup, 2008

Vancouver Island lies wholly within the Insular Superterrane of the Canadian Cordillera that makes up one of the five tectonic belts produced by the collisions and accretions along the Canadian northwest edge of North America (Lithoprobe, 2007). The island is dominated by rocks of the Wrangellia Terrane, that consist of three volcano-sedimentary cycles: the oldest volcanic cycle is made up of the volcanic rocks of the Upper Palaeozoic Sicker Group which are conformably overlain by the limestone rocks of the Buttle Lake Group; the second cycle is made up of the tholeiitic volcanic rocks of the Karmutsen Formation of the Vancouver Group which are overlain by the limestone of the Quatsino Formation; and the third cycle is made up of the volcanic rocks of the Lower Jurassic Bonanza Group (Figure 7–1). These cycles have been intruded by mafic sills of the Mount Hall Gabbro (coeval with the overlying Karmutsen Formation) and subsequently intruded by various granodioritic stocks. The sedimentary rocks of the Cretaceous Nanaimo Group unconformabley overlie these older sequences (Massey, 1992). Regional-scale warping of the Vancouver Island rocks produced the 3 major geanticlinal uplifts cored by Sicker Group rocks, including the Cowichan (Horne Lake – Cowichan), Buttle and Nanoose uplifts. The oldest rocks of Wrangellia lie at the top of an imbricated stack of northeast-dipping thrust sheets and are Late Silurian to Early Permian arc sequences (Green, Scoates and Weis, 2005). The Sicker and Buttle Lake groups, the main target for volcanogenic massive sulphide deposits, are primarily exposed in the Cowichan Lake area, at the southeastern extent of the Cowichan uplift (BCMEMPR, 2007a) (Figure 7–2).

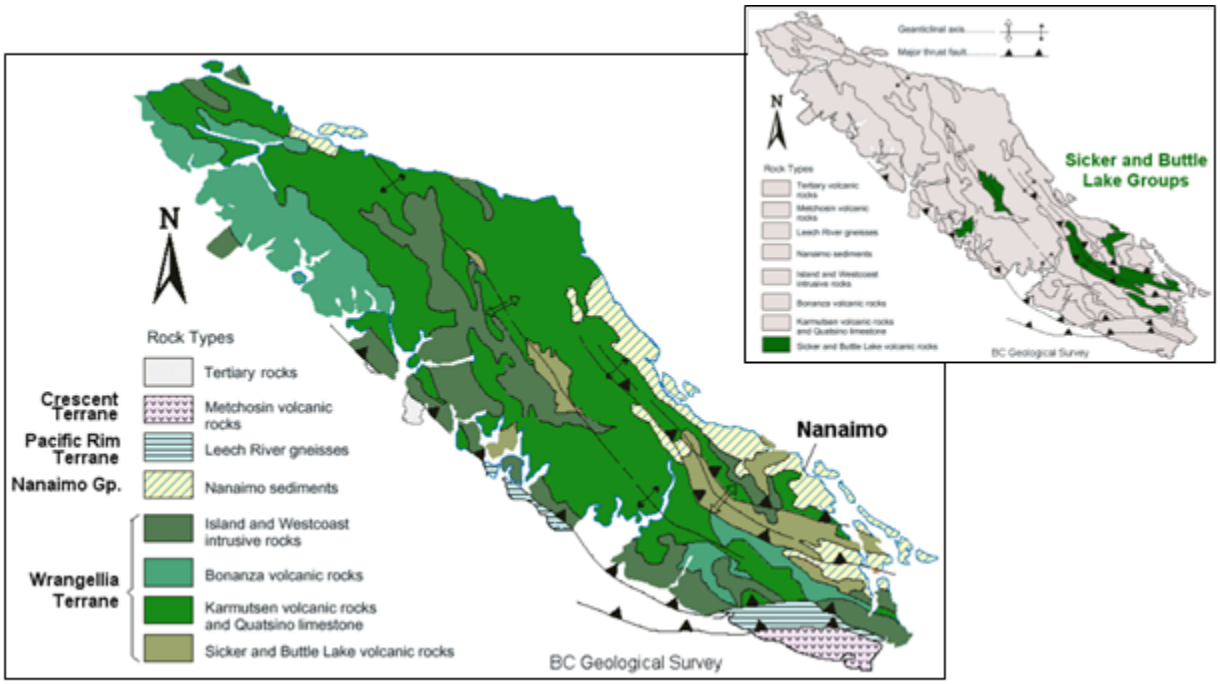

Figure 4: Geology of Vancouver Island showing major geological features, structures and components of the Insular Superterrane of the Wrangellia Terrane (after Earle, 2004).

Vancouver Island has undergone at least six periods of deformation (Massey and Friday, 1987) giving rise to a broad antiform structure with a west-northwesterly axis, with younger

units towards the west and plunging from 5° to 15° to the west-northwest to east-southeast. The schistosity and cleavage are moderate to steeply dipping to the northeast. Large-scale west to northwesterly trending thrust faults cutthe Cowichan-Horne Lake uplift into multiple slices (Figure 7–2). These in turn these are transected by northeast trending block faults. The over-thrusting of these faults pushed the older units up over the younger. Two major fault zones are recognized. The Cameron River fault runs southeast along the Cameron River valley and joins the Fulford fault. The Fulford fault is a regional west-northwest trending fault that dips at about 47° and crosscuts bedding in the volcanic rocks (McLaughlin Ridge Formation) at a shallow angle The thrusts (where exposed) are high-angle reverse faults which dip between 45° and 90° to the east or northeast, generally place older rocks over younger and become listric at mid-crustal depths. The metamorphic grade in the area is generally low but increases with the age and structural position of the rocks (Massey and Friday, 1989; MINFILE, 1990a).

The surficial geology and stratigraphy of the southern Vancouver Island have been studied in the area, and the glacial events established by Blyth and Rutter (1993). The surficial geology of area is characterized by glaciomarine drift, beach materials, till and/or glaciofluvial/fluvial sand and gravel in the low-lying (200-300 metres) coastal areas. Higher elevations (from 600 to 900 m ASL) are covered by till or colluviated till, glaciofluvial sand and gravel and more recent colluvium. Diamicton deposits are found in low-lying areas of Ladysmith (up to 12 m of massive, indurated and clay-rich). Chemainus is draped by 1 to 2 metres of silty diamicton directly on bedrock or over silty clay unit and in upland areas overlying glaciofluvial sand and gravel. Sand and gravel deposits are found west of Victoria and in the Chemainus area, throughout the lower and upper Cowichan Valley (area east of Cowichan Lake). Convoluted, interbedded sand, gravel and diamicton combined with pitted, kame and kettle topography occurs just south of Duncan. Economic aggregate deposits have been established at Metchosin, Lanford, Goldstream, Duncan and parts of the Cowichan Valley. The mountainous inland areas appear to have been completely covered by ice. Surficial materials consist of colluviated diamicton over bedrock. Exposures of well-indurated clay-rich diamicton or sandy diamicton are sometimes found in valley basins. These diamictons are usually overlain by recent fluvial sands, gravels and lacustrine silts and clays.

7.2 PROPERTY GEOLOGY

This section excerpted from report by Kelso and Wetherup, 2008

The Lara Property area is underlain primarily by the McLaughlin Ridge Formation, the uppermost unit of the Sicker Group which has been thrust over the younger rocks of the Fourth Lake Formation and the Nanaimo Group by the Fulford fault; this is referred to as the Cowichan Uplift. The McLaughlin Ridge Formation, which hosts the VMS deposits, consists of northerly dipping, west-northwest striking rhyolitic to andesitic rocks. Bedding generally dips steeply at 60° to 75° north, although dips of between 30° and 45° north are common (MINFILE, 1990a; Massey et al. 2005a). The principal stratigraphic units of the Eastern Belt of the Cowichan Uplift are presented in Table 7–1 and Figure 7–2 (Massey, 1992).

The McLaughlin Ridge Formation is a sequence of volcaniclastic sediments dominated by thickly bedded, massive tuffites and lithic tuffites with interbedded laminated tuffaceous sandstone, siltstone and argillite. Associated breccias and lapilli tuffs are usually heterolithic and include aphyric and porphyritic (feldspar, pyroxene, hornblende) lithologies, commonly mafic to intermediate in composition; felsic tuffs are rare.

In the region east (Duncan area) of the Lara Property, the tuffaceous sediments thin out and the strata is dominated by volcanic rocks with only minor tuffaceous sediments. The volcanic rocks are predominantly intermediate to felsic pyroclastics, commonly feldspar-crystal lapilli tuffs and heterolithic lapilli tuffs and breccias. A thick package of quartz- crystal, quartz-feldspar-crystal and fine dust tuffs is developed in the Chipman Creek-Mount Sicker area and is host to the massive sulphides. This package thins to the west where it interfingers with andesitic lapilli tuffs and breccias. It appears to be stratigraphically high within the formation. A distinctive maroon schistose heterolithic breccia and lapilli tuff forms the uppermost unit within the McLaughlin Ridge Formation and is seen in the southern claims of the Lara Property.

7.3 MINERALIZATION AND ALTERATION

This section excerpted from report by Kelso and Wetherup, 2008

The polymetallic, VMS deposits on Vancouver Island are hosted in the structural uplifts of the Palaeozoic Sicker Group: the Myra Falls deposit within the Buttle Lake uplift, while the Lara and Mt. Sicker mine workings are located in the Horne Lake-Cowichan uplift. The felsic volcanic rocks of the McLaughlin Ridge Formation (Horne Lake-Cowichan uplift) and the Myra Formation (Buttle Lake uplift) host the deposits of Cu, Pb, Zn, Ag and Au within several stratigraphic levels (Crick, 2003; Massey, 1992).

The mineralized zones on the Lara Property were identified from drilling and extrapolating geological units along strike. The interpretive work by various exploration companies involved primarily comparison studies to the Buttle Lake/Myra Falls up strike deposits and the Mt. Sicker deposit down strike (Archibald, 1999). Seven zones, located at various stratigraphic levels were delineated on the Lara Property: Anita, Coronation Trend, Randy North, 262, Silver Creek, 126 and the Sharon zones (from west to east).

The deposit type on the Lara Property is classified as Kuroko-type massive sulphides consisting of volcanic-hosted, stratiform accumulations of copper, lead, zinc, silver and gold. The zones are described in Table 9–1 and their locations within Treasury's registered claim boundaries (superimposed on bedrock geology) are illustrated in Figure 9–1. The most important of these zones is the Coronation Trend which is made up of the Coronation Zone, the Coronation Extension and the Hanging Wall deposit. Together the deposits of the Coronation mineralized trend make up most of the reserve and the historic resource calculations of the Lara Property. Of the mineralized zones tested, the Coronation Trend and Anita appear to be on a similar trend; whereas the "262" Zone may be a sub-parallel strFigure 9–1 Location of mineralized zones within mineral claims of Lara Property, Vancouver Island, BC, Canada.

structure. The Randy North, Silver Creek, "126" and Sharon zones appear to be on a more northerly trend as part of the northern limb of a synclinal structure (Archibald, 1999: Wells and Kapusta, 1990a)

The package of rocks hosting the Lara deposits consists of an andesitic sequence referred to as the "Green volcaniclastic Sequence" overlying rhyolite which hosts to the massive sulphide ore. The rhyolite has been subdivided into two units which are referred to as the "Rhyolite Sequence" and the "Footwall Sequence", the latter underlying the lowermost sulphide sequence. Numerous minor faults occurring in three or four directions have been observed on the Property resulting in displacement and gaps of the mineralized stratigraphy (MINFILE 1990a; Roscoe and Postle, 1988).

The mineralized zones are characterized by rapid facies changes and abrupt fault displacements. Mineralization that has been discovered above and below the Coronation Trend stratigraphy is likely repeated on the Property either by regional folds or faults.

VMS mineralization on the Property is characterized by hydrothermal alteration of the rhyolite host that is typical of VMS deposits. The mineralized zones are characterized by strong sodium depletion, enrichment in potassium (sericitization) and zinc, silicification and pyritization. The lithogeochemical surveys defined two areas of hydrothermal alteration: the Randy Zone with a strike extent of at least six kilometres where the pyritic cherts are interpreted as a distal exhalite; and the structural hanging wall east of the Coronation Zone (Peatfield and Walker, 1994; Wells and Kapusta, 1990a). The geological reconnaissance work by Nucanolan in 1998 (Archibald, 1999) suggests that the structural controls existing in the area and the alteration mineralization indicate secondary mineralization via hydrothermal processes. The original features of the host sedimentary rock appear to be upgraded or influenced by the cross-cutting fault structures and possibly by the late stage mafic or diorite intrusions.

7.3.1 Coronation Trend

The Coronation Trend consists of several stratiform massive sulphide lenses within an envelope of banded or laminated sulphides. The Trend is made up of three zones: the original discovery of the Coronation Zone, the Coronation Extension Zone (east and stratigraphically

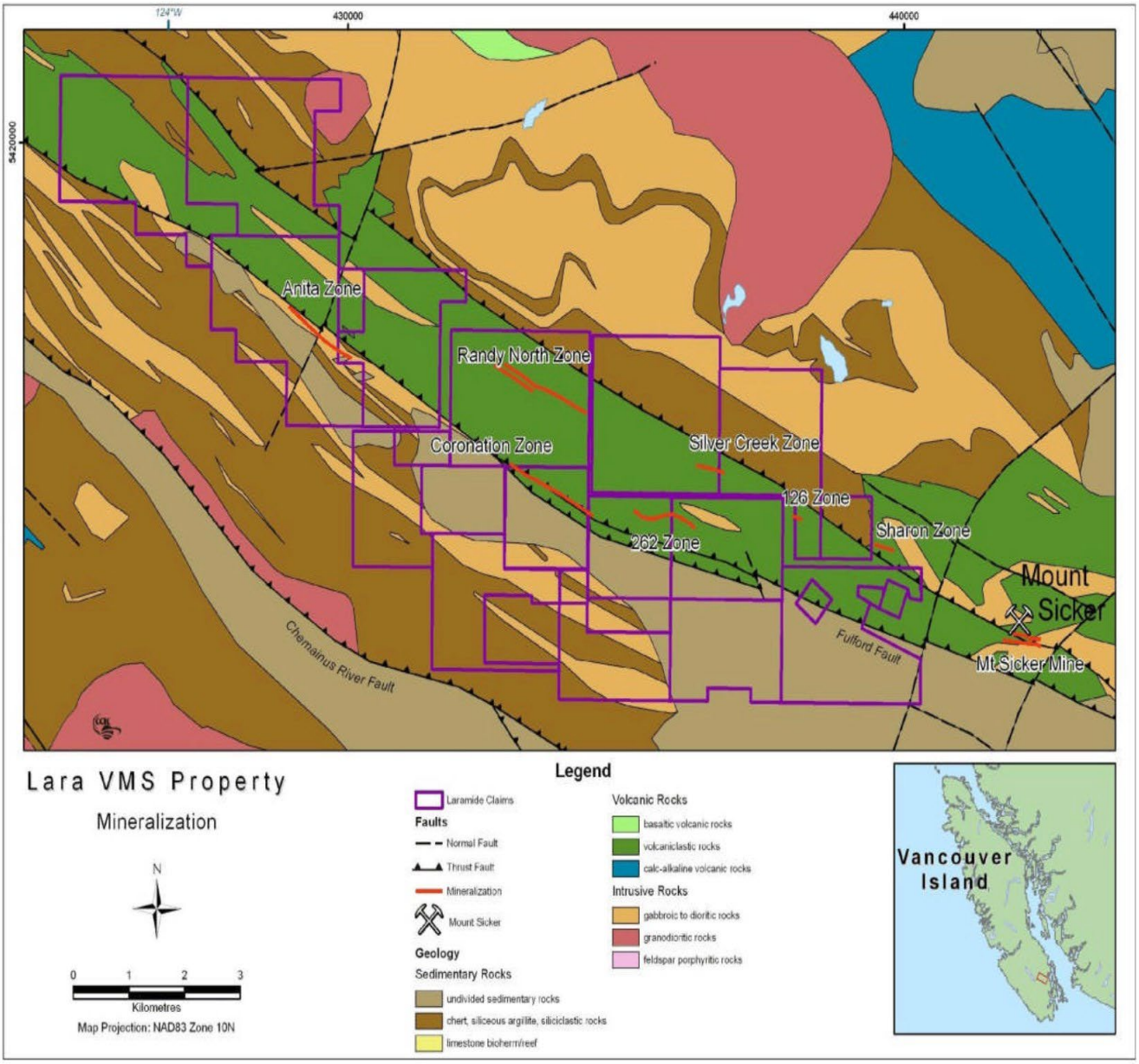

Figure 5: Historical Geology Map of Property Showing Mineral Zones

above the Coronation Zone) and the Hanging Wall Zone which consists of stringer mineralization that is also stratigraphically above the Coronation Zone (Roscoe and Postle, 1988). Although classified as massive sulphides, the predominant facies actually consist of bands, laminae and stringers of sulphide minerals in a strongly silicified rhyolite host

(intercalated with siliceous and tuffaceous debris). The Coronation sulphide mineralization strikes west-northwest, dips to the northeast at 60° and exhibits variation in thickness from 3 to 16 metres, averaging about 6 metres (Crick, 2003; MINFILE, 1990a). The distribution of mineralization along the Coronation Trend is influenced by a strong linear structural fabric which plunges at a low angle to the east (Roscoe and Postle, 1988).

The Coronation Zone is hosted by the southern Rhyolite Sequence (one of the 4 members of the McLaughlin Ridge Formation), and which consists of coarse-grained rhyolite crystal tuff and ash tuff. Black argillite beds and buff-coloured mudstones occur at the boundaries of pyritic units and enclose the polymetallic zones. The Footwall Sequence underlying the Member 1 Rhyolite consists of coarse-grained quartz porphyries and feldspar porphyries. These appear to form domal structures which not only controlled palaeotopography and basin configuration but may have played a role in focussing mineralizing fluids. Only a few diamond drill holes have penetrated the Footwall Sequence, and these have intersected another similar rhyolite porphyry package which is mineralized and has potential. The Member 1 Rhyolite is in fault contact with the overlying Green Volcaniclastic Sequence consisting of a 250 m thick unit of dacite to andesite fragmental rocks, minor argillite and quartz feldspar porphyry dykes (Roscoe and Postle, 1988). The footwall sequence is dominantly quartz porphyritic massive rhyolitic rocks up to 40 m thick (Crick, 2003) and is clearly from a distinct stratigraphic level compared to the above. These rocks are texturally variable but are distinguishable by the presence of abundant large quartz eyes. Feldspar porphyry dykes, rhyolite dykes, rhyolite breccia and mudstone and argillite beds are also present (MINFILE, 1990a).

Mineralogical studies carried out on drill core samples in 1989 (Peatfield and Walker, 1994) show that the mineralogy of the Coronation Trend is complex. The minerals include sphalerite, pyrite, chalcopyrite, galena and tetrahedrite [$(Cu, Ag, Zn, Fe)_{12}As_4S_{13}$], with small amounts of bornite, rutile and arsenopyrite and locally abundant barite. Tetrahedrite appears to be the preferred host for gold whereas pyrite shows very few included gold grains, but gold and silver are found dispersed in tennantite [$(Cu, Ag, Zn, Fe)_{12}As_4S_{13}$]. Gangue consists mostly of quartz and calcite with lesser amounts of muscovite, feldspar, and barium-bearing feldspar (Peatfield and Walker, 1994; MINFILE, 1990a).

The predominant facies of the Coronation deposits are the banded and laminated facies which consist of sulphide laminae and bands up to a few cm thick in a siliceous host. The host rock varies from a silicified rhyolite to a very fine-grained siliceous mass with various amounts of felsic tuffaceous debris. The mineralization is broadly conformable, however, crosscutting features are common within the conformable zones. Crosscutting mineralization varies from occasional sulphide stringers to well-developed breccia zones with sulphides in the matrix. Sulphides also occur disseminated in the rhyolite host. Primar textures are masked by pronounced cataclastic overprint. Although these features to some extent mask the primary depositional style, the overall stratiform character of the facies is demonstrated by the presence of sedimentary units which enclose and occur within the

deposit, and which can be correlated over considerable distances. The banded and laminated facies vary up to 16 metres true thickness.

Although not as high grade as the massive sulphide facies, laminated and banded sulphides can achieve significant grade (MINFILE, 1990a). One massive sulphide lens exposed by trenching in the Coronation Zone graded **24.58 g/t Au, 513.6 g/t Ag, 3.04% Cu, 43.01% Zn and 8.30% Pb over 3.51 m**.

7.3.2 "126" Zone

Diamond drill hole data indicates stringer style mineralization with long intersection of alteration and scattered mineralization at the "126" Zone. This zone consists of chalcopyrite in quartz veins hosted by chloritic volcanic flows/tuffs, which overlie a thick sequence of felsic volcanic rocks (Peatfield and Walker, 1994). Drilling indicates the presence of a gabbro intrusion (Peatfield and Walker, 1994). This zone is located in an area of deep overburden therefore geophysical and geochemical data cannot be interpreted.

7.3.3 "262" Zone

Drilling in 1990 by Minnova tested the felsic sequence at variable depths over a strike length of 6.5 km. The "262" Zone felsic volcanic rocks host a distal exhalite composed of pyritic cherts, ashes, and thin, copper-rich, semi-massive to massive sulphides and occurs within 40 m of the contact between the felsic and the underlying andesite rocks. The best development of exhalative sulphides, cherts and stringer mineralization is found in shallow, near surface holes. At depth, there is a fine-grained, siliceous felsic ash that is depleted in base metals and hosted in unaltered felsic rocks, suggesting that this zone has limited opportunity for development (Wells and Kapusta, 1991).

8 AIRBORNE MAGNETIC DATA INTERPRETATION

8.1 AIRBORNE MAGNETIC SURVEY PARAMETERS

The airborne magnetic survey was flown over the Lara Property in October 2007 by Aeroquest International. It consisted of a helicopter-borne magnetometer, an AeroTEM II time domain EM survey, and a radiometric survey. The Lara Property was much larger than now and thus the survey area was much larger. The present property area is as shown on the flight line map below, which is figure GP-3D1.

The lines were flown in a 15°E direction with a line spacing of 100 meters and 200 meters and the tie lines were flown in a perpendicular direction of 105°E with a line spacing of 1000 meters and 2000 meters. The number of kilometers consisted of 478 for the survey lines and 45 for the tie lines. That part of the survey area that covers the Lara Property was flown with a 200-meter line spacing and a 2000-meter tie line spacing.

The instrumentation consisted of a Geometrics model G-825A cesium vapor magnetometer that had a sensitivity of 0.001 nT, a sampling rate of 0.1 seconds, and an ambient range of 20,000 to 100,000 nT. A base station magnetometer, which was a Geometrics cesium vapor type, model G-859, was used to monitor the diurnal variation.

8.2 REGIONAL MAGNETIC DATA OVER THE PROJECT AREA

Aeroquest created magnetic survey maps with a minimum curvature routine and a grid resolution of 100 meters. The coordinates used were based on the 1983 North American Datum.

8.3 MAGNETIC DATA 2D FILTERING

The data set was processed using Geosoft software in order to produce 10 different types of filtered magnetic maps of the survey area. These have been reproduced for this report and are located within Appendix I.

- Total Magnetic Intensity (TMI), Figure GP-1, - This is the original data that has been diurnally corrected.
- Reduce to the Pole, Figure GP-2, - Reduction-to-the-pole transforms magnetic intensity data to equivalent data that would have been recorded as if the survey was at a magnetic pole. The magnetic anomalies, therefore, are placed directly over their causative bodies, greatly simplifying the geological interpretation of the data. It is intended to remove the skewness of the anomalies due to the inclination of the geomagnetic field.
- Downward Continuation, Figure GP-3, - Downward continuation takes the data and produces from it the data which would have been measured had the sensor been closer to the source. For this data set, downward continuation has been calculated to 100 meters.
- 1st Vertical Derivative, Figure GP-4, - The first vertical derivative (1VD) is the mathematical equivalent of physically measuring the magnetic field simultaneously at two points, with one point located vertically above the other. By subtracting one measurement from the other and dividing the result by the vertical separation of the two measurements, a vertical gradient is derived. The 1VD enhances short-wavelength anomalies, often separating overlapping adjacent anomalies and eliminating long-wavelength regional anomalies. The vertical derivative is commonly applied to total magnetic field data to enhance the shallowest geological sources in the data and is commonly used in conjunction with total field grids to enhance and highlight structural trends.
- 2nd Vertical Derivative, Figure GP-5, - The second vertical derivative (2VD) carries out a double differentiation with respect to vertical distance and thus tends to emphasize, even further than the 1VD, the anomalies associated with small, shallow geologic structures at the expense of larger, regional features. The 2VD map can help identify additional near-surface anomalies not clearly imaged in the 1VD map.
- East Horizontal Derivative (HXD) – GP-6, is similar to the 1st vertical derivative, except that it is calculated horizontally along the east-west direction by subtracting one reading from the other and dividing it by the distance. The

horizontal x derivative map is used to show contacts, especially those striking in northerly directions.

- North Horizontal Derivative (HYD) – GP-7, is the same as the horizontal X derivative, except that it is calculated horizontally along the north-south direction. The horizontal y derivative map is used to show contacts, especially those striking in easterly directions.

- General Derivative - GP-8, is a linear combination of the horizontal and vertical field derivatives normalized by the analytic signal amplitude. It is good for small anomalies as well as finding the edges of larger magnetic bodies.

- Tilt Derivative – GP-9, is defined as the arctangent of the ratio of the vertical derivative of the TMI (numerator) to the total horizontal derivative of the TMI (denominator). The total horizontal derivative is defined as the square root of the sum of the squares of the two horizontal derivatives in the X and Y grid directions. As the TDR is an angle, it is often referred to as the 'tilt angle' or 'local phase' of the magnetic field. Tilt derivative is good for enhancing smaller targets
- Analytic Signal – GP-10, is calculated by taking the square root of the sum of the squares of each of the three directional first derivatives (in the X and Y horizontal grid directions and in the vertical Z direction). The resulting shape of the analytic signal is independent of the orientation of the magnetization of the source, whether induced or remanent. Analytic signal maps are characterized by 'ridges' located above the geological contacts of larger bodies or at the centre of narrow bodies and thus AS is particularly good at outlining edges or boundaries of magnetic sources.

8.4 3D Magnetic Modelling Methodology

The airborne magnetic data was first loaded into Geosoft. A brief review of the data was then carried out As it had been professionally processed, no major changes were required.

A 3D mesh was first created utilizing a 50 x 50 cell size. Topographic data was then incorporated into the model based on DEM data included with the airborne survey. The modelling utilized the Geosoft Voxi platform, and both magnetic vector inversion (MVI) and traditional magnetic susceptibility inversion were performed. The model was unconstrained, since very little work has been carried out on the property. Future work might include a further exploration of relevant constraints and further expanding upon the initial modelling.

The magnetic susceptibility models were then presented with specific susceptibility ranges as 3D voxels with relevant data overlaying within the report.

To examine the magnetic features and trends around and beyond the property, a larger area encompassing the claims was chosen. The modelling region spans from easting 442000 to 450000 and northing 6597500 to 6606500, with the coordinates being NAD83 UTM, zone 9.

The inverted magnetic susceptibility model was visually depicted using 3D iso-volumes to depict areas of magnetic lows (in blue) and highs (in green to red).

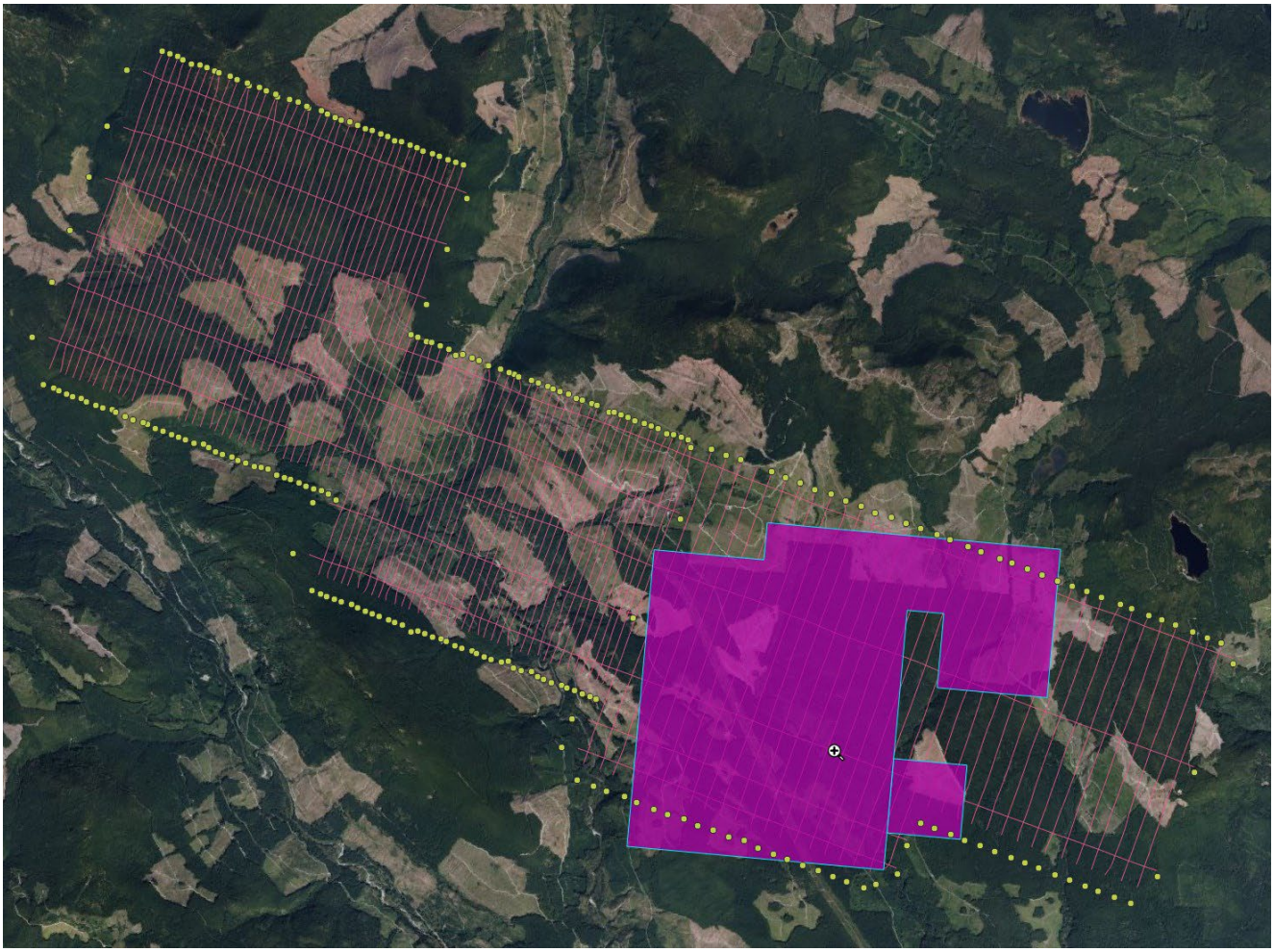

Fig GP-3D1 - Airborne Flight Line Map Showing Lara Claims

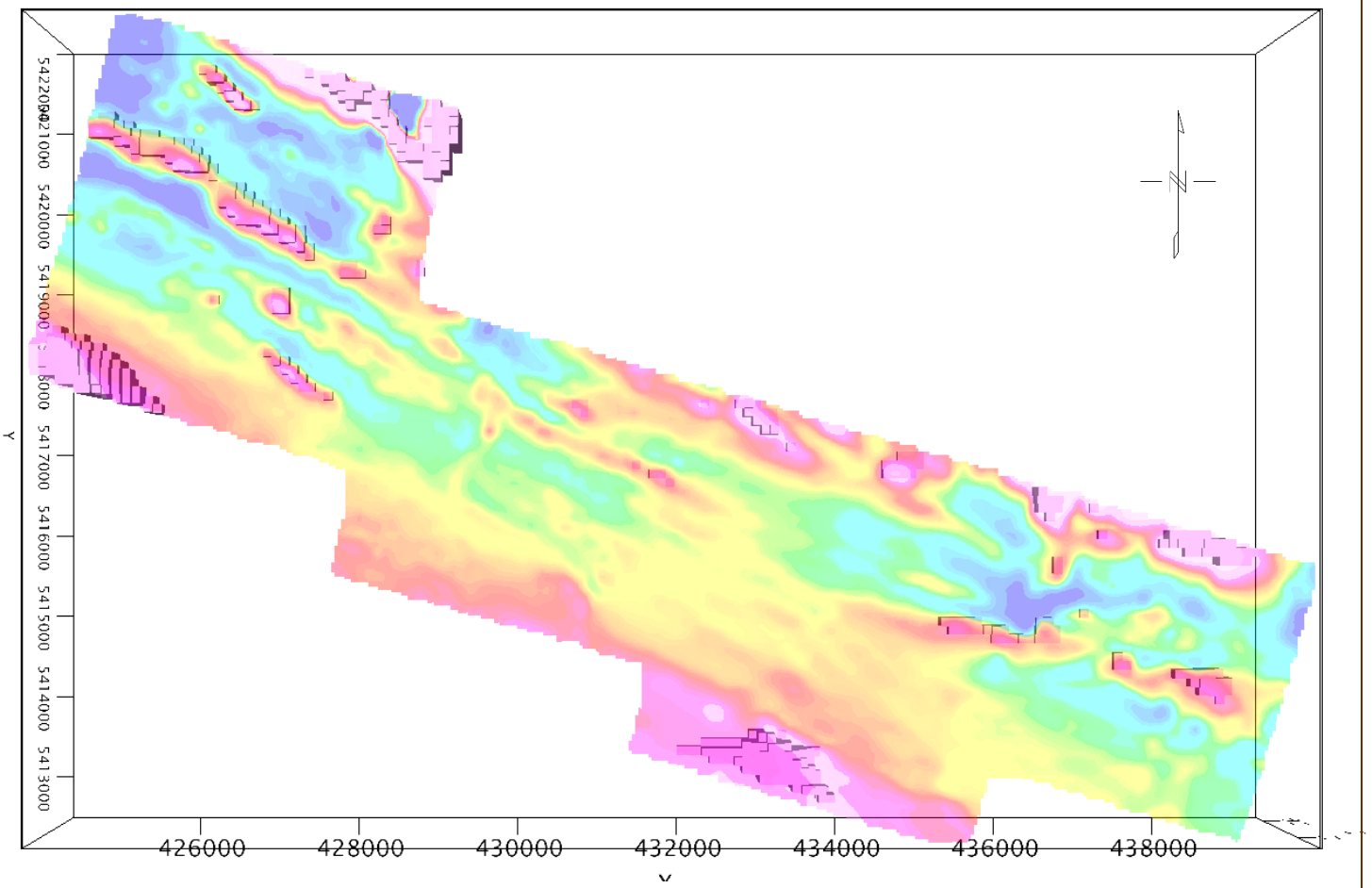

Fig GP-3D2 - 3D Plan View Susceptibility Map with Overlying Magnetic TMI Map
(Red tones are magnetic highs and blue tones are magnetic lows.)

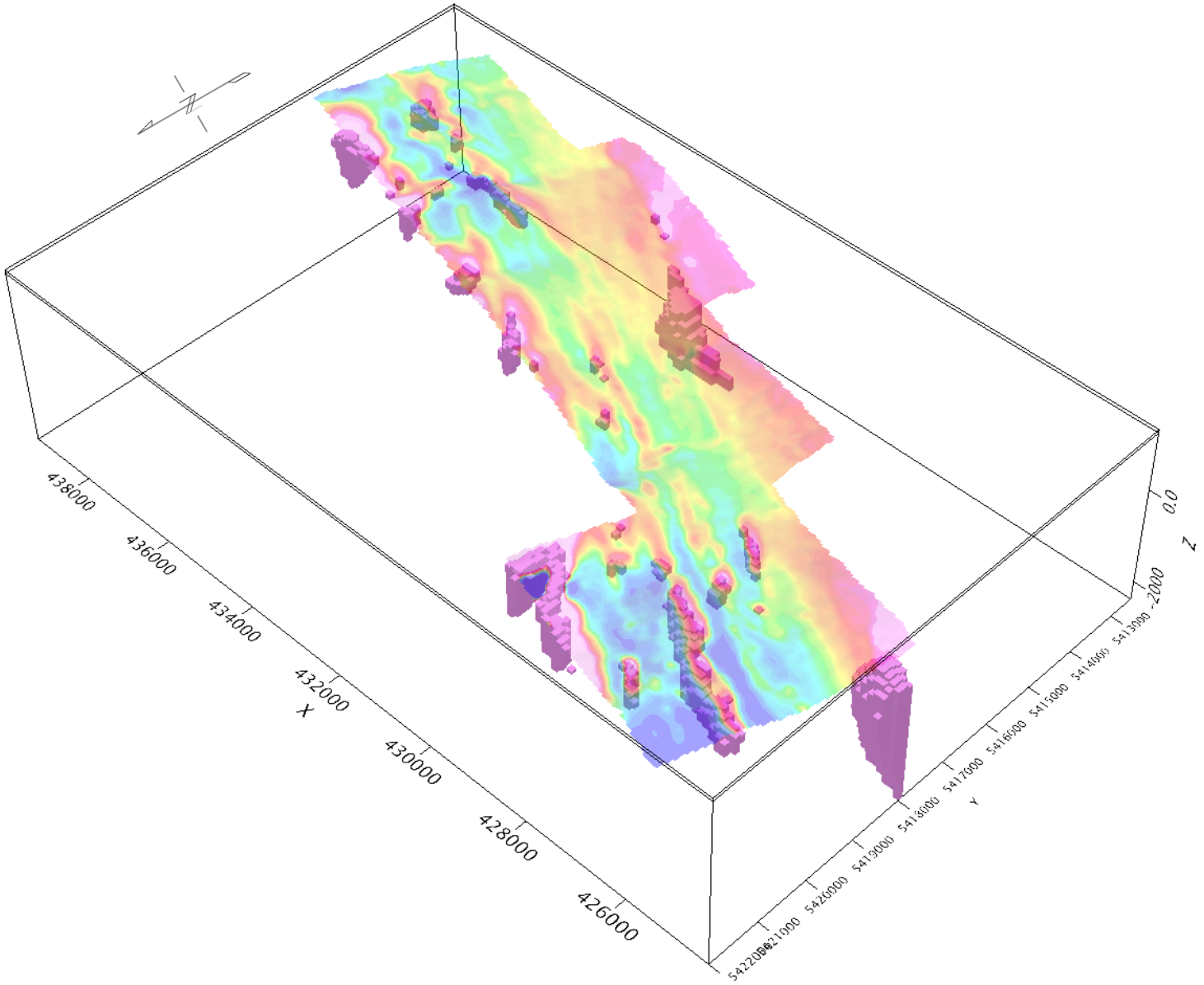

Fig GP-3D3 - 3D Susceptibility Map with Overlying Magnetic TMI Map – View from Northwest

(Red tones are magnetic highs and blue tones are magnetic lows.)

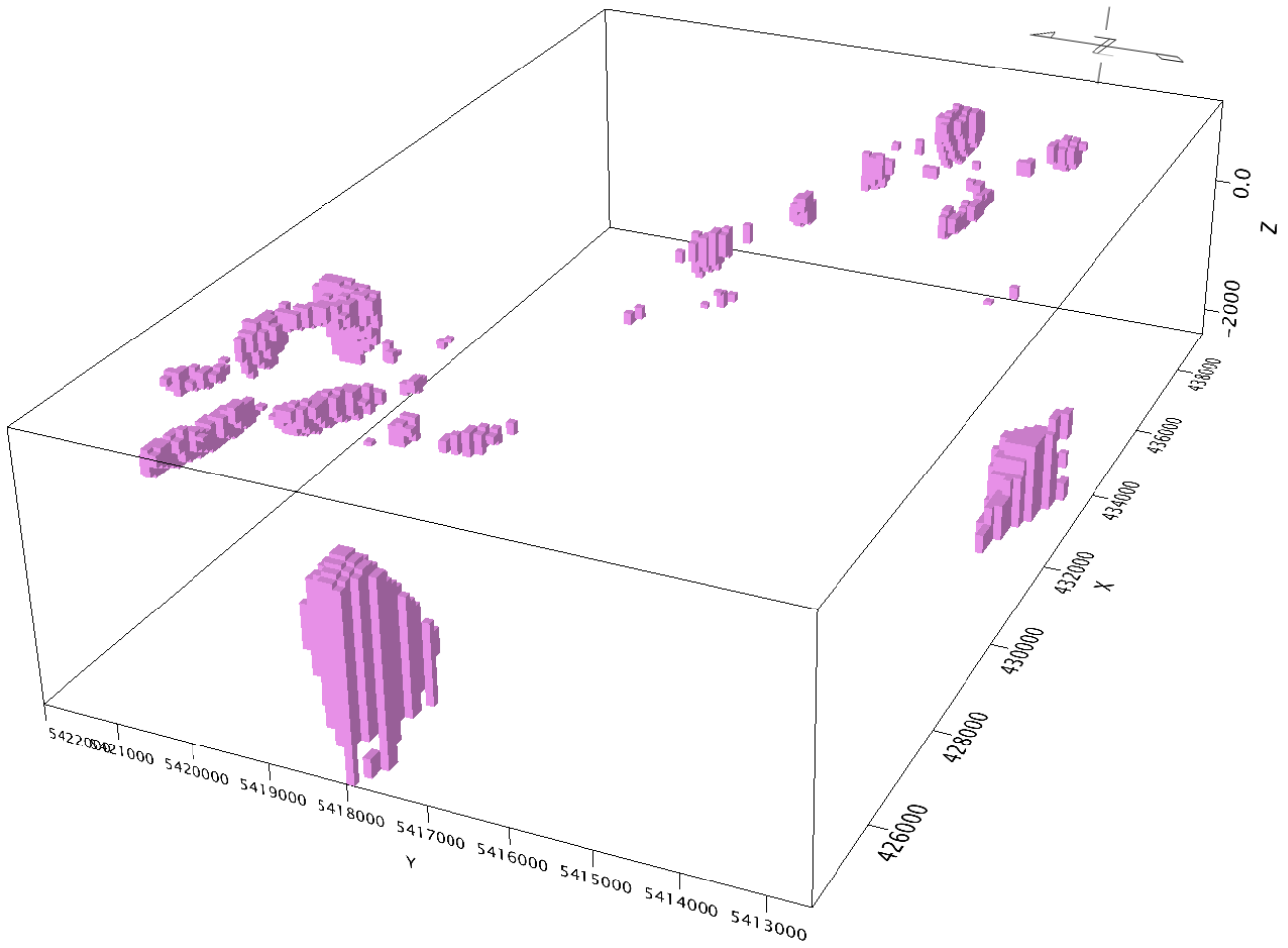

Fig GP-3D4 - 3D View of Magnetic Bodies - from Southwest

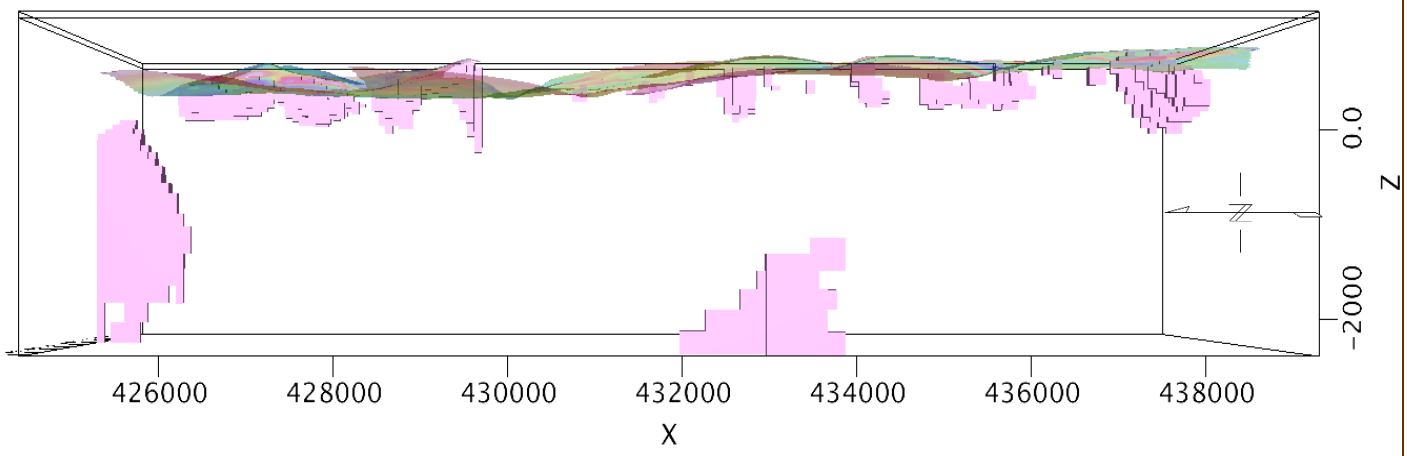

Fig GP-3D5 - 3D Susceptibility Map with Overlying Magnetic TMI Map – View from West
(Red tones are magnetic highs and blue tones are magnetic lows.)

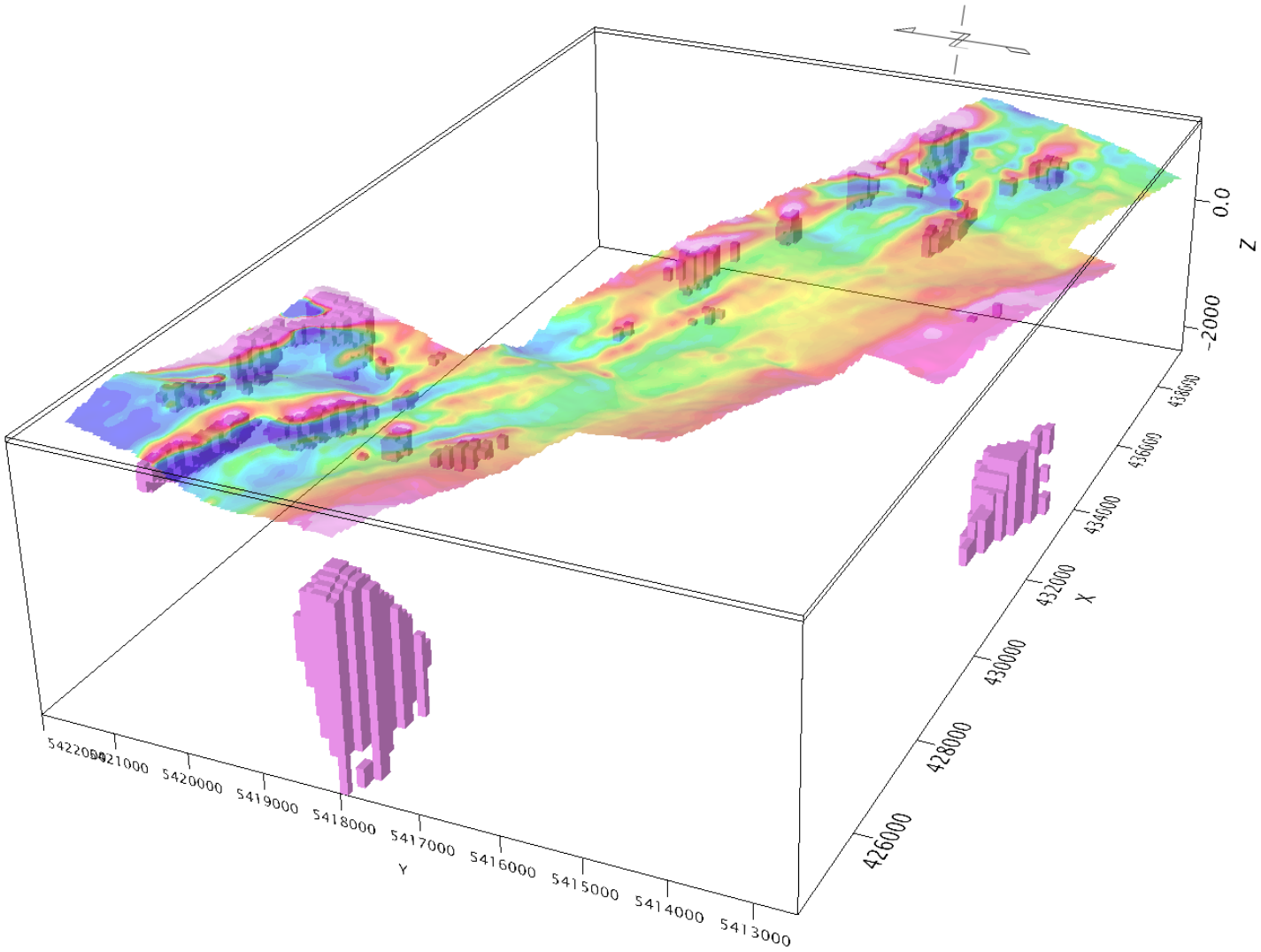

Fig GP-3D6 - 3D Susceptibility Map with Overlying Magnetic TMI Map – View from Southwest
(Red tones are magnetic highs and blue tones are magnetic lows.)

10 DISCUSSION OF RESULTS

The main feature of the magnetic survey maps is a west-northwesterly to northwesterly trend to the magnetic field which can be seen on all the magnetic maps within this report, and which correlates directly with the known geology. The north-northeastern part of the survey area and property shows a magnetic high which is probably reflecting andesitic to basaltic rock-types. The 3D maps show the causative sources to be a series of relatively shallow magnetic bodies occurring along the northern edge of the property. These magnetic bodies may simply consist of higher concentrations of magnetite within the suggested andesites and/or basalts.

The south-southwestern part of the survey area and property has a relatively low magnetic field which is interpreted to be reflecting volcaniclastic and/or sedimentary rock-types. However, a low level, lineal-shaped magnetic high strikes through the southern part of the property as is shown on

the total magnetic intensity, reduce to pole, and downward continuation maps. The 3D maps show that the causative source of this magnetic high is a magnetic body at about a depth of 1,800 meters with a strike length of 2,000 meters and a width of 800 meters. Considering its depth, this magnetic body is interpreted to be relatively strongly magnetic suggesting that the rock type may be an intrusive containing magnetite such as a gabbro, which is known to occur within the area. Perhaps it is the heat engine for the Coronation (Lara) mineralization.

Lineations of magnetic lows have been drawn on the 10 2D magnetic plan maps. These are interpreted to be reflecting geological structure such as faults, shear zones, and/or contacts and thus are exploration targets, especially where they intersect. They reflect zones of weakness which are conducive to the pooling of mineralizing fluids. The primary direction for these lineations, as would be expected, is west-northwesterly with the secondary direction being north-northeasterly.

One of these lineations strikes northwesterly through the Coronation mineral zone and thus may be reflecting the mineralization directly. The Bonbon showing occurs almost directly on a west-northwesterly lineation indicating that its mineralization may be fault related. The Poly showing occurs on the edge of the survey area and thus cannot be correlated with any magnetic features.

11 SELECTED BIBLIOGRAHY

Aeroquest International Ltd. (2007) Report on a Helicopter-Borne AeroTEM System Electromagnetic, Radiometric & Magnetic Survey. Aeroquest Job # 08022, Lara Project, Vancouver Island, British Columbia, NTS 092B13, 092C16. For Laramide Resources Ltd., 38 pp, with data DVD.

Archibald, J.C. (1999) Summary Report on the Laramide Property Diamond Drill Program, Lara VMS Project, Vancouver Island, B.C., 103 pp.

Bailes, R.J., Blackadar, D.W. and Kapusta, J.D. (1987) The Lara Polymetallic Massive Sulphide Deposit. Vancouver Island, British Columbia. Abermin Corporation, 31 pp.

B.C. MEMPR (2006) Legacy Claim Conversion to Cell Claim *in* Information Update, Number 13, revision date November 26, 2006; British Columbia Ministry of Energy, Mines and Petroleum Resources, online http://www.em.gov.bc.ca/mining/titles/infoupdate/default.htm [accessed October 1, 2007].

B.C. MEMPR (2007) Geology of Vancouver Island; British Columbia Ministry of Energy, Mines and Petroleum Resources online at http://www.em.gov.bc.ca/Mining/Geolsurv/GeologyBC/default.htm [accessed October 1, 2007].

B.C. MEMPR (2007) Mineral Titles Online; British Columbia Ministry of Energy, Mines and Petroleum Resources; online at http://www.mtonline.gov.bc.ca/ [accessed October 1, 2007].

Belik, G. and Associates Ltd. (1981) Trenching, geophysical and geochemical report on the Mt. Sicker Property; Victoria Mining Division, British Columbia (NTS 92B/13W) for Laramide Resources Ltd., 49 pp.

Blyth, H.E. and Rutter, N.W. (1993) Quaternary Geology of Southeastern Vancouver Island and Gulf Islands (92B/5, 6, 11, 13 and 14); *in* Geological Fieldwork 1992, British Columbia Ministry of Energy, Mines and Petroleum Resources, Paper 1993-1, p. 209-220.

Breakwater Resources Ltd. (2004) NVI Mining Ltd., A Wholly-owned subsidiary of Breakwater Resources Ltd. Myra Falls Operation; Vancouver Island, British Columbia, NI-43101 Technical Report. July 30, 2004, by Torben Jensen, 54 pp.

Breakwater Resources Ltd. (2007a) 2006 Annual Report, www.breakwater.ca [accessed September 26, 2007].

Breakwater Resources Ltd. (2007b) Operations: Myra Falls.

www.breakwater.ca/operations/myra.cfm [accessed October 1, 2007].

Broughton, L.J. (1987) Exploratory Metallurgical Testwork, Report No. 1; Prepare for Abermin Corporation, Lara Property by Coastech Research Inc., 39 pp.

Earle, Steven (2004) The Geology and Geological History of Vancouver Island; a Powerpoint Presentation, accessed online at http://web.mala.bc.ca/geoscape/ [accessed October 1, 2007].

Chong, A., Becherer, M., Sawyer, R., Wasteneys, H., Baldwin, R., Bakker, F. and McWIlliams, Deposits at Myra Falls Operations, I. (2005) Massive Sulphide Vancouver Island, British Columbia *in* GAC Field Trip Guide (Part 1) Cordilleran Round-Up Field Trip, January 2005, Geological Association of Canada Geofile 2005-20; B.C. Ministry of Energy, Mines and Petroleum Resources, GeoFile 2006-07, 42 pp.

Crick, D. B. (2003) Vancouver Island Opportunities - Junior Custom Feed Exploration Unpublished report to Laramide Resources Ltd.

Franklin, J. M. (1996) Volcanic-Associated Massive Sulphide Base Metals; Geology of Canadian Mineral Deposit Types, (ed.) O.R. Eckstrand, W. D. Sinclair and R. I. Thorpe; Geological Survey of Canada, no. 8, p.158-183.

Franklin, J. M. (1999). Systematic Analysis of Lithogeochemical Data in. Exploration Tools for Volcanogenic Massive Sulphide Deposits short course sponsored by Mineral Deposits Research Unit, University of British Columbia.

Franklin, J. M., Gibson, H. L., Jonasson, I. R., and Galley, A. G. (2005) Volcanogenic Massive Sulphides; Economic Geology 100th Anniversary Volume p. 523-560.

Galley, A.G., Hannington, M.D., and Jonasson, I.R. (2007) Volcanogenic Massive Sulphide Deposits *in* Goodfellow, W.D., ed. Mineral Deposits of Canada: A Synthesis of Major Deposit-Types, District Metallogeny, The Evolution of Geological Provinces, and Exploration Methods: Geological Association of Canada, Mineral Deposits Division, Special Publication No. 5, p. 141-161.

Harris, M.W. (1989) Observations on the Geology, Structure and Mineralization of the Coronation Zone Polymetallic Horizon Lara Project, 1988 Underground Exploration Program. 112 pp.

Hart, T. R., Gibson, H. L. and Lesher, C.M. (2004) Trace Element Geochemistry and Petrogenesis of Felsic Volcanic Rocks Associated with Volcanogenic Massive Cu-Zn-Pb Sulfide Deposits; Economic Geology, v.99, p. 1003-1013.

Höy, T. (1991) Volcanogenic Massive Sulphide Deposits in British Columbia; Ore Deposits, Tectonics and Metallogeny in the Canadian Cordillera, W.J. McMillan, Coordinator, British Columbia Ministry of Energy, Mines and Petroleum Resources, Paper 1991-4, p. 89-123.

Kapusta, J.D. (1991) 1990 Diamond Drilling Report on the Lara Group II: Solly, T.L., Jennie, Ugly, Wimp, Nero, Face and Plant claims, B.C. Ministry of Energy, Mines and Petroleum Resources, Assessment File #20980, 50 pp.

Kelso, I,H,B,Sc and Wetherup, S., 2008 Independent Technical Report and Mineral Resource Estimation, Lara Polymetallic Property, British Columbia, Canada; unpublished report, 121 p.

Laramide Resources Inc (2007). 2006 Annual Report, available online at www.laramide.com.

Lesher, C. M., Goodwin, A. M., Campbell, I. H., Gorton, M. P. (1986) Rare element geochemistry of ore-associated and barren, felsic metavolcanic rocks in the Superior Province Canada; Canadian Journal of Earth Sciences, v.23, p. 222-237.

Lithoprobe Geoscience Project (2007) http://www.lithoprobe.ca/media/studies/terrane.asp [accessed October 1, 2007].

Long, S. D. (2003): Assay Quality Assurance-Quality Control Program for Drilling Projects at the Pre-Feasibility to Feasibility Level (3rd Ed.). Amec Mining Consulting Group.

Massey, N.W.D. and Friday, S.J. (1989) Geology of the Alberni-Nanaimo Lakes Area, Vancouver Island (92F/1W, 92F/2E and part of 92F/7); *in* Geological Fieldwork 1988; B.C. Ministry of Energy, Mines and Petroleum Resources, Paper 1989-1, p. 61-74.

Massey, N.W.D. (1992) Geology and Mineral Resources of the Duncan Sheet, Vancouver Island (92B/13); British Columbia Ministry of Energy, Mines and Petroleum Resources, Paper 1992-4, 124 pp.

Massey, N.W.D., MacIntyre, D.G., Desjardins, P.J., and Cooney, R.T. (2005a) Geology of British Columbia, B.C. Ministry of Energy, Mines and Petroleum Resources, Geoscience Map 2005-3, (3 sheets), scale 1:1 000 000.

Massey, N.W.D., MacIntyre, D.G., Desjardins, P.J. and Cooney, R.T. (2005b) Digital Map of British Columbia: Tile NM9 Mid Coast, B.C. Ministry of Energy and Mines, GeoFile 2005-2, scale 1:250,000.

Massey, N.W.D., MacIntyre, D.G., Desjardins, P.J. and Cooney, R.T. (2005c) Digital Geology Map of British Columbia: Tile NM10 Southwest British Columbia, B.C. Ministry of Energy and Mines, GeoFile 2005-3, scale 1:250,000.

MINFILE (1990a) Lara, Coronation, 262, Coronation Extension, NTS 092B13W (1990/08/10), MinFile Number 092B-129; British Columbia Ministry of Energy, Mines and Petroleum Resources, MINFILE data.

MINFILE (1990b) Anita NTS 092B 13W (1990/10/13), Minfile Number 092B-037; British Columbia Ministry of Energy, Mines and Petroleum Resources, MINFILE data.

MINFILE (1990c). Sharon Copper NTS NTS 092B 13W (1990/08/02), Minfile Number 092B-

040; British Columbia Ministry of Energy, Mines and Petroleum Resources, MINFILE data.

MINFILE (1997) Mount Sicker Mine: Lenora (L.35G), Twin J Mine, Mount Sicker, Lenora-Tyee, Tyee, Richard III, barite Ore, NTS092B13W (1997/04/30), MinFile Number 092B-001; British Columbia Ministry of Energy, Mines and Petroleum Resources, MINFILE data.

Mortensen, J. (2006) Stratigraphic and Paleotectonic Studies of the middle Paleozoic Sicker Group, Poster presented at Roundup 2006; Association for Mineral Exploration in British Columbia

Nucanolan Resources Ltd. (1998) Update on the Lara Project in British Columbia, Press Release December 11, 1998.

Peatfield, G. R. and Walker, R.R. (1994) Review of Technical Reports and Field Observations with a Re-interpretation of Geological Relationships on the Cowichan Uplift Polymetallic Mineral Property, Laramide Resources Summary Report; Victoria Mining Divisions, British Columbia (NTS 93B/13W; 93 C/16E.

Roberts, S.A. (2007) Lara Project Order of Magnitude Study, Vancouver Island, BC for Laramide Resources Limited, Unpublished report by Watts, Griffis and McQuat Limited, Toronto, Canada, 46 pp.

Roscoe, W. (1988) Report on the Lara Project, Vancouver Island, B.C. for Laramide Resources. Roscoe Postle Associates Inc., Toronto, Ontario, 46 pp.

Roscoe and Postle Associates (1988) Report on the Lara Project, Vancouver Island, British Columbia, for Laramide Resources Ltd.

Stewart, R. (1991) Project 116: Project Summary of Chemainus Property (NTS 92B/13 and 92C/16), Falconbridge Ltd.

Wells, G.S. and Kapusta, J.D. (1990a) 1989 Exploration Program, Lara Property, Victoria Mining Division (NTS 92B/13W), Minnova Inc.

Wells, G.S. (1990b) Summary Report, Mount Sicker Property: 1983-1990. Minnova Inc.

Wells, G.S. and Kapusta, J.D. (1991) 1990 Exploration Program, Lara Property, Victoria Mining Division (NTS 92B/13W), Minnova Inc.

12 GEOSCIENTIST'S CERTIFICATE

I, DAVID G. MARK, of the City of Surrey, in the Province of British Columbia, do hereby certify that:

I am registered as a Professional Geoscientist with the Association of Professional Engineers and Geoscientists of the Province of British Columbia.

I am a Consulting Geophysicist of Geotronics Consulting Inc., with offices at 132 Saddlehorn Drive, Kaleden, British Columbia.

I further certify that:

1. I am a graduate of the University of British Columbia (1968) and hold a B.Sc. degree in Geophysics.
2. I have been practicing my profession for the past 55 years and have been active in the mining industry for the past 58 years.
3. This report is a 2D and 3D interpretation of magnetic data obtained from an airborne geophysical survey carried out during September 2007 over the entire Lara Property by Aeroquest International. The interpretive work was done during the period of May 05th, 2022 to March 27th, 2023
4. I am a 25% owner of the Lara Property.

David Mark

David G. Mark, P.Geo. May 31, 2024
Geoscientist

13 AFFIDAVIT OF EXPENSES

Inversion 3D modelling of airborne magnetic surveying over the Lara Property, which is located on Solly Creek 17 km northwest of the town of Duncan, during the period of May 05th, 2022 to March 27th, 2023, was carried out to the value of the following:

Geoscientist, 43 hours @ $150/hour	$6,450.00	
Geophysical technician with advanced computer and		
software, 32 hours @ $150/hour	$4,800.00	
TOTAL	$11,250.00	$11,250.00
Administration @10%		$1,125.00
GRAND TOTAL		$12,375.00

Respectfully submitted,
Geotronics Consulting Inc.

David Mark

David G. Mark, P.Geo,
Geoscientist

May 31, 2024

14 APPENDIX I – MAGNETIC CONTOUR PLAN MAPS

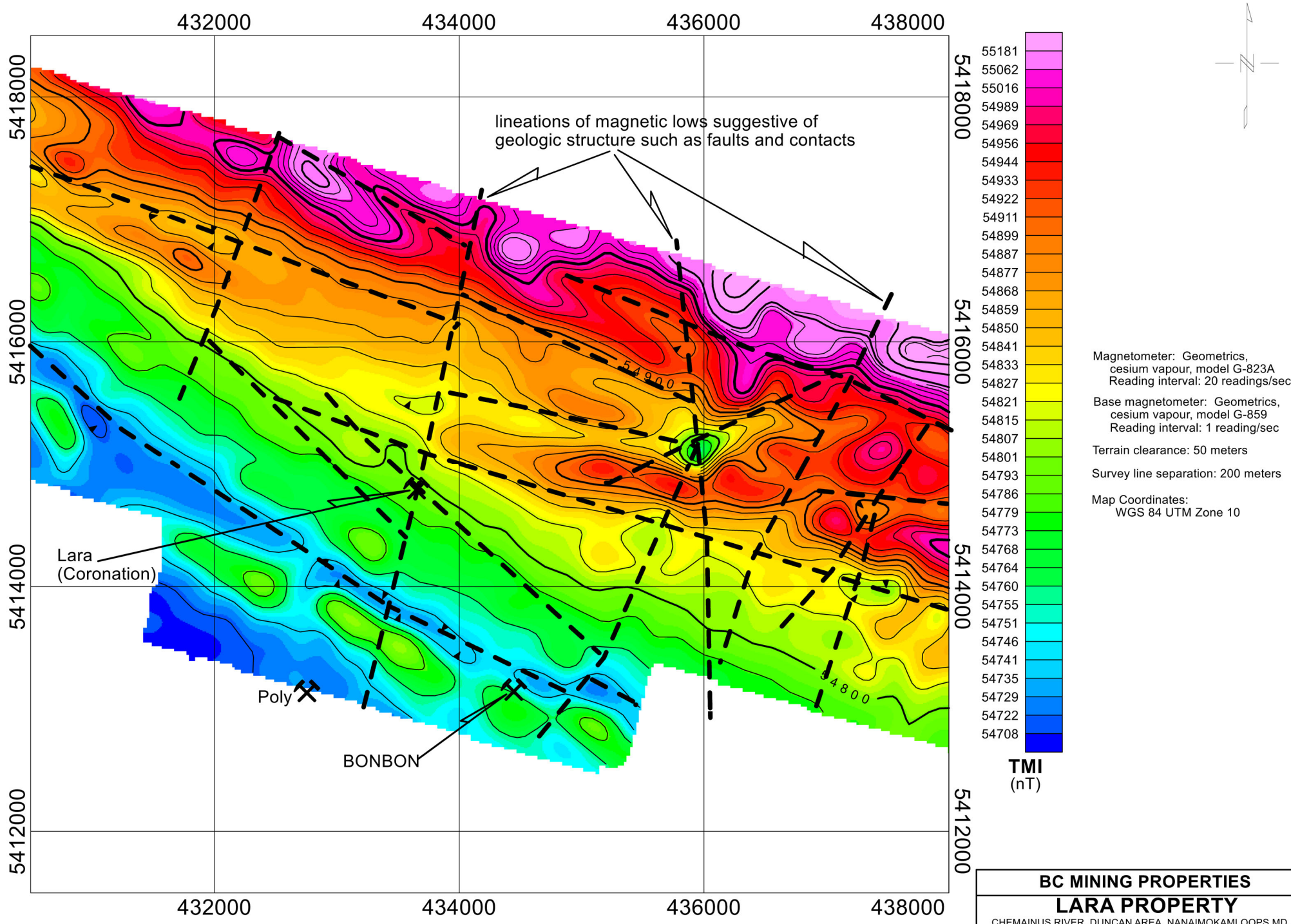

Magnetometer: Geometrics, cesium vapour, model G-823A
Reading interval: 20 readings/sec

Base magnetometer: Geometrics, cesium vapour, model G-859
Reading interval: 1 reading/sec

Terrain clearance: 50 meters

Survey line separation: 200 meters

Map Coordinates:
WGS 84 UTM Zone 10

BC MINING PROPERTIES

LARA PROPERTY

CHEMAINUS RIVER, DUNCAN AREA, NANAIMOKAMLOOPS MD, BC

AIRBORNE MAGNETIC SURVEY
TOTAL MAGNETIC INTENSITY (TMI)
CONTOUR PLAN

DRAWN BY:	JOB NO:	NTS: / BCGS:	DATE:	FIG NO:
DGM	23-04	92B/13 / 092B.081	MAY '24	GP-1

Geotronics Consulting Inc
Exploration done right

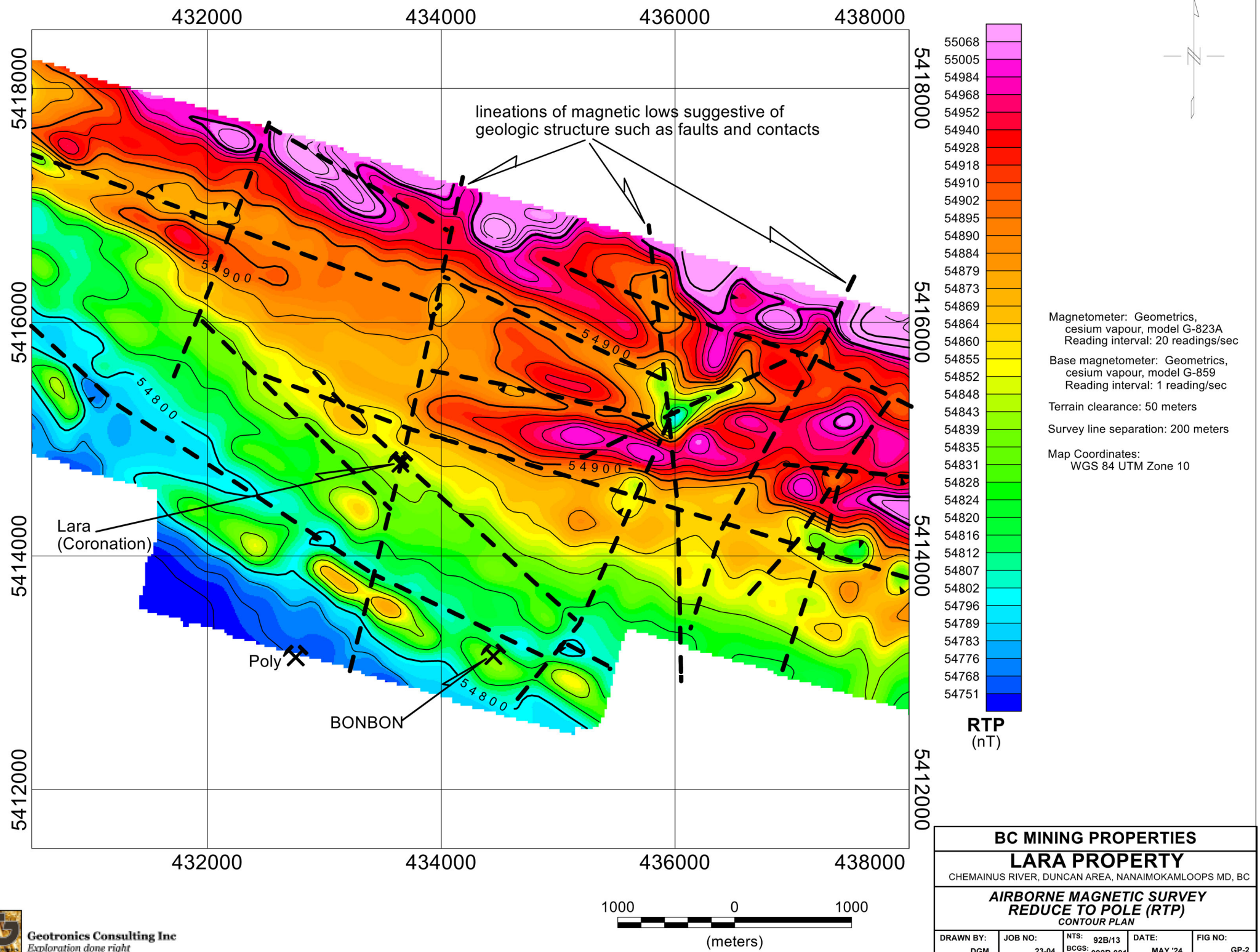

Geotronics Consulting Inc
Exploration done right

BC MINING PROPERTIES

LARA PROPERTY

CHEMAINUS RIVER, DUNCAN AREA, NANAIMOKAMLOOPS MD, BC

AIRBORNE MAGNETIC SURVEY
REDUCE TO POLE (RTP)
CONTOUR PLAN

DRAWN BY:	JOB NO:	NTS: / BCGS:	DATE:	FIG NO:
DGM	23-04	92B/13 / 092B.081	MAY '24	GP-2

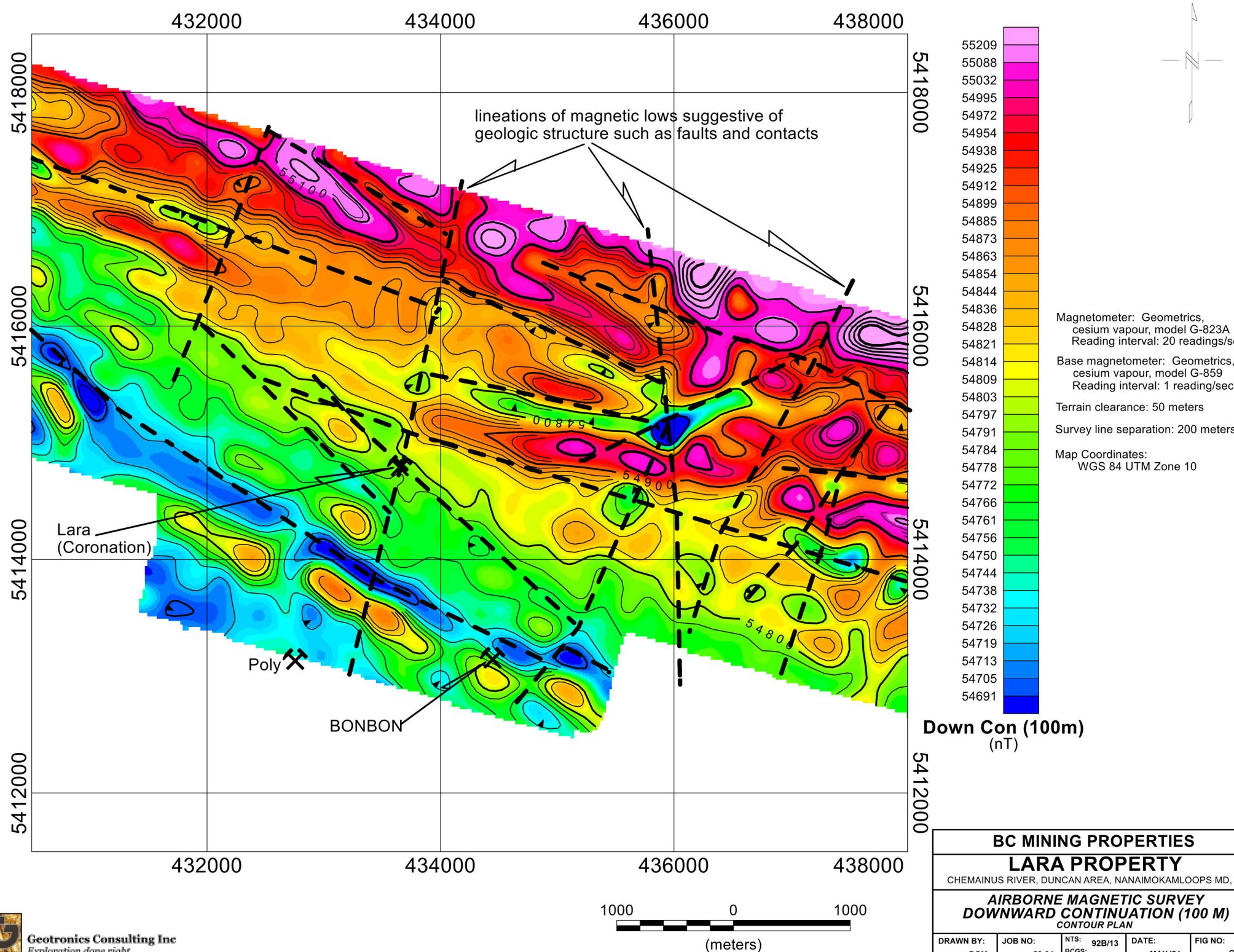

Geotronics Consulting Inc
Exploration done right

BC MINING PROPERTIES

LARA PROPERTY

CHEMAINUS RIVER, DUNCAN AREA, NANAIMOKAMLOOPS MD, BC

AIRBORNE MAGNETIC SURVEY
DOWNWARD CONTINUATION (100 M)
CONTOUR PLAN

DRAWN BY:	JOB NO:	NTS: / BCGS:	DATE:	FIG NO:
DGM	23-04	92B/13 / 092B.081	MAY '24	GP-3

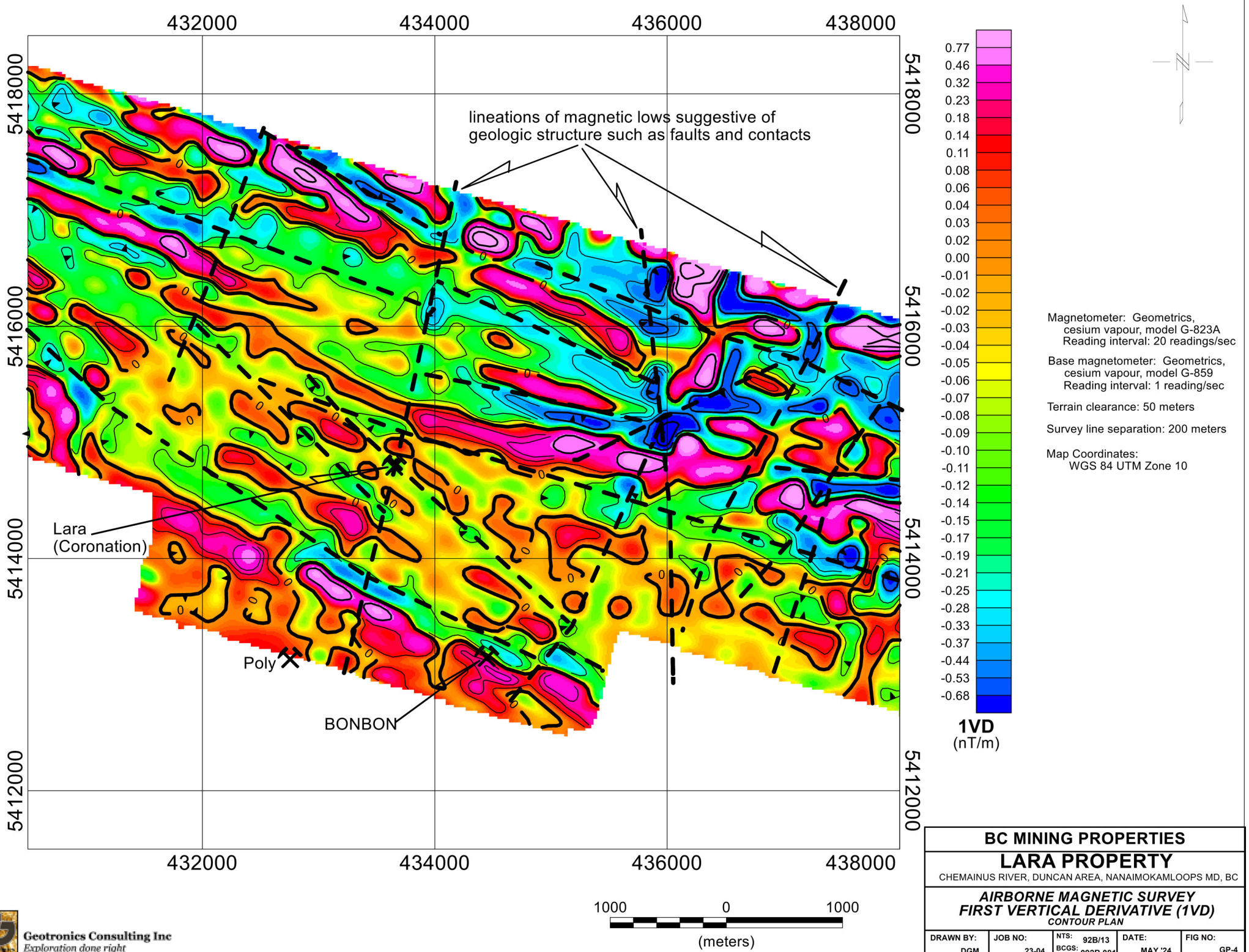

Magnetometer: Geometrics, cesium vapour, model G-823A
Reading interval: 20 readings/sec

Base magnetometer: Geometrics, cesium vapour, model G-859
Reading interval: 1 reading/sec

Terrain clearance: 50 meters

Survey line separation: 200 meters

Map Coordinates:
WGS 84 UTM Zone 10

Geotronics Consulting Inc
Exploration done right

BC MINING PROPERTIES

LARA PROPERTY

CHEMAINUS RIVER, DUNCAN AREA, NANAIMOKAMLOOPS MD, BC

AIRBORNE MAGNETIC SURVEY
FIRST VERTICAL DERIVATIVE (1VD)
CONTOUR PLAN

DRAWN BY:	JOB NO:	NTS: / BCGS:	DATE:	FIG NO:
DGM	23-04	92B/13 / 092B.081	MAY '24	GP-4

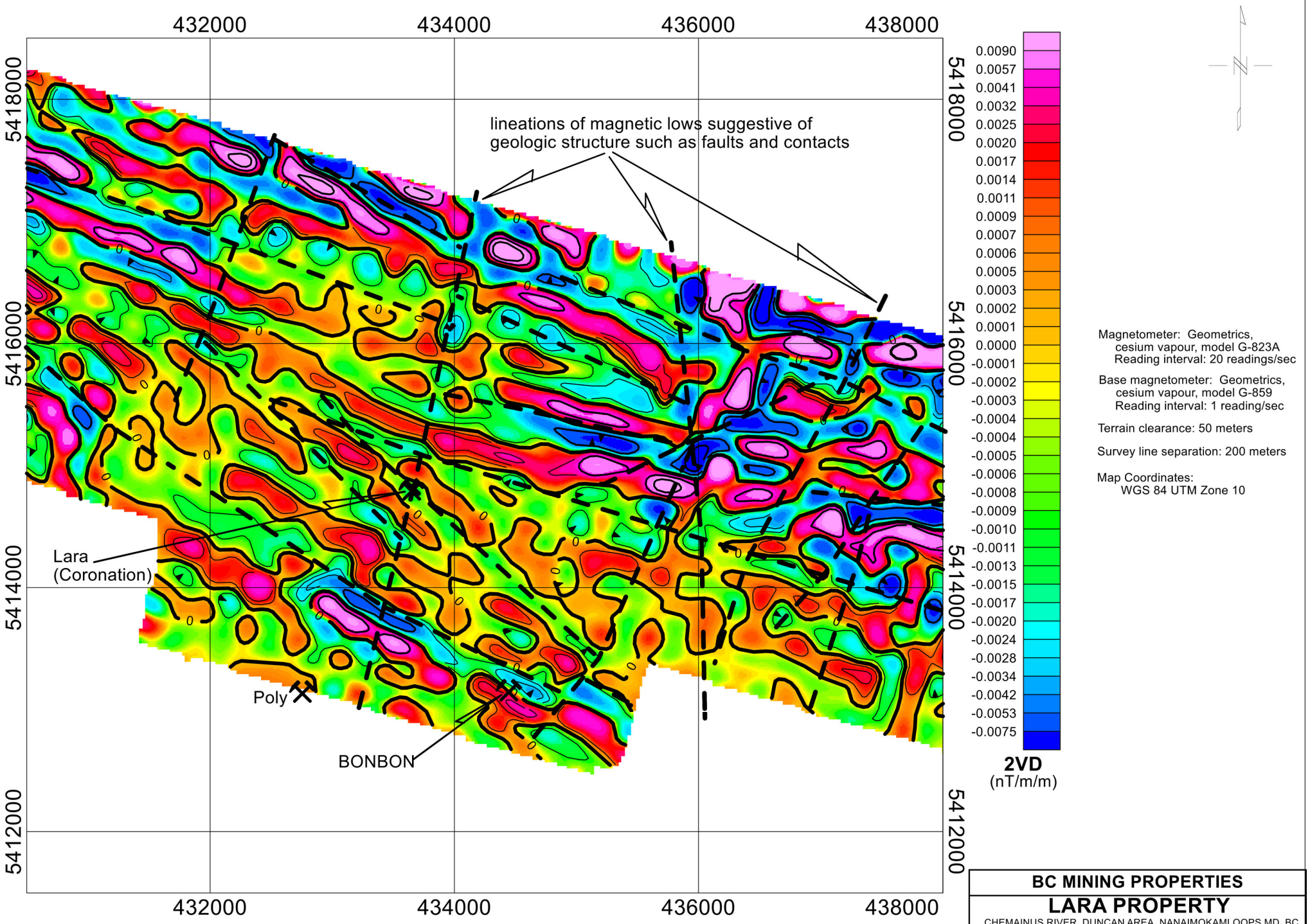

Magnetometer: Geometrics, cesium vapour, model G-823A
Reading interval: 20 readings/sec

Base magnetometer: Geometrics, cesium vapour, model G-859
Reading interval: 1 reading/sec

Terrain clearance: 50 meters

Survey line separation: 200 meters

Map Coordinates:
WGS 84 UTM Zone 10

Geotronics Consulting Inc
Exploration done right

BC MINING PROPERTIES

LARA PROPERTY

CHEMAINUS RIVER, DUNCAN AREA, NANAIMOKAMLOOPS MD, BC

AIRBORNE MAGNETIC SURVEY
SECOND VERTICAL DERIVATIVE (2VD)
CONTOUR PLAN

DRAWN BY:	JOB NO:	NTS: / BCGS:	DATE:	FIG NO:
DGM	23-04	92B/13 / 092B.081	MAY '24	GP-5

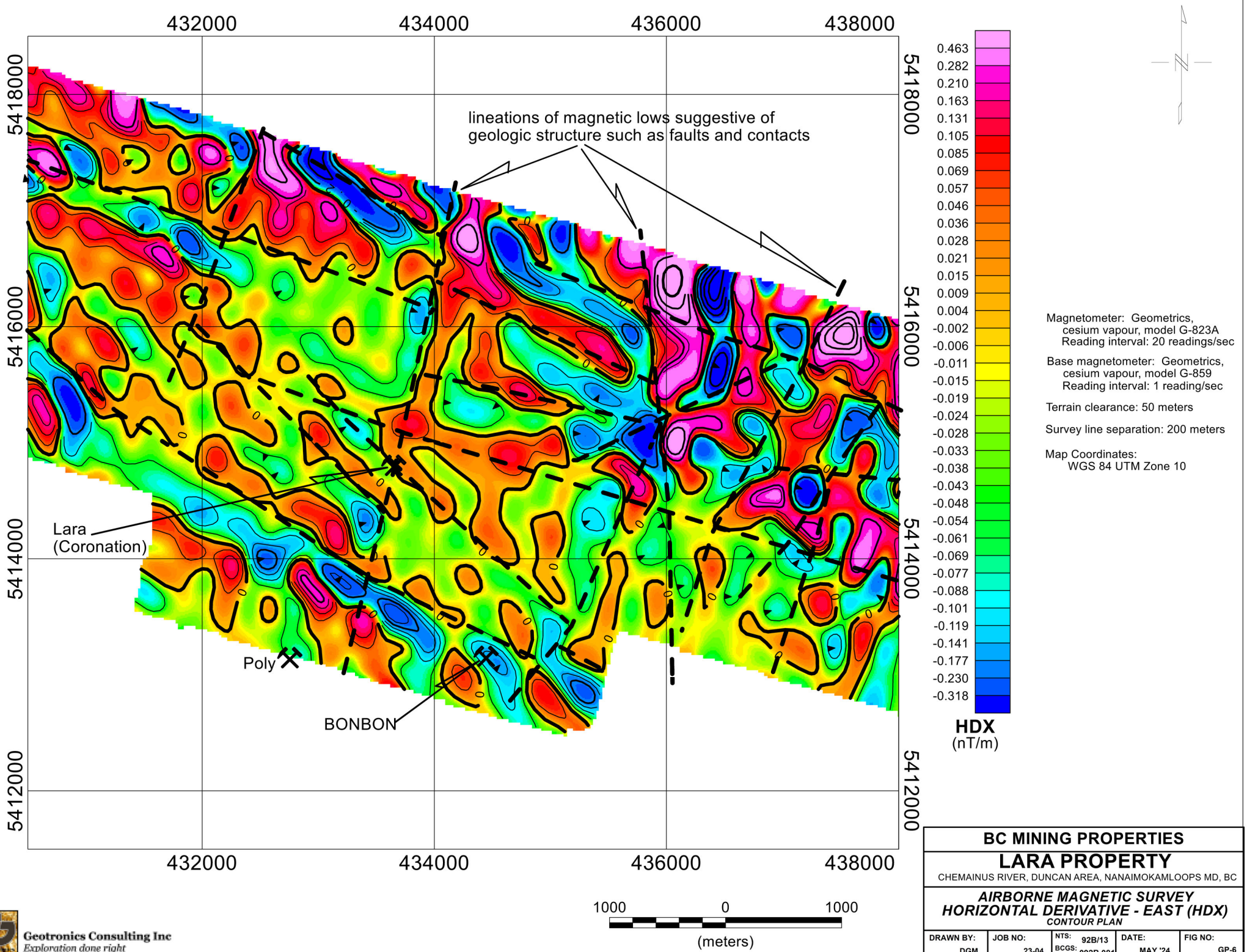

Magnetometer: Geometrics, cesium vapour, model G-823A
Reading interval: 20 readings/sec

Base magnetometer: Geometrics, cesium vapour, model G-859
Reading interval: 1 reading/sec

Terrain clearance: 50 meters

Survey line separation: 200 meters

Map Coordinates:
WGS 84 UTM Zone 10

Geotronics Consulting Inc
Exploration done right

BC MINING PROPERTIES

LARA PROPERTY

CHEMAINUS RIVER, DUNCAN AREA, NANAIMOKAMLOOPS MD, BC

AIRBORNE MAGNETIC SURVEY
HORIZONTAL DERIVATIVE - EAST (HDX)
CONTOUR PLAN

DRAWN BY:	JOB NO:	NTS: / BCGS:	DATE:	FIG NO:
DGM	23-04	92B/13 / 092B.081	MAY '24	GP-6

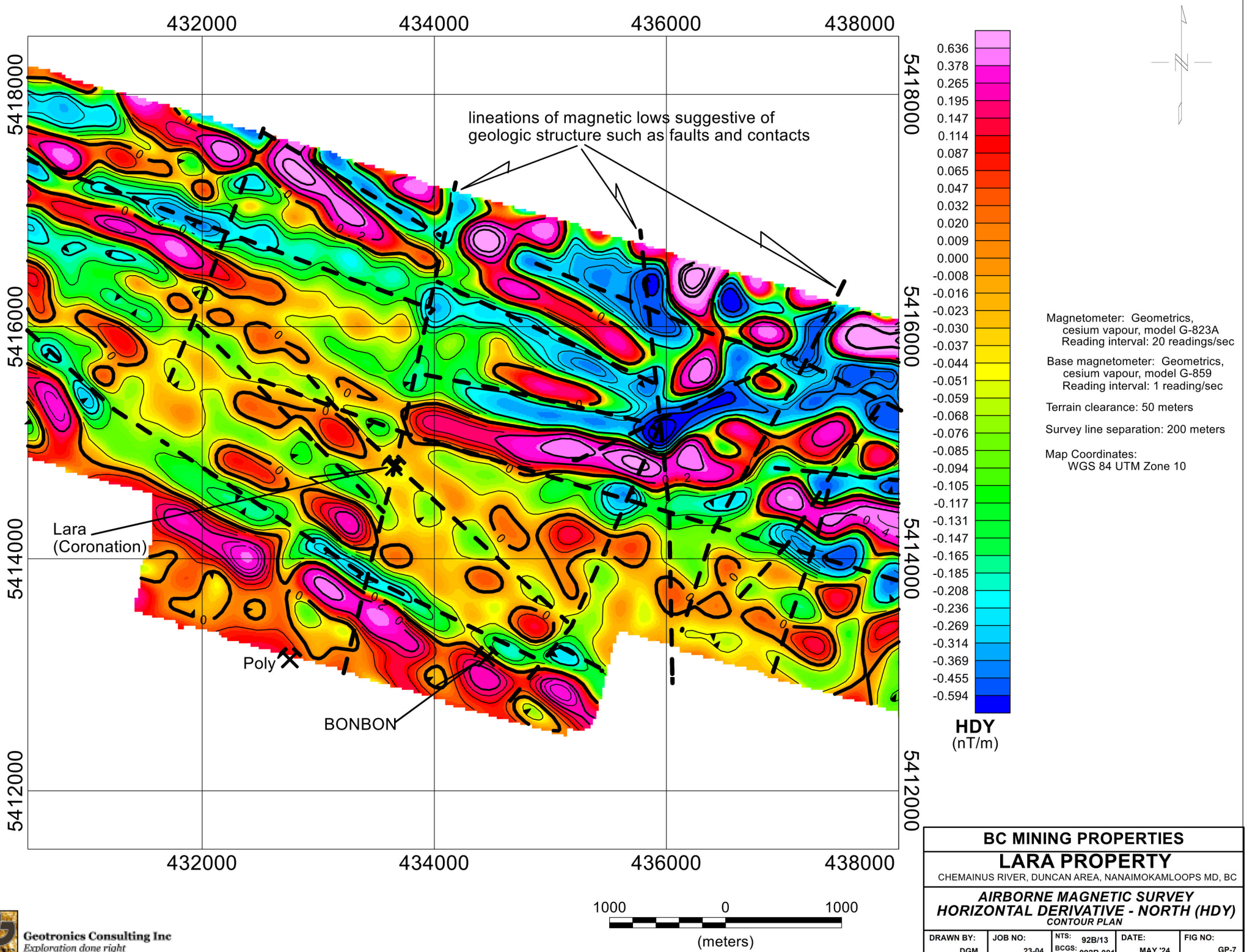

Magnetometer: Geometrics, cesium vapour, model G-823A
Reading interval: 20 readings/sec

Base magnetometer: Geometrics, cesium vapour, model G-859
Reading interval: 1 reading/sec

Terrain clearance: 50 meters

Survey line separation: 200 meters

Map Coordinates:
WGS 84 UTM Zone 10

BC MINING PROPERTIES

LARA PROPERTY

CHEMAINUS RIVER, DUNCAN AREA, NANAIMOKAMLOOPS MD, BC

AIRBORNE MAGNETIC SURVEY
HORIZONTAL DERIVATIVE - NORTH (HDY)
CONTOUR PLAN

DRAWN BY:	JOB NO:	NTS: / BCGS:	DATE:	FIG NO:
DGM	23-04	92B/13 / 092B.081	MAY '24	GP-7

Geotronics Consulting Inc
Exploration done right

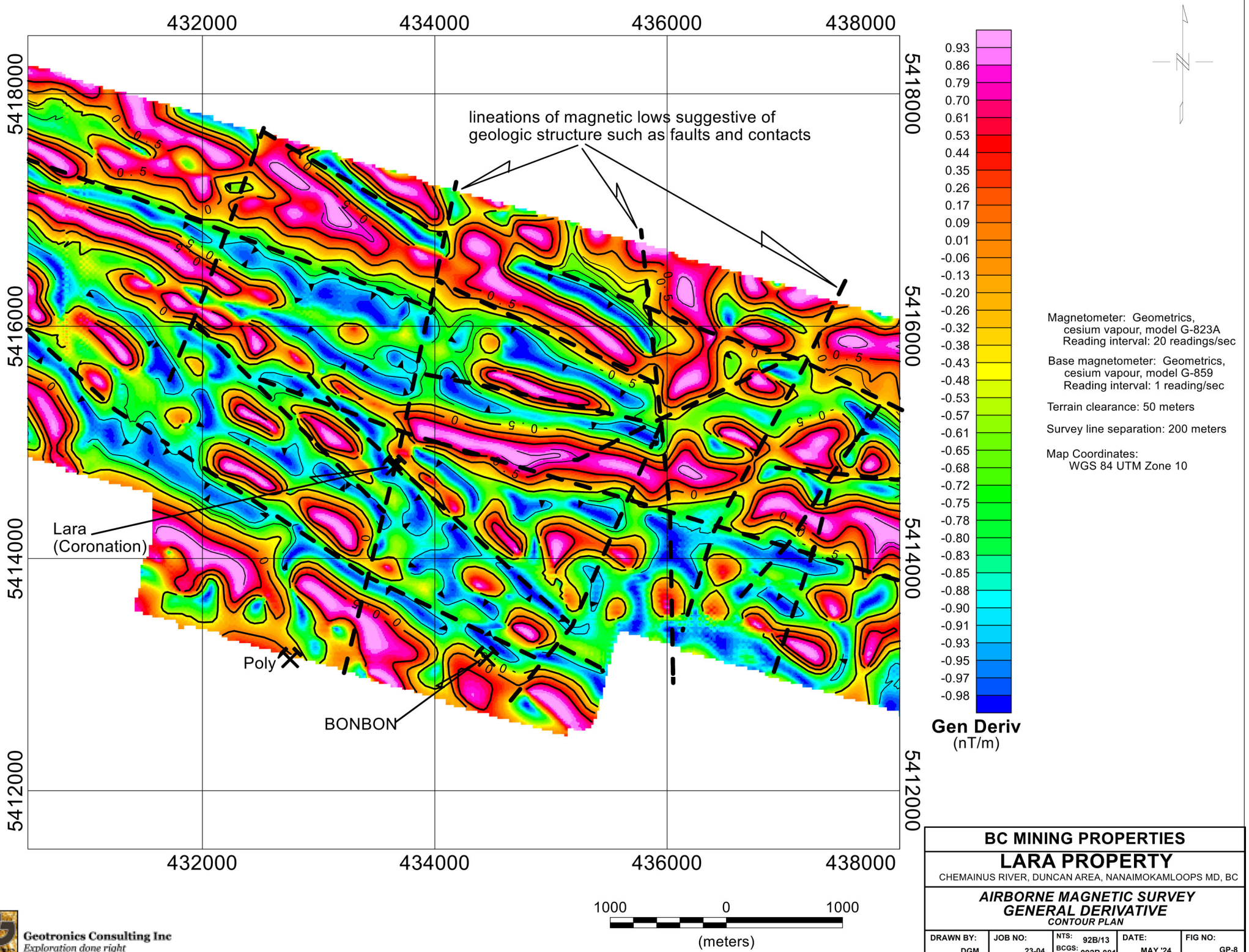

Magnetometer: Geometrics, cesium vapour, model G-823A
Reading interval: 20 readings/sec

Base magnetometer: Geometrics, cesium vapour, model G-859
Reading interval: 1 reading/sec

Terrain clearance: 50 meters

Survey line separation: 200 meters

Map Coordinates:
WGS 84 UTM Zone 10

Geotronics Consulting Inc
Exploration done right

BC MINING PROPERTIES

LARA PROPERTY

CHEMAINUS RIVER, DUNCAN AREA, NANAIMOKAMLOOPS MD, BC

AIRBORNE MAGNETIC SURVEY
GENERAL DERIVATIVE
CONTOUR PLAN

DRAWN BY:	JOB NO:	NTS: / BCGS:	DATE:	FIG NO:
DGM	23-04	92B/13 / 092B.081	MAY '24	GP-8

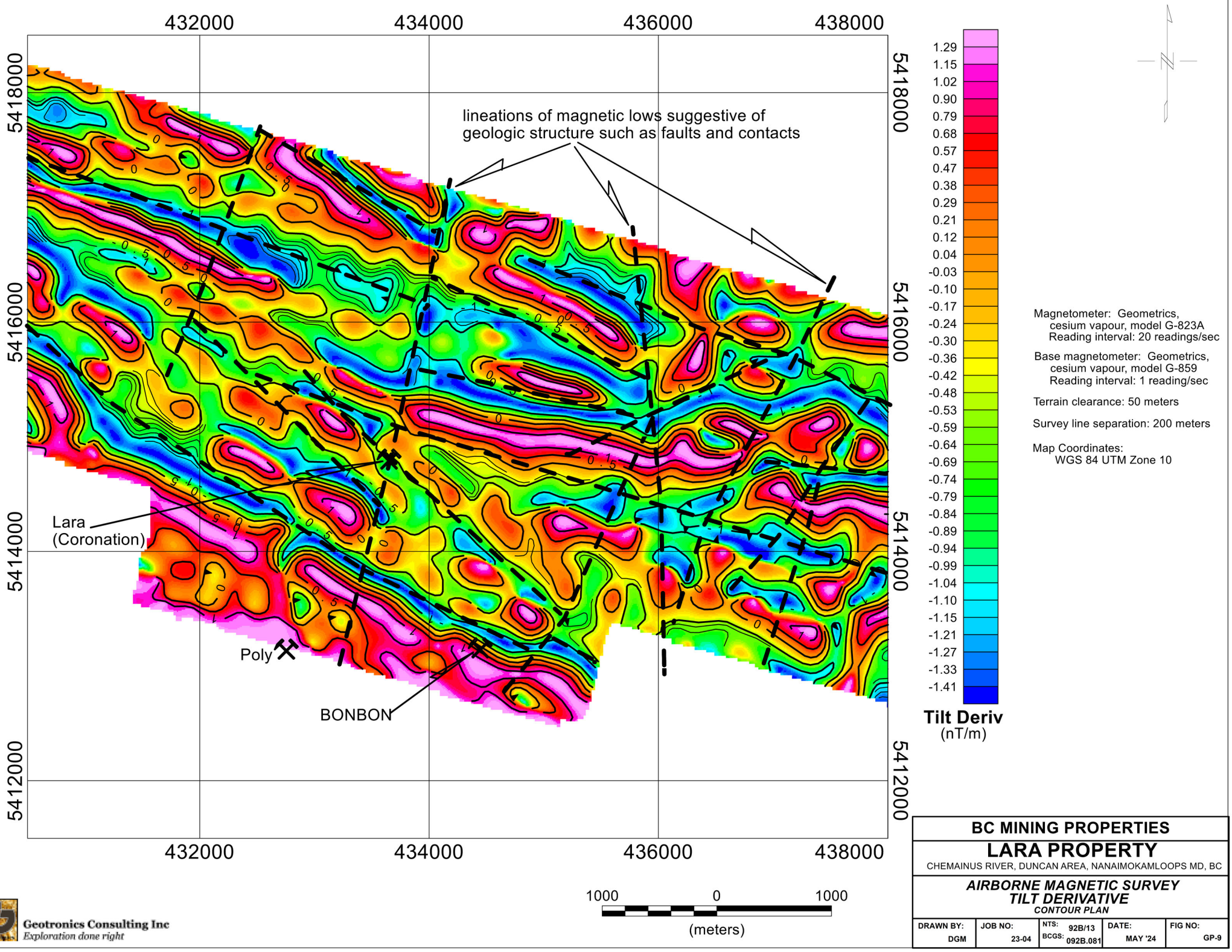

Geotronics Consulting Inc
Exploration done right

BC MINING PROPERTIES

LARA PROPERTY

CHEMAINUS RIVER, DUNCAN AREA, NANAIMOKAMLOOPS MD, BC

AIRBORNE MAGNETIC SURVEY
TILT DERIVATIVE
CONTOUR PLAN

DRAWN BY:	JOB NO:	NTS: 92B/13 BCGS: 092B.081	DATE:	FIG NO:
DGM	23-04		MAY '24	GP-9

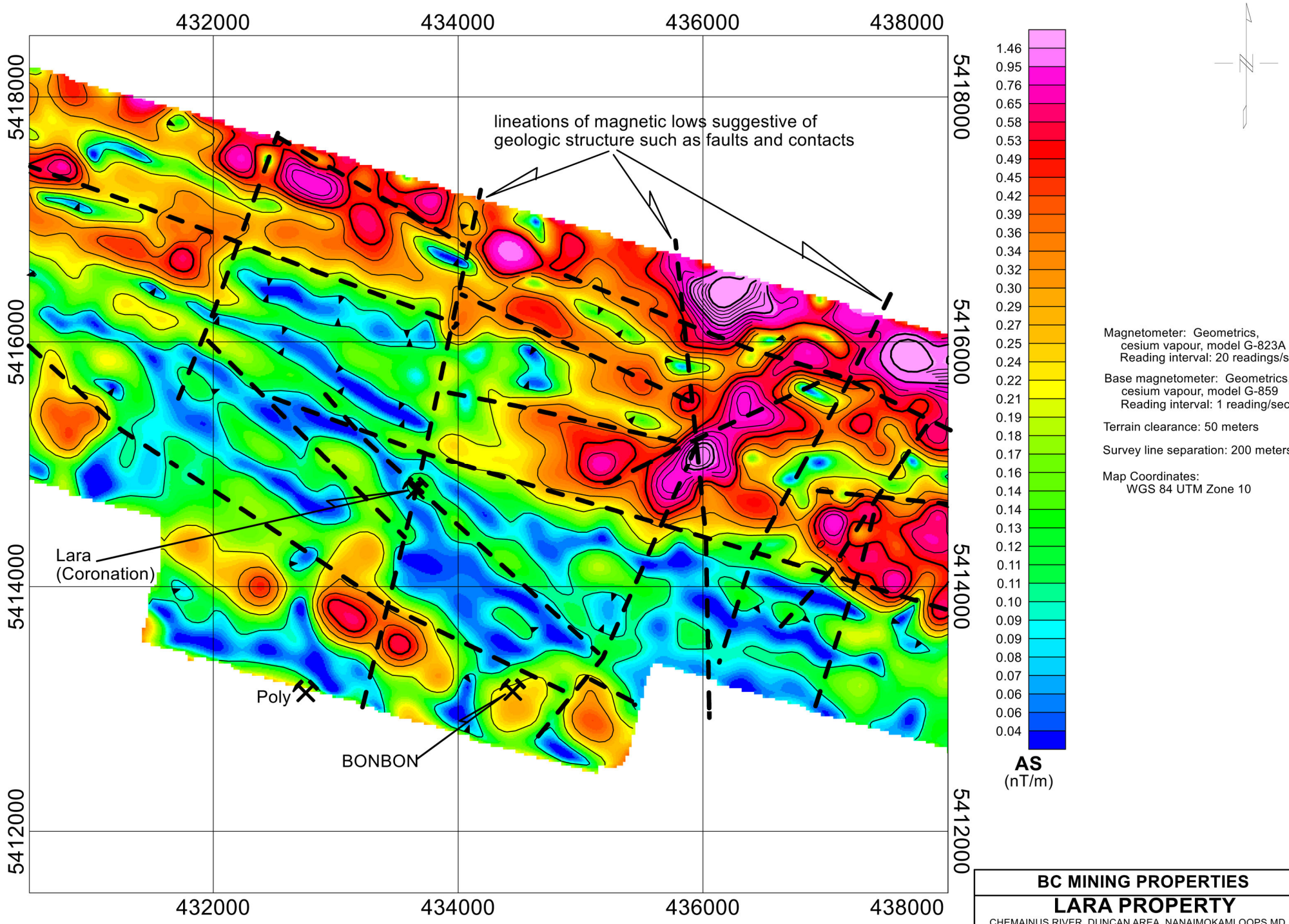

Magnetometer: Geometrics, cesium vapour, model G-823A
Reading interval: 20 readings/sec

Base magnetometer: Geometrics, cesium vapour, model G-859
Reading interval: 1 reading/sec

Terrain clearance: 50 meters

Survey line separation: 200 meters

Map Coordinates:
WGS 84 UTM Zone 10

Geotronics Consulting Inc
Exploration done right

BC MINING PROPERTIES

LARA PROPERTY

CHEMAINUS RIVER, DUNCAN AREA, NANAIMOKAMLOOPS MD, BC

AIRBORNE MAGNETIC SURVEY
ANALYTICAL SIGNAL (AS)
CONTOUR PLAN

DRAWN BY:	JOB NO:	NTS: 92B/13 BCGS: 092B.081	DATE:	FIG NO:
DGM	23-04		MAY '24	GP-10

15 APPENDIX II – AIRBORNE REPORT BY AEROQUEST

Report on a Helicopter-Borne AeroTEM System Electromagnetic, Radiometric & Magnetic Survey

Aeroquest Job # 08022

Lara Project

Vancouver Island, British Columbia
NTS 092B13, 092C16

For

LARAMIDE RESOURCES LTD.

by

AEROQUEST INTERNATIONAL
ADVANCED AIRBORNE GEOPHYSICS

7687 Bath Road,
Mississauga, ON, L4T 3T1
Tel: (905) 672-9129
Fax: (905) 672-7083
www.aeroquest.ca

Report date: October 2007

Report on a Helicopter-Borne AeroTEM System Electromagnetic, Radiometric & Magnetic Survey

Aeroquest Job # 08022

Lara Project

Vancouver Island, British Columbia
NTS 092B13, 092C16

For

Laramide Resources Ltd.

3680-130 King Street W.,
Toronto, ON
Tel: 416 599 7363

By

7687 Bath Road,
Mississauga, ON, L4T 3T1
Tel: (905) 672-9129
Fax: (905) 672-7083
www.aeroquest.ca

Report date: October 2007

TABLE OF CONTENTS

TABLE OF CONTENTS i

LIST OF FIGURES 2

LIST OF MAPS 2

1. INTRODUCTION 1

2. SURVEY AREA 1

3. SURVEY SPECIFICATIONS AND PROCEDURES 3

3.1. Navigation 3
3.2. System Drift 3
3.3. Field QA/QC Procedures 3

4. AIRCRAFT AND EQUIPMENT 4

4.1. Aircraft 4
4.2. Magnetometer 4
4.3. Magnetometer II 5
4.4. Electromagnetic System 5
4.5. AeroDAS Acquisition System 6
4.6. RMS DGR-33 Acquisition System 7
4.7. Airborne Gamma Ray Spectrometer (AGRS) System 8
4.8. Magnetometer Base Station 9
4.9. Radar Altimeter 9
4.10. Video Tracking and Recording System 9
4.11. GPS Navigation System 10
4.12. Digital Acquisition System 10

5. PERSONNEL 10

6. DELIVERABLES 11

6.1. Hardcopy Deliverables 11
6.2. Digital Deliverables 11
6.2.1. Final Database of Survey Data (.GDB, .XYZ) 11
6.2.2. Geosoft Grid files (.GRD) 11
6.2.3. Digital Versions of Final Maps (.MAP, .PDF) 12
6.2.4. Free Viewing Software 12
6.2.5. Digital Copy of this Document (.PDF) 12

7. DATA PROCESSING AND PRESENTATION 12

7.1. Base Map 12
7.2. Flight Path & Terrain Clearance 13
7.3. Electromagnetic Data 13
7.4. Magnetic Data 14
7.5. Radiometric Data 14
7.5.1. Equipment and General Adherence to IAEA Standards 14
7.5.2. Spectral Calibration 14
7.5.3. Data Quality Assurance and Control 14
7.5.4. Dead-time Correction 14
7.5.5. Filtering to Prepare for Background Corrections 15

7.5.6. Cosmic and Aircraft Background *15*
7.5.7. Radon Background *15*
7.5.8. Computation of Effective Height Above Ground Level *15*
7.5.9. Compton Stripping Correction *15*
7.5.10. Altitude Attenuation Correction *16*
7.5.11. Apparent Radioelement Concentrations *16*
7.5.12. Computation of Radioelement Ratios *16*

8. General Comments 16

8.1. Magnetic Response 16
8.2. EM Anomalies 16
8.3. Radiometric response 19

APPENDIX 1: Survey Boundaries 20

APPENDIX 2: Mining Claims 21

APPENDIX 3: Description of Database Fields 23

APPENDIX 4: AEROTEM ANOMALY LISTING 25

APPENDIX 5: AeroTEM Design Considerations 28

APPENDIX 6: AeroTEM Instrumentation Specification Sheet 34

LIST OF FIGURES

Figure 1. Project Area 2
Figure 2. Project Flight Path and Mining Claims 2
Figure 3. Helicopter registration number C-FPTG 4
Figure 4. AeroTEM II EM bird. Arrow indicates the location of the second cesium magnetometer sensor. 5
Figure 5. The magnetometer bird (A) and AeroTEM II EM bird (B) 6
Figure 6. Schematic of Transmitter and Receiver waveforms 6
Figure 7. AeroTEM II Instrument Rack., including AeroDAS and RMS DGR-33 systems, AeroTEM power supply, data acquisition computer and AG-NAV2 navigation system. 8
Figure 8. Aeroquest AGRS system. A. AGRS Sensor (Crystal Pack), B. Data acquisition computer 9
Figure 9. Digital video camera typical mounting location. 10
Figure 10. AeroTEM response to a 'thin' vertical conductor 17
Figure 11. AeroTEM response for a 'thick' vertical conductor. 18
Figure 12. AeroTEM response over a 'thin' dipping conductor. 18

LIST OF MAPS

- TMI – Coloured Total Magnetic Intensity (TMI) with line contours and EM anomaly symbols.
- ZOFF1 – AeroTEM Z1 Off-time with line contours and EM anomaly symbols.
- EM – AeroTEM off-time profiles Z3 – Z15 and EM anomaly symbols.
- TDR – Tilt Derivative of TMI with EM anomaly symbols.
- ThKRAD – Gamma Ray Spectrometer, Equivalent Thorium/Potassium Ratio (eTh/K%)
- TCRAD – Gamma Ray Spectrometer, Natural Air Absorbed Dose Rate

1. INTRODUCTION

This report describes a helicopter-borne geophysical survey carried out on behalf of Laramide Resources Ltd. for their Lara Project, Vancouver Island, British Columbia.

The principal geophysical sensor is Aeroquest's exclusive AeroTEM II (Bravo) time domain helicopter electromagnetic system which is employed in conjunction with a high-sensitivity caesium vapour magnetometer. The secondary sensor was Aeroquest's Airborne Gamma Ray Spectrometer (AGRS) system. The AGRS system utilizes four (4) downward looking NaI crystals used as the main gamma-ray sensors and one upward looking crystal for monitoring non-geologic sources. Ancillary equipment includes a real-time differential GPS navigation system, radar altimeter, video recorder, and a base station magnetometer. Full-waveform streaming EM data is recorded at 36,000 samples per second. The streaming data comprise the transmitted waveform, and the X component and Z component of the resultant field at the receivers. A secondary acquisition system (RMS) records the ancillary data.

The total survey coverage is 500.1 line-km, of which 477.8 line-km fell within the defined project area (Appendix 1). Survey flight direction was NNE-SSW (15º) and flight spacing was 100 and 200m. The survey flying described in this report took place from September 22-26, 2007. This report describes the survey logistics, the data processing, presentation, and provides the specifications of the survey.

2. SURVEY AREA

The Project area (Figure 1) is located in the southeast section of Vancouver Island approximately 35 km south of Nanaimo and 20 km northwest of Duncan. The survey comprised a single area (53 km²) made up of 4 adjoining blocks (Blocks A,B,C,D). Project terrain is mountainous ranging from 400-1200m. Accessibility is good, the project area is surrounded by road and rail.

There are 70 mining claims in the project area (Figure 2) with Laramide Resources Ltd. holding most of the ground in the survey area (see Appendix 2 for full details)

The base of survey operations was at Nanaimo.

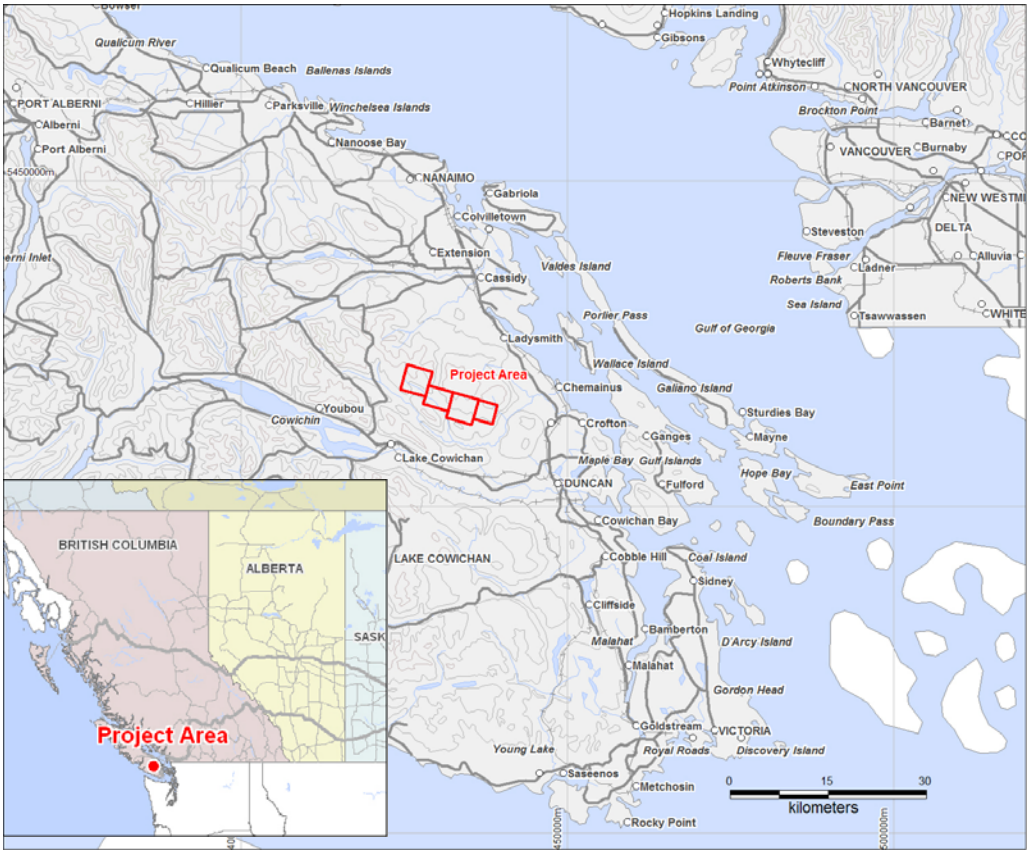

Figure 1. Project Area

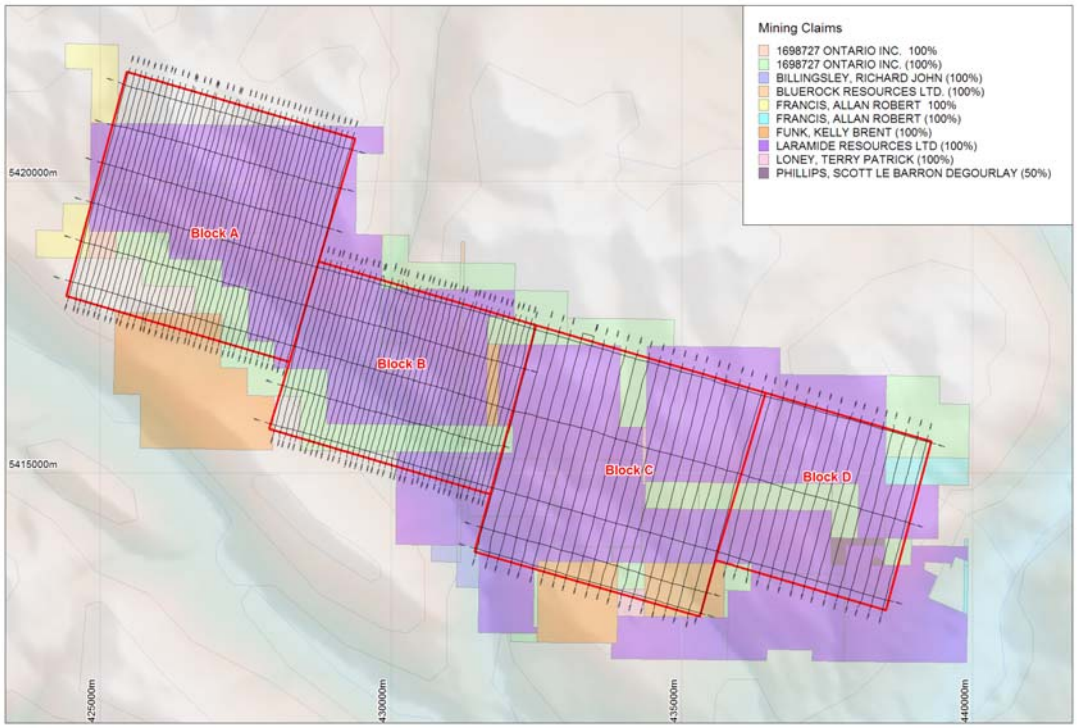

Figure 2. Project Flight Path and Mining Claims

3. SURVEY SPECIFICATIONS AND PROCEDURES

The survey specifications are summarised in the following table:

Project Name	Line Spacing (metres)	Line Direction	Survey Coverage (line-km)	Date flown
Lara	100 & 200	NNE-SSW (15º)	477.8	September 22 – 26, 2007

Table 1. Survey specifications summary

The survey coverage was calculated by adding up the along-line distance of the survey lines and control (tie) lines as presented in the final Geosoft database. The survey was flown with a line spacing of 100 metres for Block A and B and 200 metres for Block C and D. The control (tie) lines were flown perpendicular to the survey lines with a spacing of 1000 and 2000 metres.

The nominal EM bird terrain clearance is 30 metres, but can be higher in more rugged terrain due to safety considerations and the capabilities of the aircraft. The magnetometer sensor is mounted in a smaller bird connected to the tow rope 17 metres above the EM bird and 21 metres below the helicopter (Figure 4). A second magnetometer is installed on the tail of the EM bird. Nominal survey speed over relatively flat terrain is 75 km/hr and is generally lower in rougher terrain. Scan rates for ancillary data acquisition is 0.1 second for the magnetometer and altimeter, and 0.2 second for the GPS determined position. The EM data is acquired as a data stream at a sampling rate of 36,000 samples per second and is processed to generate final data at 10 samples per second. The 10 samples per second translate to a geophysical reading about every 1.5 to 2.5 metres along the flight path.

3.1. NAVIGATION

Navigation is carried out using a GPS receiver, an AGNAV2 system for navigation control, and an RMS DGR-33 data acquisition system which records the GPS coordinates. The x-y-z position of the aircraft, as reported by the GPS, is recorded at 0.2 second intervals. The system has a published accuracy of under 3 metres. A recent static ground test of the Mid-Tech WAAS GPS yielded a standard deviation in x and y of under 0.6 metres and for z under 1.5 metres over a two-hour period.

3.2. SYSTEM DRIFT

Unlike frequency domain electromagnetic systems, the AeroTEM II system has negligible drift due to thermal expansion. The operator is responsible for ensuring the instrument is properly warmed up prior to departure and that the instruments are operated properly throughout the flight. The operator maintains a detailed flight log during the survey noting the times of the flight and any unusual geophysical or topographic features. Each flight included at least two high elevation 'background' checks. During the high elevation checks, an internal 5 second wide calibration pulse in all EM channels was generated in order to ensure that the gain of the system remained constant and within specifications.

3.3. FIELD QA/QC PROCEDURES

On return of the pilot and operator to the base, usually after each flight, the AeroDAS streaming EM data and the RMS data are carried on removable hard drives and FlashCards, respectively and transferred to the data processing work station. At the end of each day, the base station magnetometer data on FlashCard is retrieved from the base station unit.

Data verification and quality control includes a comparison of the acquired GPS data with the flight plan; verification and conversion of the RMS data to an ASCII format XYZ data file; verification of the base station magnetometer data and conversion to ASCII format XYZ data; and loading, processing and conversion of the steaming EM data from the removable hard drive. All data is then merged to an ASCII XYZ format file which is then imported to an Oasis database for further QA/QC and for the production of preliminary EM, magnetic contour, and flight path maps.

Survey lines which show excessive deviation from the intended flight path are re-flown. Any line or portion of a line on which the data quality did not meet the contract specification was noted and reflown.

4. AIRCRAFT AND EQUIPMENT

4.1. AIRCRAFT

A Eurocopter (Aerospatiale) AS350B2 "A-Star" helicopter - registration C-FPTG was used as survey platform. The helicopter was owned and operated by Hi-Wood Helicopters, Calgary, Alberta. Installation of the geophysical and ancillary equipment was carried out by Aeroquest Limited personnel in conjunction with a licensed aircraft. The survey aircraft was flown at a nominal terrain clearance of 220 ft (65 metres).

Figure 3. Helicopter registration number C-FPTG

4.2. MAGNETOMETER

The AeroTEM II airborne survey system employs the Geometrics G-823A caesium vapour magnetometer sensor installed in a two metre towed bird airfoil attached to the main tow line, 17 metres below the helicopter (Figure 4). The sensitivity of the magnetometer is 0.001 nanoTesla at a 0.1 second sampling rate. The nominal ground clearance of the magnetometer bird is 51 metres (170 ft.). The magnetic data is recorded at 10 Hz by the RMS DGR-33.

4.3. MAGNETOMETER II

In addition to the main magnetometer bird on the main tow line, the AeroTEM II system includes an additional G-828A magnetometer installed on the tail of the EM bird (Figure 4). The sensor is located 37 metres below the helicopter and has a superior nominal terrain clearance of 31 m. Data is recorded at 300 samples a second and down sampled to 10 Hz by the AeroDAS acquisition system.

Figure 4. AeroTEM II EM bird. Arrow indicates the location of the second cesium magnetometer sensor.

4.4. ELECTROMAGNETIC SYSTEM

The electromagnetic system is an Aeroquest AeroTEM II time domain towed-bird system (Figure 4, Figure 5). The current AeroTEM II transmitter dipole moment is 38.8 kNIA. The AeroTEM bird is towed 38 metres (125 ft) below the helicopter. More technical details of the system may be found in Appendix 4.

The wave-form is triangular with a symmetric transmitter on-time pulse of 1.10 ms and a base frequency of 150 Hz (Figure 5). The current alternates polarity every on-time pulse. During every Tx on-off cycle (300 per second), 120 contiguous channels of raw X and Z component (and a transmitter current monitor, itx) of the received waveform are measured. Each channel width is 27.778 microseconds starting at the beginning of the transmitter pulse. This 120 channel data is referred to as the raw streaming data. The AeroTEM system has two separate EM data recording streams, the conventional RMS DGR-33 and the AeroDAS system which records the full waveform (Figure 6).

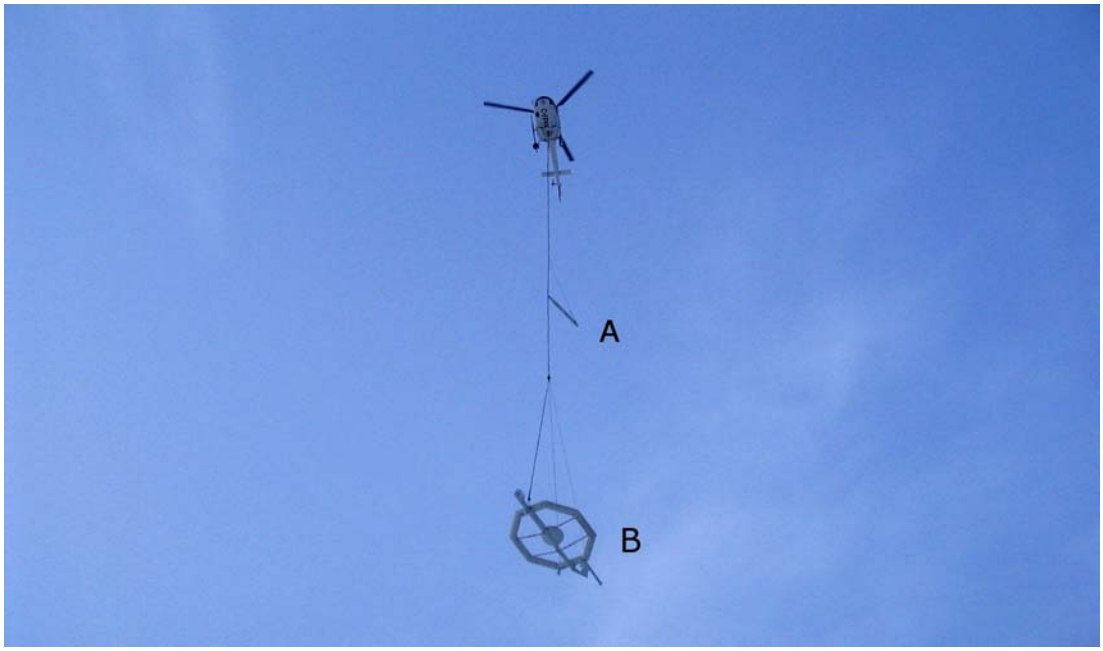

Figure 5. The magnetometer bird (A) and AeroTEM II EM bird (B)

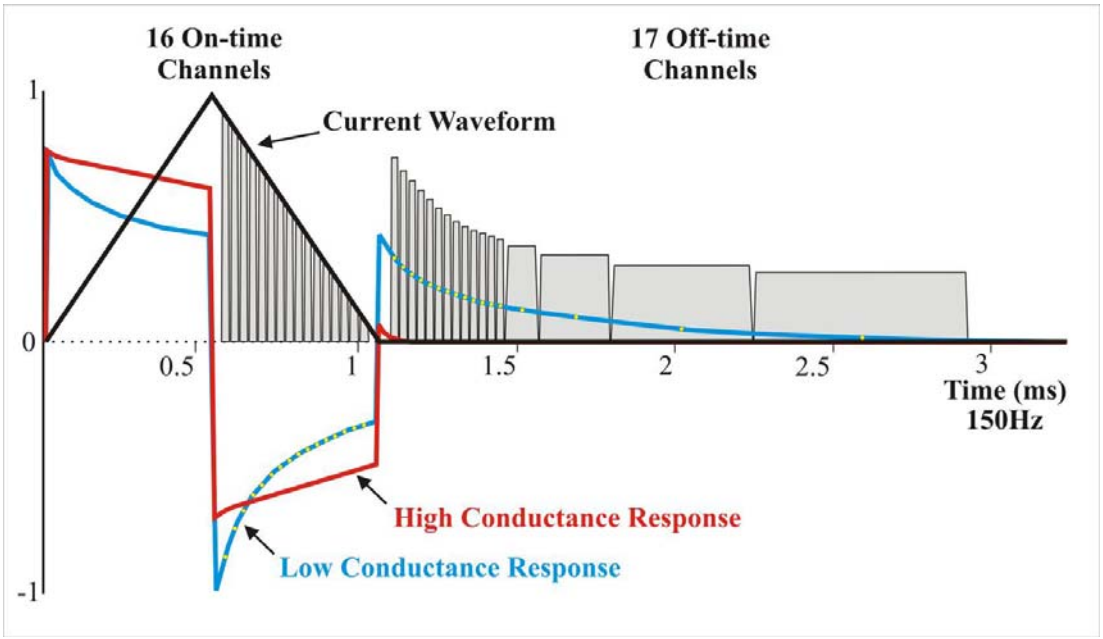

Figure 6. Schematic of Transmitter and Receiver waveforms

4.5. AERODAS ACQUISITION SYSTEM

The 120 channels of raw streaming data are recorded by the AeroDAS acquisition system (Figure 7) onto a removable hard drive. The streaming data are processed post-survey to yield 33 stacked and binned on-time and off-time channels at a 10 Hz sample rate. The timing of the final processed EM channels is described in the following table:

Average TxOn -3.0044 us
Average TxSwitch 583.5513 us
Average TxOff 1127.0493 us

Channel	Sample Range	Time Width (us)	Time Center (us)	Time After TxOn (us)
On1	3 - 3	27.778	69.444	72.449
On2	4 - 4	27.778	97.222	100.227
On3	5 - 5	27.778	125.000	128.004
On4	6 - 6	27.778	152.778	155.782
On5	7 - 7	27.778	180.556	183.560
On6	8 - 8	27.778	208.333	211.338
On7	9 - 9	27.778	236.111	239.115
On8	10 - 10	27.778	263.889	266.893
On9	11 - 11	27.778	291.667	294.671
On10	12 - 12	27.778	319.444	322.449
On11	13 - 13	27.778	347.222	350.227
On12	14 - 14	27.778	375.000	378.004
On13	15 - 15	27.778	402.778	405.782
On14	16 - 16	27.778	430.556	433.560
On15	17 - 17	27.778	458.333	461.338
On16	18 - 18	27.778	486.111	489.116

Channel	Sample Range	Time Width (us)	Time Center (us)	Time After TxOff (us)
Off0	44 - 44	27.778	1208.333	81.284
Off1	45 - 45	27.778	1236.111	109.062
Off2	46 - 46	27.778	1263.889	136.840
Off3	47 - 47	27.778	1291.667	164.617
Off4	48 - 48	27.778	1319.444	192.395
Off5	49 - 49	27.778	1347.222	220.173
Off6	50 - 51	55.556	1388.889	261.840
Off7	52 - 53	55.556	1444.444	317.395
Off8	54 - 55	55.556	1500.000	372.951
Off9	56 - 57	55.556	1555.556	428.506
Off10	58 - 60	83.333	1625.000	497.951
Off11	61 - 63	83.333	1708.333	581.284
Off12	64 - 67	111.111	1805.556	678.506
Off13	68 - 73	166.667	1944.444	817.395
Off14	74 - 81	222.222	2138.889	1011.840
Off15	82 - 94	361.111	2430.556	1303.506
Off16	95 - 114	555.556	2888.889	1761.840

4.6. RMS DGR-33 ACQUISITION SYSTEM

In addition to the magnetics, altimeter and position data, six channels of real time processed off-time EM decay in the Z direction and one in the X direction are recorded by the RMS DGR-33 acquisition system at 10 samples per second and plotted real-time on the analogue chart recorder. These channels are derived by a binning, stacking and filtering procedure on the raw streaming data. The primary use of the RMS EM data (Z1 to Z6, X1) is to provide for real-time QA/QC on board the aircraft.

The channel window timing of the RMS DGR-33 6 channel system is described in the table below.

RMS Channel	Start time (µs)	End time (µs)	Width (µs)	Streaming Channels
Z1, X1	1269.8	1322.8	52.9	48-50
Z2	1322.8	1455.0	132.2	50-54
Z3	1428.6	1587.3	158.7	54-59
Z4	1587.3	1746.0	158.7	60-65
Z5	1746.0	2063.5	317.5	66-77
Z6	2063.5	2698.4	634.9	78-101

Figure 7. AeroTEM II Instrument Rack., including AeroDAS and RMS DGR-33 systems, AeroTEM power supply, data acquisition computer and AG-NAV2 navigation system.

4.7. AIRBORNE GAMMA RAY SPECTROMETER (AGRS) SYSTEM

The Aeroquest AGRS system consists of a GRS410 sensor pack (Figure 4) and a acquisition system designed and manufactured by Pico Envirotec. The sensor pack was installed on the port side basket of the Lama aircraft, and was installed in the cabin of the UH-1 aircraft. The system has 4 downward looking NaI crystals used as the main sensors and 1 upward looking crystal for monitoring non-geologic sources. The system features automatic peak detection and real-time calibration to ensure spectrum stability and a high quality final product. The full

spectrum is recorded (256 or 512 channels) to allow for subsequent noise reduction processing such as NASVD. The data are processed to produce the standard IAGA ROI channels – Total Count, Potassium, Uranium and Thorium. The potassium, and equivalent uranium and thorium concentrations are also derived and ratios of these concentrations are computed to enhance the interpretation of the survey results.

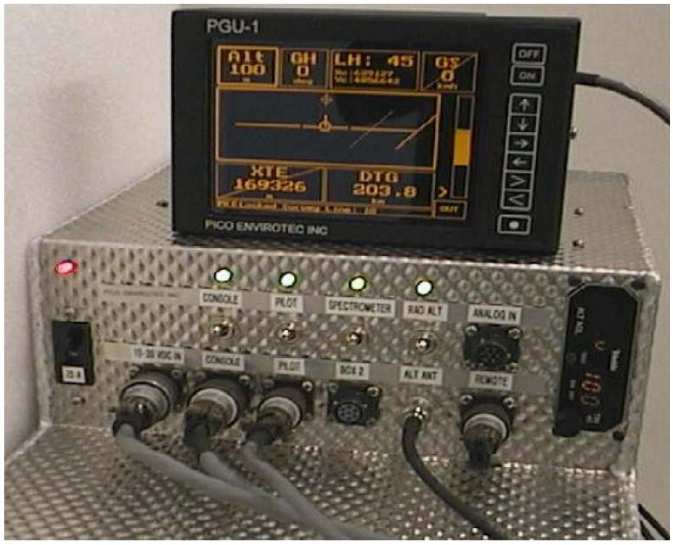

Figure 8. Aeroquest AGRS system. A. AGRS Sensor (Crystal Pack), B. Data acquisition computer.

4.8. MAGNETOMETER BASE STATION

The base magnetometer was a Geometrics G-859 cesium vapour magnetometer system with integrated GPS. Data logging and UTC time synchronisation was carried out within the magnetometer, with the GPS providing the timing signal. The data logging was configured to measure at 1.0 second intervals. Digital recording resolution was 0.001 nT. The sensor was placed on a tripod in an area of low magnetic gradient and free of cultural noise sources. A continuously updated display of the base station values was available for viewing and regularly monitored to ensure acceptable data quality and diurnal variation.

4.9. RADAR ALTIMETER

A Terra TRA 3500/TRI-30 radar altimeter is used to record terrain clearance. The antenna was mounted on the outside of the helicopter beneath the cockpit. Therefore, the recorded data reflect the height of the helicopter above the ground. The Terra altimeter has an altitude accuracy of +/- 1.5 metres.

4.10. VIDEO TRACKING AND RECORDING SYSTEM

A high resolution digital colour 8 mm video camera is used to record the helicopter ground flight path along the survey lines. The video is digitally annotated with GPS position and time and can be used to verify ground positioning information and cultural causes of anomalous geophysical responses.

Figure 9. Digital video camera typical mounting location.

4.11. GPS NAVIGATION SYSTEM

The navigation system consists of an Ag-Nav Incorporated AG-NAV2 GPS navigation system comprising a PC-based acquisition system, navigation software, a deviation indicator in front of the aircraft pilot to direct the flight, a full screen display with controls in front of the operator, a Mid-Tech RX400p WAAS-enabled GPS receiver mounted on the instrument rack and an antenna mounted on the magnetometer bird. WAAS (Wide Area Augmentation System) consists of approximately 25 ground reference stations positioned across the United States that monitor GPS satellite data. Two master stations located on the east and west coasts collect data from the reference stations and create a GPS correction message. This correction accounts for GPS satellite orbit and clock drift plus signal delays caused by the atmosphere and ionosphere. The corrected differential message is then broadcast through one of two geostationary satellites, or satellites with a fixed position over the equator. The corrected position has a published accuracy of less than 3 metres.

Survey co-ordinates are set up prior to the survey and the information is fed into the airborne navigation system. The co-ordinate system employed in the survey design was WGS84 [World] using the UTM zone 10N projection. The real-time differentially corrected GPS positional data was recorded by the RMS DGR-33 in geodetic coordinates (latitude and longitude using WGS84) at 0.2 s intervals.

4.12. DIGITAL ACQUISITION SYSTEM

The AeroTEM received waveform sampled during on and off-time at 120 channels per decay, 300 times per second, was logged by the proprietary AeroDAS data acquisition system. The channel sampling commences at the start of the Tx cycle and the width of each channel is 27.778 microseconds. The streaming data was recorded on a removable hard-drive and was later backed-up onto DVD-ROM from the field-processing computer.

The RMS Instruments DGR33A data acquisition system was used to collect and record the analogue data stream, i.e. the positional and secondary geophysical data, including processed 6 channel EM, magnetics, radar altimeter, GPS position, and time. The data was recorded on 128 Mb capacity FlashCard. The RMS output was also directed to a thermal chart recorder.

5. PERSONNEL

The following Aeroquest personnel were involved in the project:

- Manager of Operations: Bert Simon
- Manager of Data Processing: Jonathan Rudd
- Field Data Processor: Emilio Schein
- Field Operator: Gabriel Ganier
- Data processing, interpretation, mapping and reporting: Gord Smith, Eric Steffler, Marion Bishop
- The survey pilot, Ted Slavin, was employed directly by the helicopter operator – Hi-Wood Helicopters.

6. DELIVERABLES

6.1. HARDCOPY DELIVERABLES

The report includes a set of ten 1:10,000 maps. The survey area is covered by a two map plates and five geophysical data products are delivered as listed below:

- TMI – Coloured Total Magnetic Intensity (TMI) with line contours and EM anomaly symbols.
- ZOFF1 – AeroTEM Z1 Off-time with line contours and EM anomaly symbols.
- EM – AeroTEM off-time profiles Z3 – Z15 and EM anomaly symbols.
- TDR – Tilt Derivative of TMI with EM anomaly symbols.
- ThKRAD – Gamma Ray Spectrometer, Equivalent Thorium/Potassium Ratio (eTh/K%)
- TCRAD – Gamma Ray Spectrometer, Natural Air Absorbed Dose Rate

The coordinate/projection system for the maps is NAD83 – UTM Zone 10N. For reference, the latitude and longitude in WGS84 are also noted on the maps.

All the maps show flight path trace, skeletal topography, and conductor picks represented by an anomaly symbol classified according to calculated off-time conductance. The anomaly symbol is accompanied by postings denoting the calculated off-time conductance, a thick or thin classification and an anomaly identifier label. The anomaly symbol legend is given in the margin of the maps.

6.2. DIGITAL DELIVERABLES

6.2.1. Final Database of Survey Data (.GDB, .XYZ)

The geophysical profile data is archived digitally in a Geosoft GDB binary format database. A description of the contents of the individual channels in the database can be found in Appendix 2. A copy of this digital data is archived at the Aeroquest head office in Mississauga.

6.2.2. Geosoft Grid files (.GRD)

Levelled Grid products used to generate the geophysical map images.

- Total Magnetic Intensity lower sensor (MagL)
- Total Magnetic Intensity lower sensor (MagU)
- AeroTEM Z Offtime Channel 1 (Zoff1_s)
- Digital terrain Model (DTMF.grd)

- Tilt Derivative of TMI (TDRF)
- Gamma Ray Spectrometer – Natural Air Absorbed Dose Rate (TCcoorF)
- Gamma Ray Spectrometer – Equivalent Thorium/Potassium Ratio (eTHK_RATIOF)
- Gamma Ray Spectrometer – Equivalent Uranium/Thorium Ratio (eUeK_RATIOF)
- Gamma Ray Spectrometer – eU/%K concentration (eUK_RATIOF)
- Gamma Ray Spectrometer – Potassium (Kcorrf)
- Gamma Ray Spectrometer – Thorium (ThcorrF)
- Gamma Ray Spectrometer – Uranium (UcorrfF)
- Gamma Ray Spectrometer – Exposure rate (TCexpF)

6.2.3. Digital Versions of Final Maps (.MAP, .PDF)

Map files in Geosoft .map and Adobe PDF format.

6.2.4. Free Viewing Software

- Geosoft Oasis Montaj Viewing Software
- Adobe Acrobat Reader

6.2.5. Digital Copy of this Document (.PDF)

7. DATA PROCESSING AND PRESENTATION

All in-field and post-field data processing was carried out using Aeroquest proprietary data processing software and Geosoft Oasis Montaj software. Maps were generated using 42-inch wide Hewlett Packard ink-jet plotters.

7.1. BASE MAP

The geophysical maps accompanying this report are based on positioning in the WGS84 datum. The survey geodetic GPS positions have been projected using the Universal Transverse Mercator projection in Zone 10 North. A summary of the map datum and projection specifications is given following:

- Ellipse: GRS 1980
- Ellipse major axis: 6378137m eccentricity: 0.081819191
- Datum: North American 1983 - Canada Mean
- Datum Shifts (x,y,z) : 0, 0, 0 metres
- Map Projection: Universal Transverse Mercator Zone 10 (Central Meridian 123ºW)
- Central Scale Factor: 0.9996
- False Easting, Northing: 500,000m, 0m

For reference, the latitude and longitude in WGS84 are also noted on the maps.

The background vector topography supplied by the client and the background shading was derived from NASA Shuttle Radar Topography Mission (SRTM) 90 metres resolution DEM data.

7.2. FLIGHT PATH & TERRAIN CLEARANCE

The position of the survey helicopter was directed by use of the Global Positioning System (GPS). Positions were updated five times per second (5 Hz) and expressed as WGS84 latitude and longitude calculated from the raw pseudo range derived from the C/A code signal. The instantaneous GPS flight path, after conversion to UTM co-ordinates, is drawn using linear interpolation between the x/y positions. The terrain clearance was maintained with reference to the radar altimeter. The raw Digital Terrain Model (DTM) was derived by taking the GPS survey elevation and subtracting the radar altimeter terrain clearance values. The calculated topography elevation values are relative and are not tied in to surveyed geodetic heights.

Each flight included at least two high elevation 'background' checks. These high elevation checks are to ensure that the gain of the system remained constant and within specifications.

7.3. ELECTROMAGNETIC DATA

The raw streaming data, sampled at a rate of 36,000 Hz (120 channels, 300 times per second) was reprocessed using a proprietary software algorithm developed and owned by Aeroquest Limited. Processing involves the compensation of the X and Z component data for the primary field waveform. Coefficients for this compensation for the system transient are determined and applied to the stream data. The stream data are then pre-filtered, stacked, binned to the 33 on and off-time channels and checked for the effectiveness of the compensation and stacking processes. The stacked data is then filtered, levelled and split up into the individual line segments. Further base level adjustments may be carried out at this stage. The filtering of the stacked data is designed to remove or minimize high frequency noise that can not be sourced from the geology.

The final field processing step was to merge the processed EM data with the other data sets into a Geosoft GDB file. The EM fiducial is used to synchronize the two datasets. The processed channels are merged into 'array format; channels in the final Geosoft database as Zon, Zoff, Xon, and Xoff.

Apparent bedrock EM anomalies were interpreted with the aid of an auto-pick from positive peaks and troughs in the off-time Z channel responses correlated with X channel responses. The auto-picked anomalies were reviewed and edited by a geophysicist on a line by line basis to discriminate between thin and thick conductor types. Anomaly picks locations were migrated and removed as required. This process ensures the optimal representation of the conductor centres on the maps.

At each conductor pick, estimates of the off-time conductance have been generated based on a horizontal plate source model for those data points along the line where the response amplitude is sufficient to yield an acceptable estimate. Some of the EM anomaly picks do not display a Tau value; this is due to the inability to properly define the decay of the conductor usually because of low signal amplitudes. Each conductor pick was then classified according to a set of seven ranges of calculated off-time conductance values. For high conductance sources, the on-time conductance values may be used, since it provides a more accurate measure of high-conductance sources. Each symbol is also given an identification letter label, unique to each flight line. Conductor picks that did not yield an acceptable estimate of off-time conductance due to a low amplitude response were classified as a low conductance source. Please refer to the anomaly symbol legend located in the margin of the maps.

7.4. MAGNETIC DATA

Prior to any levelling the magnetic data was subjected to a lag correction of -0.1 seconds and a spike removal filter. The filtered aeromagnetic data were then corrected for diurnal variations using the magnetic base station and the intersections of the tie lines. No corrections for the regional reference field (IGRF) were applied. The corrected profile data were interpolated on to a grid using a random grid technique with a grid cell size of 30 metres. The final levelled grid provided the basis for threading the presented contours which have a minimum contour interval of 5 nT.

7.5. RADIOMETRIC DATA

7.5.1. Equipment and General Adherence to IAEA Standards

Aeroquest Limited generally adopts the standards for airborne gamma-ray spectrometry (the radiometric method) as laid out in the IAEA Technical Report 323 – Airborne Gamma-Ray Spectrometry Surveying.

7.5.2. Spectral Calibration

When calibrated (with thorium source about once a year) linearity of the each detector is measured and linearity correction coefficients are calculated. When operating in real time (collecting data), the linearity of each detector is mathematically corrected for each measurement. Individual detector tracking (tuning) and linearity correction provide better fit of the individual spectra that are being summed and therefore a sharper (better resolution) spectrum is obtained.

Calibration of the 5 detectors was carried out on September 22, 2007 as follows:

Crystal	S/N	Cs resolution (%)
1	SAM359	7.9
2	SAM358	8.4
3	SAM355	8.4
4	SAM357	8.4
5	SAM356	9.1

7.5.3. Data Quality Assurance and Control

The spectrometer data are referenced to the other ancillary data sets using the Pico Envirotec data acquisition system (Figure 4). After each flight, preliminary ROI channels are generated and profiles are then plotted from the digital data to check for any missing data, spikes or data corrupted by other noise sources. Where necessary, the data are corrected or flagged for re-flight depending on the severity or duration of the noise.

7.5.4. Dead-time Correction

Generally, the first data reduction step for radiometric data is dead-time correction. Because the GRS-10 dead time is virtually nil, this correction is only applied where the total count rates are extremely high. Dead-time correction is made to each window using the expression N=n/(1-T) where N is the corrected count; n is the raw recorded count; and T is the dead-time.

7.5.5. Filtering to Prepare for Background Corrections

The radar altimeter data are filtered in order to ensure that no noise sources from the altimeter data are introduced to the radiometric data processing. The upward looking data are also filtered to improve the count statistics. A typical filter width ranges from 10 to 20s. In order to establish radon background levels from the upward-looking detector data, temporary heavily filtered upward and downward looking uranium and downward looking thorium data are utilized. The original unfiltered data are, of course, retained. All filtering will be carried out in consultation with the Client Representative if requested by the Client.

7.5.6. Cosmic and Aircraft Background

Cosmic and aircraft background expressions are determined for each spectral window as described in chapter 4 of the IAEA Technical Report 323. The general form of these expressions is N = a + bC, where N is the combined cosmic and aircraft background for each window; a is the aircraft background in the window; C is the cosmic channel count; and b is the cosmic stripping factor for the window.

The expressions are evaluated for each ROI window for each sample and used as a subtractive correction for the data.

7.5.7. Radon Background

Correction of the data for variations in background due to radon is a multi-step process. First, test flights at various elevations over water are carried out in the field to establish the contribution of atmospheric radon to the ROI windows. A least squares analysis of the data from these test flights yields the constants for equations 4.9 to 4.12 (IAEA Report 323). Second, the response of the upward looking detector to radiation from the ground is established. Here a departure from the IAEA Report has been recommended by Grasty and Hovgaard (1996). The expression for the radon component in the downward looking uranium window is given by Ur =(u – a1U – a2T + a2bT – bu)/(au – a1 – a2aT) (see Eq. 4.3 – IAEA 323) where, Ur is the radon background detected in the downward U window; u is the measured count in the upward uranium window; U is the measured count in the downward uranium window; T is the measured count in the downward thorium window; a1, a2, au and aT are proportionality factors; and bu and bT are constants determined experimentally. Using a1 or a2 (see above) in this equation will result in a good estimate of Ur permitting correction of the other ROI windows.

Survey altitude test data will be collected and used to establish atmospheric background and calibrate the upward and downward looking detector systems. Variations in count rates due to soil moisture content and altimeter variations can largely be overcome by a normalization procedure using the thorium count. The procedure correlates the thorium count to the uranium count assuming the contribution to each ROI from the ground is proportional.

7.5.8. Computation of Effective Height Above Ground Level

Radar altimeter data are used in adjusting the stripping ratios for altitude and to carry out the height attenuation corrections. They are then converted to effective height (he) at STP by the expression he = (h * 273.15)/(T + 273.15)* (P/1013), where h is the observed radar altitude; T is the temperature in degrees C; and P is the barometric pressure in mbar.

7.5.9. Compton Stripping Correction

The stripping ratios α, β, γ, a, b and g are determined during tests over calibration pads. The principal ratios a, β and g should be adjusted for temperature, pressure and altitude (above ground) before stripping is carried out. These stripping ratios are used to remove the

contribution in each of the three ROI windows from higher energy sources, leaving only the contribution from potassium, uranium and thorium.

7.5.10. Altitude Attenuation Correction

The altitude attenuation correction corrects the data in each of the ROI windows for the effects of altitude. The count rates decrease exponentially with altitude and therefore the counts are corrected to a constant altimeter datum at the nominal survey height of 30m.

7.5.11. Apparent Radioelement Concentrations

The corrected count rate data can be converted to estimate the ground concentrations of each of the three radioelements, potassium, uranium and thorium. The procedure assumes an infinite horizontal slab source geometry with a uniform radioelement concentration. The calculation assumes radioactive equilibrium in the U and Th decay series. Therefore the U and Th concentrations are assigned as equivalent concentrations using the nomenclature eU and eTh.

An estimate of the air absorbed dose rate can be made from the apparent concentrations, K%, eU ppm and eTh ppm.

7.5.12. Computation of Radioelement Ratios

Standard ratioing of the three radioelements (eU/eTh, eU/K and eTh/K) can be carried out and presented in profile or plan map form. In order to ensure statistical confidence in generating these ratios, we generally take the following precautions:

- Reject all data point where the apparent potassium concentration is less than 0.25% as these measurements are likely taken over water.
- Carry out cumulative summing along the survey line of each radioelement, rejecting areas where the summation does not exceed a certain threshold value (usually 10 counts for both numerator and denominator).
- Compute the ratios using the cumulative sums.

8. GENERAL COMMENTS

The survey was successful in mapping the magnetic and conductive properties of the geology throughout the survey area. Below is a brief interpretation of the results. For a detailed interpretation please contact Aeroquest Limited.

8.1. MAGNETIC RESPONSE

The magnetic data provide a high resolution map of the distribution of the magnetic mineral content of the survey area. This data can be used to interpret the location of geological contacts and other structural features such as faults and zones of magnetic alteration. The sources for anomalous magnetic responses are generally thought to be predominantly magnetite because of the relative abundance and strength of response (high magnetic susceptibility) of magnetite over other magnetic minerals such as pyrrhotite.

8.2. EM ANOMALIES

The EM anomalies on the maps are classified by conductance (as described earlier in the report) and also by the thickness of the source. A thin, vertically orientated source produces a double peak anomaly in the z-component response and a positive to negative crossover in the x-component response (Figure 8). For a vertically orientated thick source (say, greater than

10 metres), the response is a single peak in the z-component response and a negative to positive crossover in the x-component response (Figure 9). Because of these differing responses, the AeroTEM system provides discrimination of thin and thick sources and this distinction is indicated on the EM anomaly symbols (N = thin and K = thick). Where multiple, closely spaced conductive sources occur, or where the source has a shallow dip, it can be difficult to uniquely determine the type (thick vs. thin) of the source (Figure 10). In these cases both possible source types may be indicated by picking both thick and thin response styles. For shallow dipping conductors the 'thin' pick will be located over the edge of the source, whereas the 'thick' pick will fall over the downdip 'heart' of the anomaly.

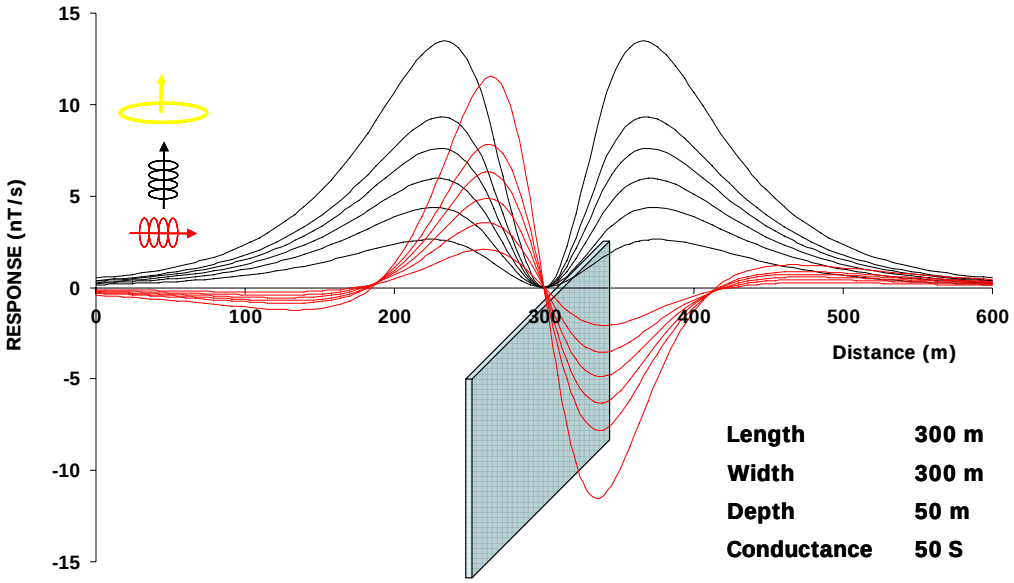

Figure 10. AeroTEM response to a 'thin' vertical conductor.

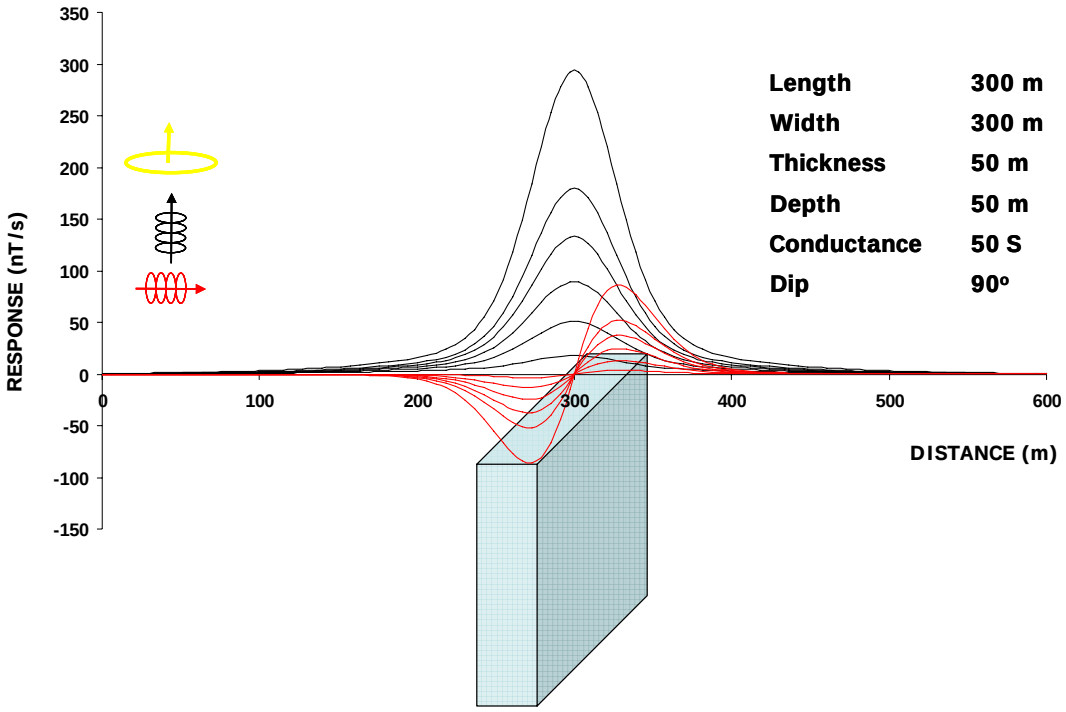

Figure 11. AeroTEM response for a 'thick' vertical conductor.

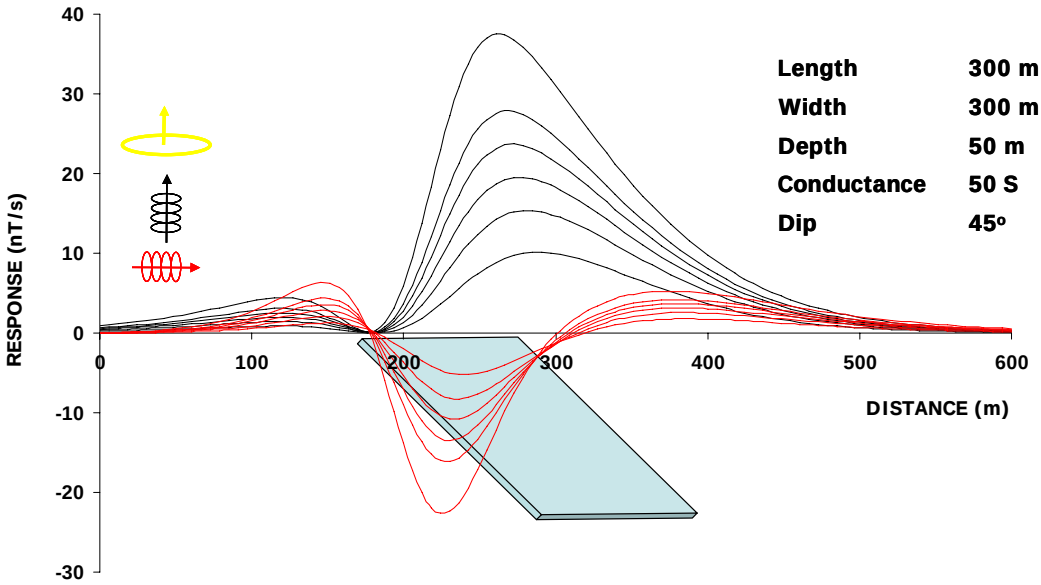

Figure 12. AeroTEM response over a 'thin' dipping conductor.

All cases should be considered when analyzing the interpreted picks and prioritizing for follow-up. Specific anomalous responses which remain as high priority should be subjected to numerical modeling prior to drill testing to determine the dip, depth and probable geometry of the source.

8.3. RADIOMETRIC RESPONSE

The radiometric data indicate the apparent concentrations of potassium, uranium, and thorium in the rocks and soils at the very near surface. The depth of measurement is on the order of 30 cm and the vast majority of information comes from a circular area with a diameter equal to twice the survey height.

Within different lithologies, concentrations of potassium, uranium and thorium tend to diagnostically vary. The radiometric data provide a remote measurement of these concentrations and can be used to characterise the lithology and distribution of the overlying geologic materials.

The dose rate and thorium-potassium (eTh/K) were selected fro presentation on the final maps. The Natural Air Absorbed Dose Rate can be though of as the total radioactivity from natural sources. It is a combined measure of K, U, and Th gamma ray energies. Measurement units are in nanoGrays per hour (nGy/h).

The eTh/K ratio was selected since it can be a sensitive indicator of potassium alteration associated with mineralization. Thorium enrichment generally does not accompany potassium enrichment during the hydrothermal alteration processes. Therefore a ratio of these signals provide excellent distinction between anomalies associated with alteration and anomalies related to normal lithological variations (i.e. felsic rocks). Note that potassic alteration zones would be expected to appear as lows in the eTh/K grid.

Respectfully submitted,

Gord Smith
Aeroquest Limited
October, 2007

Reviewed By:

Doug Garrie
Aeroquest Limited
October, 2007

APPENDIX 1: SURVEY BOUNDARIES

The following table presents the Lara block boundaries. All geophysical data presented in this report have been windowed to 100m outside these outlines. X and Y positions are in NAD83 UTM Zone 10N.

100 m spacing (Blocks A and B)

X	Y
425449.59	5421875.67
429380.79	5420728.76
428757.82	5418614.97
432493.50	5417526.07
431708.16	5414637.97
427902.04	5415756.40
428250.00	5416891.92
424415.24	5418027.79

200 m spacing (Blocks C and D)

X	Y
425449.6	5421875.7
429380.8	5420728.8
428757.8	5418615.0
432493.5	5417526.1
439296.1	5415538.3
438514.9	5412641.6
435579.6	5413506.3
435314.3	5412536.4
431439.4	5413651.5
431708.2	5414638.0
427902.0	5415756.4
428250.0	5416891.9
424415.2	5418027.8

APPENDIX 2: MINING CLAIMS

Taken from Government of British Columbia Mineral Titles Online, October, 2007

Tenure Number	Claim Name	Owner	Date Due	Mining Division
260341	FANG	Laramide Resources Ltd	2010/jan/21	VICTORIA
260342	SILVER 1	Laramide Resources Ltd	2010/jan/21	VICTORIA
260343	SILVER 2	Laramide Resources Ltd	2010/jan/21	VICTORIA
260344	SOLLY	Laramide Resources Ltd	2010/jan/21	VICTORIA
260345	TL	Laramide Resources Ltd	2010/jan/21	VICTORIA
260395		Laramide Resources Ltd	2010/jan/21	VICTORIA
260419	UGLY	Laramide Resources Ltd	2010/jan/21	VICTORIA
260420	WIMP	Laramide Resources Ltd	2010/jan/21	VICTORIA
260420	WIMP	Laramide Resources Ltd	2010/jan/21	VICTORIA
260420	WIMP	Laramide Resources Ltd	2010/jan/21	VICTORIA
260421	NERO	Laramide Resources Ltd	2010/jan/21	VICTORIA
260521	JENNIE	Laramide Resources Ltd	2010/jan/21	VICTORIA
260607	COR 1 FR.	Laramide Resources Ltd	2010/jan/21	VICTORIA
260608	COR 2 FR.	Laramide Resources Ltd	2010/jan/21	VICTORIA
260609	COR 3 FR.	Laramide Resources Ltd	2010/jan/21	VICTORIA
260610	COR 4 FR.	Laramide Resources Ltd	2010/jan/21	VICTORIA
260611	COR 5 FR.	Laramide Resources Ltd	2010/jan/21	VICTORIA
260612	COR 6 FR.	Laramide Resources Ltd	2010/jan/21	VICTORIA
260613	COR 7 FR.	Laramide Resources Ltd	2010/jan/21	VICTORIA
260624	TOUCHE	Laramide Resources Ltd	2010/jan/21	VICTORIA
260625	CAVITY	Laramide Resources Ltd	2010/jan/21	VICTORIA
260626	PLANT	Laramide Resources Ltd	2010/jan/21	VICTORIA
260627	FACE	Laramide Resources Ltd	2010/jan/21	VICTORIA
260627	FACE	Laramide Resources Ltd	2010/jan/21	VICTORIA
260627	FACE	Laramide Resources Ltd	2010/jan/21	VICTORIA
397311	LADY	Bluerock Resources Ltd.	2009/dec/31	NANAIMO
512321		Laramide Resources Ltd	2010/jan/21	
512325	LADY 6	Laramide Resources Ltd	2010/jan/21	
512327	LADY 7	Laramide Resources Ltd	2010/jan/21	
512331	LADY 8	Laramide Resources Ltd	2010/jan/21	
512331	LADY 8	Laramide Resources Ltd	2010/jan/21	
512331	LADY 8	Laramide Resources Ltd	2010/jan/21	
512355	LADY 9	Laramide Resources Ltd	2010/jan/21	
512358	LADY 9	Laramide Resources Ltd	2010/jan/21	
512359		Laramide Resources Ltd	2010/jan/21	
512362		Laramide Resources Ltd	2010/jan/21	
513291		Francis, Allan Robert	2007/nov/07	
516963		Francis, Allan Robert	2007/oct/31	
533072	HOLYOAK	Francis, Allan Robert	2007/nov/20	
543043	LE BARON	Phillips, Scott Le Barron Degourlay	2009/oct/11	
549799	TL LARA 07	Loney, Terry Patrick	2008/jan/18	
549807	TL LARA 07A	Loney, Terry Patrick	2008/jan/18	
555207	COW 2	Funk, Kelly Brent	2008/mar/28	
566136	LARA 2	Funk, Kelly Brent	2008/sep/18	
566137	LARA 1	Funk, Kelly Brent	2008/sep/18	
566138	LARA 4	Funk, Kelly Brent	2008/sep/18	
566169	LARATL07A	1698727 Ontario Inc.	2008/sep/18	
566170	LARATL04A	1698727 Ontario Inc.	2008/sep/18	

566171	LARATL05A	1698727 Ontario Inc.	2008/sep/18	
566172	LARATL05B	1698727 Ontario Inc.	2008/sep/18	
566173	LARATL05C	1698727 Ontario Inc.	2008/sep/18	
566174	LARATL06A	1698727 Ontario Inc.	2008/sep/18	
566175	LARATL06B	1698727 Ontario Inc.	2008/sep/18	
566552	LARATLB2	1698727 Ontario Inc.	2008/sep/23	
566553	LARATLB3	1698727 Ontario Inc.	2008/sep/23	
566553	LARATLB3	1698727 Ontario Inc.	2008/sep/23	
566553	LARATLB3	1698727 Ontario Inc.	2008/sep/23	
566565	LARATLB4	1698727 Ontario Inc.	2008/sep/24	
567270	LARATLA08	1698727 Ontario Inc.	2008/oct/02	
567271	LARATLA09	1698727 Ontario Inc.	2008/oct/02	
567274	TLLARA11	1698727 Ontario Inc.	2008/oct/02	
567274	TLLARA11	1698727 Ontario Inc.	2008/oct/02	
567274	TLLARA11	1698727 Ontario Inc.	2008/oct/02	
567276	TL LARA A 11	1698727 Ontario Inc.	2008/oct/02	
568158	NEVER SWEAT	Billingsley, Richard John	2008/oct/17	
568158	NEVER SWEAT	Billingsley, Richard John	2008/oct/17	
568158	NEVER SWEAT	Billingsley, Richard John	2008/oct/17	
566167	LARATL09A	1698727 Ontario Inc.	2008/sep/18	
514351	KIDS EAST	Francis, Allan Robert	2007/nov/01	
514360	DEPOSIT S	Francis, Allan Robert	2007/nov/01	

APPENDIX 3: DESCRIPTION OF DATABASE FIELDS

The magnetic/EM GDB file is a Geosoft binary database. In the database, the Survey lines and Tie Lines are prefixed with an "L" for "Line" and "T" for "Tie".

COLUMN	UNITS	DESCRIPTOR
x	m	UTM Easting (NAD83, Zone 10N)
y	m	UTM Northing (NAD83, Zone 10N)
Line		Line number
emfid		AERODAS Fiducial
utctime	hh:mm:ss.ss	UTC time
bheight	m	Terrain clearance of EM bird
dtm	m	Digital Terrain Model
galtf	m	GPS - Z
Basemagf	nT	Base station total magnetic intensity
Magu	nT	Total magnetic firld from upper senor
Magl	nT	Total magnetic field from sensor on EM bird
Zon	nT/s	Processed Streaming On-Time Z component Channels 1-16
Zoff	nT/s	Processed Streaming Off-Time Z component Channels 0-16
Xon	nT/s	Processed Streaming On-Time X component Channels 1-16
Xoff	nT/s	Processed Streaming Off-Time X component Channels 0-16
Anom_ID		Anomaly Character (K= thicK, N = thiN)
Anom_labels		Alphanumeric label of conductor pick
grade		Classification from 1-7 based on conductance of conductor pick
Off_allcon	S	Off-time conductance
Off_AllTau	µs	Off-time decay constant
Off_Con	S	Off-time conductance at conductor pick
Off_Tau	µs	Off-time decay constant at conductor pick
pwrline		powrline monitor data channel

The spectometer GDB file is a Geosoft binary database. In the database, the Survey lines and Tie Lines are prefixed with an "L" for "Line" and "T" for "Tie".

COLUMN	UNITS	DESCRIPTOR
X	m	UTM Easting (NAD83, Zone 10N)
y	m	UTM Northing (NAD83, Zone 10N)
Line		Line number
Fid		Fiducial
utctime	hh:mm:ss.ss	UTC time
alth_m	m	Radar altitude of aircraft
altbf	m	Barometric altitude
Barotf	°C	Barometric temperature
Galt_m	m	Elevation of GPS antenna (AMSL) (WGS84)
Cos_raw	cps	Uncorrected Cosmic counts
Isp1d_cpt		256 channel spectral data (downward looking)
Isp1u_cpt		256 channel spectral data (upward looking)
K_raw	cps	Uncorrected Potassium counts
Kcorr	%	Radiometric – potassium (%K)
Tc_raw	cps	Uncorrected Total counts
Tccorr	nGy/hr	Radiometric – dose rate
Tcexp	uR/hr	Radiometric – exposure rate
Th_raw	cps	Uncorrected Thorium counts
Thcorr	ppm	Radiometirc – equivalent Thorium
Thkratio		Thorium/Potassium Ratio
U_raw	cps	Uncorrected Uranium counts
Ucorr	ppm	Radiometirc – equivalent Uranium
Ukratio		Uranium/potassium counts
Upu_raw	cps	Uncorrected Uranium upward looking counts
Uthratio		Uranium/Thorium Ratio

APPENDIX 4: AEROTEM ANOMALY LISTING

Line	Anom	ID	Cond(S)	Tau (µs)	Flight#	UTC Time	Bird height (m)	Easting (m)	Northing (m)
10010	A	N	1.0	72.7	739.14	2:38:24	33.4	424880.1	5419216.2
10010	B	N	1.0	46.9	1005.37	13:12:00	74.1	425480.1	5421422.7
10020	A	N	2.0	46.8	1047.81	9:07:12	117.2	425653.1	5421308.6
10020	B	N	3.0	53.9	747.1	23:31:12	244.6	425056.2	5419083.7
10020	C	N	1.0	32.5	848.73	*	*	424970.1	5418717.0
10030	A	N	1.0	52.5	1112.63	18:57:36	88.7	425843.3	5421271.3
10040	A	N	1.0	35.7	1162.92	5:45:36	49.1	426042.0	5421225.8
10040	B	N	1.0	39.0	1152.94	2:24:00	31.3	426021.3	5421143.3
10040	C	N	1.0	34.6	778.38	*	*	425418.7	5418884.6
10040	D	N	1.0	38.7	878.65	23:45:36	140.9	425291.6	5418387.1
10050	A	N	1.0	50.3	823.47	*	*	425583.1	5418709.3
10050	B	N	1.0	39.1	1173.06	1:55:12	28.8	426207.2	5421089.6
10060	A	N	1.0	41.2	1152.6	23:16:48	98.3	426423.7	5421107.6
10060	B	K	1.0	38.8	1144	3:07:12	35.7	426305.4	5420710.8
10060	C	N	1.0	46.7	820.73	*	*	425729.4	5418544.0
10070	A	N	1.0	49.7	812.37	*	*	425886.6	5418325.9
10070	B	N	1.0	40.8	1109.49	7:12:00	54.7	426580.1	5420975.1
10080	A	K	3.0	43.4	1046	15:07:12	237.3	426784.1	5420917.5
10080	B	N	1.0	61.3	730.91	*	*	426265.9	5418942.5
10080	C	N	1.0	46.3	797.04	*	*	426050.9	5418173.9
10090	A	N	2.0	49.0	776.68	12:14:24	122.9	426252.0	5418136.7
10090	B	K	3.0	72.8	692.4	12:00:00	255.0	426417.4	5418714.6
10090	C	N	2.0	65.3	1029.23	8:09:36	182.7	426950.1	5420733.7
10100	A	K	5.0	58.7	1048.6	4:19:12	521.3	427338.4	5421361.8
10100	B	K	4.0	54.1	967.39	23:31:12	387.1	427155.7	5420711.6
10100	C	N	2.0	41.6	992.17	18:28:48	194.1	427119.9	5420563.0
10100	D	N	2.0	56.4	710.91	9:21:36	154.5	426600.4	5418660.1
10100	E	N	1.0	44.5	770.83	*	*	426408.4	5417949.2
10110	A	N	2.0	61.7	678.06	12:28:48	123.5	426763.2	5418488.1
10110	B	N	3.0	62.8	986.94	4:48:00	228.1	427287.1	5420467.6
10120	A	K	3.0	50.8	1021.7	12:57:36	292.2	427686.7	5421140.6
10120	B	K	3.0	48.5	917.94	10:19:12	253.6	427487.8	5420428.8
10120	C	N	2.0	44.1	935.86	6:43:12	151.1	427454.9	5420302.5
10130	A	N	3.0	58.1	899.55	22:48:00	263.6	427634.1	5420226.6
10130	B	N	4.0	65.2	887.16	14:38:24	325.7	427688.9	5420407.4
10130	C	N	4.0	37.0	980.65	19:26:24	384.8	427779.6	5420758.0
10130	D	K	4.0	47.0	1038.22	9:07:12	351.8	427854.2	5421042.2
10140	A	N	4.0	40.5	1073.07	20:52:48	372.4	428046.1	5420962.6
10140	B	K	3.0	60.9	1040.2	22:33:36	299.0	427991.3	5420795.1
10140	C	N	4.0	52.5	988.64	13:12:00	368.2	427932.6	5420567.8
10140	D	K	3.0	81.4	910.18	13:26:24	256.1	427861.3	5420293.1
10150	A	K	3.0	45.7	908.65	0:43:12	224.2	428038.1	5420148.6
10150	B	N	5.0	38.3	1060.03	23:31:12	458.0	428185.6	5420731.7
10160	A	K	2.0	37.8	1075.4	7:55:12	182.5	428374.9	5420671.6
10160	B	K	2.0	53.1	1042.37	4:04:48	178.1	428289.4	5420365.6

Line	Anom	ID	Cond(S)	Tau (µs)	Flight#	UTC Time	Bird height (m)	Easting (m)	Northing (m)
10160	C	K	3.0	68.3	909.55	5:31:12	268.8	428157.2	5419890.3
10170	A	N	2.0	47.1	966.28	4:04:48	147.2	428360.6	5419852.0
10170	B	K	2.0	43.7	1092.93	20:38:24	136.4	428574.4	5420632.9
10170	C	N	3.0	43.4	1097.93	4:48:00	286.3	428593.3	5420702.7
10180	A	K	5.0	43.7	1137.65	22:04:48	590.9	428825.7	5420824.9
10180	B	K	2.0	43.9	1127.4	21:21:36	197.3	428784.7	5420643.5
10180	C	K	3.0	45.2	1120.08	3:50:24	267.5	428755.8	5420551.4
10180	D	K	3.0	48.5	1082.65	2:09:36	284.4	428689.6	5420298.4
10180	E	N	2.0	54.4	958	0:14:24	100.4	428525.2	5419683.6
10190	A	N	2.0	57.2	984.59	18:28:48	133.1	428708.4	5419623.1
10190	B	K	3.0	38.1	1144.14	12:43:12	308.7	428938.1	5420444.3
10200	A	N	1.0	48.5	1024.39	*	*	428887.3	5419516.0
10210	A	K	1.0	72.6	724.58	14:09:36	76.7	428183.6	5416035.8
10260	A	N	1.0	42.4	579.09	*	*	429318.7	5417208.3
10270	A	N	1.0	48.9	564.42	*	*	429483.7	5417097.5
10540	A	K	2.0	54.0	678.88	0:28:48	100.9	434490.2	5414110.4
10540	B	K	4.0	49.4	1009.28	17:16:48	432.6	435131.0	5416516.4
10550	A	N	2.0	49.1	990.39	8:38:24	153.7	435317.8	5416475.1
10550	B	K	1.0	50.3	669.2	14:38:24	78.4	434667.6	5413988.5
10560	A	K	1.0	49.9	661.69	17:16:48	84.8	434859.6	5413933.2
10560	B	N	3.0	55.4	966.48	21:36:00	243.0	435540.2	5416472.1
10570	A	K	3.0	57.0	931.42	0:00:00	244.0	435671.9	5416244.3
10580	A	K	4.0	57.6	934.63	23:16:48	345.9	435871.8	5416170.4
10590	A	K	4.0	46.0	931.02	5:02:24	349.5	436054.6	5416062.5
10600	A	K	2.0	48.3	929.58	16:04:48	163.5	436248.6	5415953.6
10630	A	N	1.0	47.3	959.26	6:28:48	52.0	436863.8	5415993.8
10640	A	N	1.0	47.8	993.88	16:19:12	82.3	437061.6	5415930.3
10650	A	K	4.0	52.2	1015.66	19:40:48	445.2	437239.2	5415853.8
10660	A	K	4.0	43.9	1035.4	19:55:12	329.1	437452.9	5415807.0
10670	A	K	4.0	54.5	1055.05	0:00:00	346.4	437630.5	5415779.4
10680	A	K	2.0	45.6	1045.52	14:38:24	214.8	437826.6	5415736.6
10690	A	N	1.0	34.8	1045.5	8:52:48	61.2	438050.3	5415784.6
10700	A	N	1.0	30.9	1058.36	6:43:12	52.7	438248.0	5415746.6
20010	A	N	1.0	38.0	960.53	23:45:36	99.4	425376.2	5421455.2
20010	B	N	1.0	62.8	720.47	23:16:48	98.7	424794.1	5419284.3
20020	A	N	1.0	77.2	745.68	*	*	424981.3	5419179.9
20020	B	N	2.0	44.2	1024.43	15:21:36	128.1	425570.3	5421375.9
20030	A	N	1.0	42.2	1073.79	5:45:36	49.0	425754.0	5421282.4
20040	A	N	1.0	63.8	783.36	*	*	425330.8	5418943.8
20040	B	N	1.0	42.7	1138.09	3:36:00	38.3	425936.8	5421201.3
20040	C	K	1.0	43.0	1152.61	22:19:12	96.6	425979.7	5421360.6
20050	A	K	1.0	30.0	1169.12	19:26:24	90.2	426149.2	5421231.7
20050	B	N	1.0	40.9	1166.28	2:24:00	31.7	426116.1	5421081.4
20050	C	N	2.0	37.7	799	3:07:12	177.0	425495.1	5418802.5
20060	A	N	1.0	55.5	823.85	*	*	425664.5	5418645.9
20060	B	N	1.0	47.7	1180.99	2:52:48	34.9	426321.8	5421088.3
20070	A	N	1.0	41.7	1129.41	3:21:36	37.0	426509.3	5420983.5
20070	B	K	1.0	36.9	1151.01	0:43:12	15.7	426415.3	5420655.4

Line	Anom	ID	Cond(S)	Tau (µs)	Flight#	UTC Time	Bird height (m)	Easting (m)	Northing (m)
20070	C	N	1.0	44.8	825.74	4:48:00	44.8	425788.7	5418370.0
20080	A	K	2.0	49.3	1076.02	23:45:36	141.2	426702.7	5421019.0
20090	A	N	2.0	45.6	1034.89	0:57:36	101.8	426852.3	5420722.2
20090	B	N	1.0	60.4	729.46	*	*	426347.1	5418874.3
20100	A	N	1.0	47.6	775.18	*	*	426340.8	5418057.6
20100	B	K	2.0	60.3	694.67	19:40:48	134.9	426503.3	5418670.3
20100	C	N	1.0	59.4	1012.5	19:26:24	90.3	427026.4	5420673.3
20110	A	N	2.0	43.1	987.73	3:21:36	146.3	427205.7	5420488.6
20110	B	N	1.0	69.6	711.85	6:43:12	53.3	426678.3	5418580.6
20120	A	N	2.0	59.7	973.44	9:36:00	154.9	427364.0	5420386.6
20120	B	K	3.0	50.2	1029.52	12:00:00	308.2	427602.7	5421225.7
20130	A	N	4.0	51.1	1067.69	8:09:36	321.5	427784.5	5421215.3
20130	B	K	3.0	55.4	898.09	5:16:48	228.6	427576.6	5420357.2
20140	A	K	3.0	48.7	910.49	17:16:48	295.3	427790.5	5420400.4
20140	B	K	4.0	40.4	1033.11	7:55:12	336.7	427928.7	5420932.9
20150	A	K	3.0	53.3	1047.62	7:12:00	250.9	428081.1	5420715.7
20150	B	K	3.0	69.0	918.4	20:09:36	241.6	427940.6	5420209.3
20160	A	K	3.0	54.5	917.15	7:26:24	270.3	428106.7	5420033.0
20160	B	K	3.0	43.0	1093.96	20:09:36	297.3	428361.0	5420982.9
20170	A	N	3.0	40.8	1106.16	14:09:36	293.0	428551.8	5420971.6
20170	B	N	3.0	47.5	1064.63	4:48:00	286.4	428417.1	5420413.1
20170	C	N	2.0	57.6	953.56	12:14:24	158.4	428276.9	5419908.4
20180	A	N	2.0	41.9	957.82	10:19:12	156.0	428439.7	5419793.9
20180	B	K	4.0	38.3	1076.48	17:45:36	327.7	428607.9	5420403.3
20180	C	K	3.0	43.6	1113.25	9:07:12	306.3	428675.4	5420657.4
20190	A	N	2.0	68.7	980.34	8:24:00	116.3	428614.8	5419625.2
20200	A	N	1.0	44.2	998.4	11:31:12	69.0	428804.9	5419559.5
20210	A	N	1.0	39.1	1025.4	*	*	428996.7	5419498.2
20210	B	K	1.0	54.7	720.48	5:31:12	47.9	428074.6	5416047.2
20220	A	K	1.0	58.4	707.58	18:43:12	88.3	428292.5	5416057.4
20260	A	N	1.0	39.8	571.21	*	*	429411.7	5417184.8
19010	A	K	2.0	67.1	1139.84	20:52:48	136.9	428769.4	5420693.8
19010	B	K	3.0	58.8	1051.16	11:16:48	291.0	427903.0	5420941.0
19010	C	K	2.0	63.8	952.16	12:57:36	188.2	425355.8	5421678.2
19060	A	N	2.0	48.2	820.1	6:28:48	206.7	425623.3	5418694.6

APPENDIX 5: AEROTEM DESIGN CONSIDERATIONS

Helicopter-borne EM systems offer an advantage that cannot be matched from a fixed-wing platform. The ability to fly at slower speed and collect data with high spatial resolution, and with great accuracy, means the helicopter EM systems provide more detail than any other EM configuration, airborne or ground-based. Spatial resolution is especially important in areas of complex geology and in the search for discrete conductors. With the advent of helicopter-borne high-moment time domain EM systems the fixed wing platforms are losing their *only* advantage – depth penetration.

Advantage 1 – Spatial Resolution

The AeroTEM system is specifically designed to have a small footprint. This is accomplished through the use of concentric transmitter-receiver coils and a relatively small diameter transmitter coil (5 m). The result is a highly focused exploration footprint, which allows for more accurate "mapping" of discrete conductors. Consider the transmitter primary field images shown in Figure 1, for AeroTEM versus a fixed-wing transmitter.

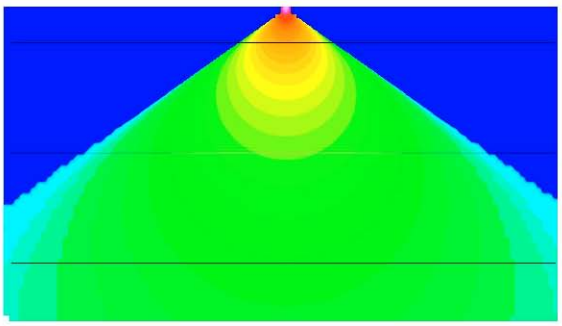

The footprint of AeroTEM at the earth's surface is roughly 50m on either side of transmitter

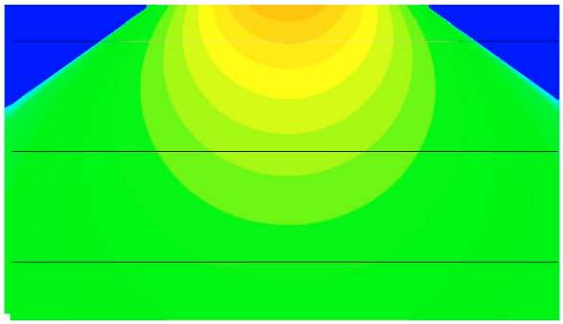

The footprint of a fixed-wing system is roughly 150 m on either side of the transmitter

Figure 1. A comparison of the footprint between AeroTEM and a fixed-wing system, highlights the greater resolution that is achievable with a transmitter located closer to the earth's surface. The AeroTEM footprint is one third that of a fixed-wing system and is symmetric, while the fixed-wing system has even lower spatial resolution along the flight line because of the separated transmitter and receiver configuration.

At first glance one may want to believe that a transmitter footprint that is distributed more evenly over a larger area is of benefit in mineral exploration. In fact, the opposite is true; by energizing a larger surface area, the ability to energize and detect discrete conductors is reduced. Consider, for example, a comparison between AeroTEM and a fixed-wing system over the Mesamax Deposit (1,450,000 tonnes of 2.1% Ni, 2.7% Cu, 5.2 g/t Pt/Pd). In a test survey over three flight lines spaced 100 m apart, AeroTEM detected the Deposit on all three flight lines. The fixed-wing system detected the Deposit only on two flight lines. In exploration programs that seek to expand the flight line spacing in an effort to reduce the cost of the airborne survey, discrete conductors such as the Mesamax Deposit can go undetected. The argument often put forward in favour of using fixed-wing systems is that because of their larger footprint, the flight line spacing can indeed be widened. Many fixed-wing surveys are flown at 200 m or 400 m. Much of the survey work performed by Aeroquest has been to survey in areas that were previously flown at these wider line spacings. One of the reasons for AeroTEM's impressive discovery record has been the strategy of flying closely spaced lines and finding all the discrete near-surface conductors. These higher resolution surveys are being flown within existing mining camps, areas that improve the chances of discovery.

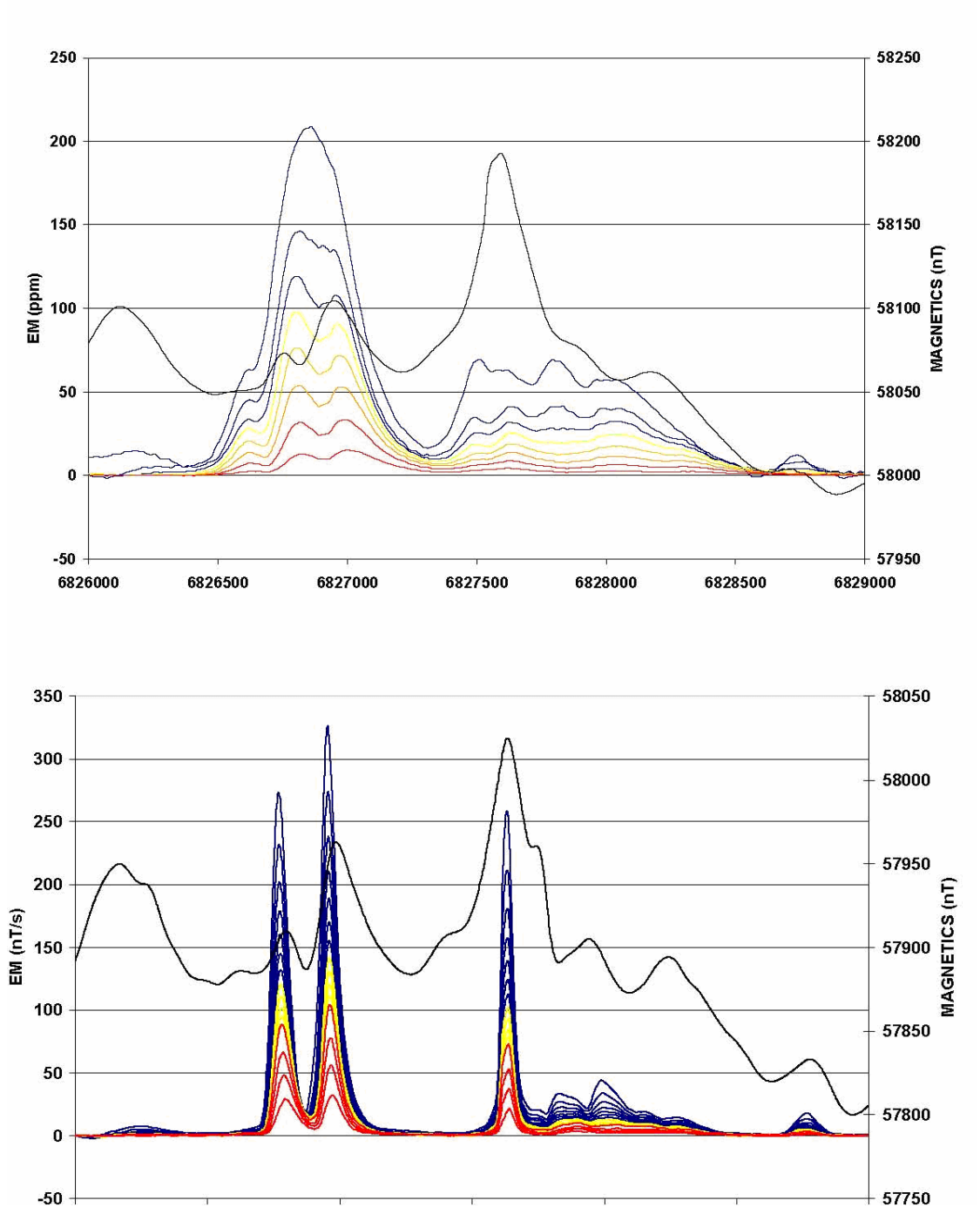

Figure 2. Fixed-wing (upper) and AeroTEM (lower) comparison over the eastern limit of the Mesamax Deposit, a Ni-Cu-PGE zone located in the Raglan nickel belt and owned by Canadian Royalties. Both systems detected the Deposit further to the west where it is closer to surface.

The small footprint of AeroTEM combined with the high signal to noise ratio (S/N) makes the system more

suitable to surveying in areas where local infrastructure produces electromagnetic noise, such as power lines and railways. In 2002 Aeroquest flew four exploration properties in the Sudbury Basin that were under option by FNX Mining Company Inc. from Inco Limited. One such property, the Victoria Property, contained three major power line corridors.

The resulting AeroTEM survey identified all the known zones of Ni-Cu-PGE mineralization, and detected a response between two of the major power line corridors but in an area of favorable geology. Three boreholes were drilled to test the anomaly, and all three intersected sulphide. The third borehole encountered 1.3% Ni, 6.7% Cu, and 13.3 g/t TPMs over 42.3 ft. The mineralization was subsequently named the Powerline Deposit.

The success of AeroTEM in Sudbury highlights the advantage of having a system with a small footprint, but also one with a high S/N. This latter advantage is achieved through a combination of a high-moment (high signal) transmitter and a rigid geometry (low noise). Figure 3 shows the Powerline Deposit response and the response from the power line corridor at full scale. The width of power line response is less than 75 m.

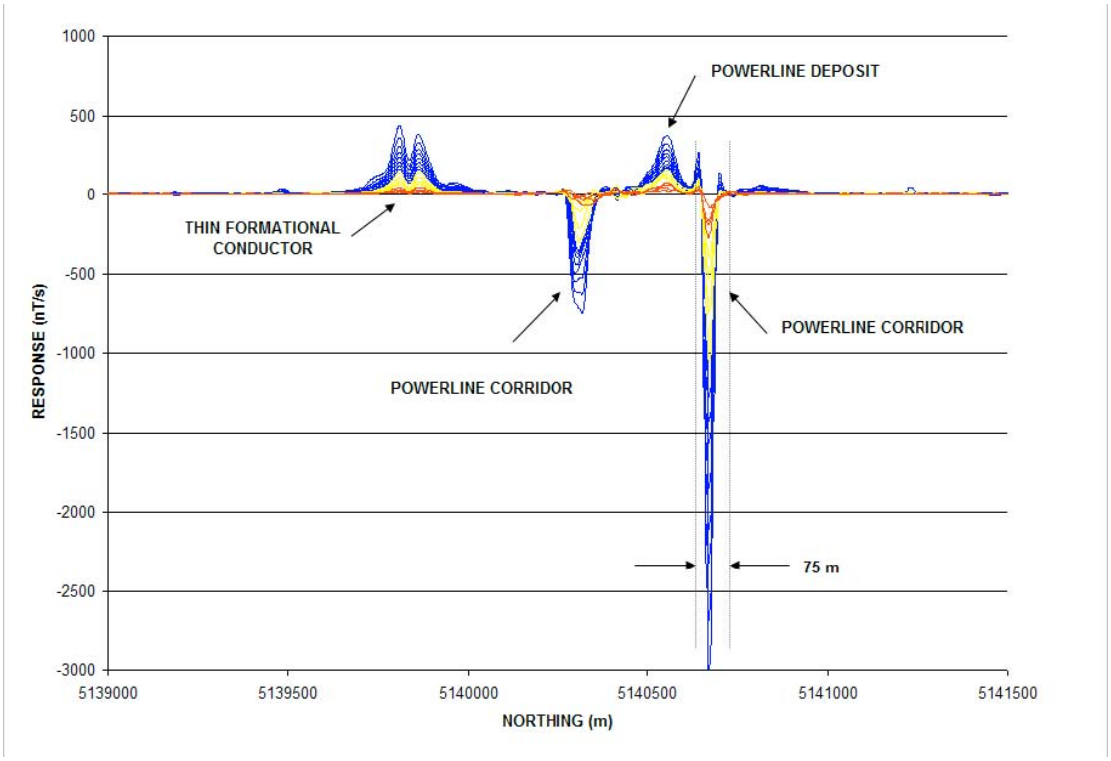

Figure 3. The Powerline Deposit is located between two major power line corridors, which make EM surveying problematic. Despite the strong response from the power line, the anomaly from the Deposit is clearly detected. Note the thin formational conductor located to the south. The only way to distinguish this response from that of two closely spaced conductors is by interpreting the X-axis coil response.

Advantage 2 – Conductance Discrimination

The AeroTEM system features full waveform recording and as such is able to measure the on-time response due to high conductance targets. Due to the processing method (primary field removal), there is attenuation of the response with increasing conductance, but the AeroTEM on-time measurement is still superior to systems that rely on lower base frequencies to detect high conductance targets, but do not measure in the on-time.

The peak response of a conductive target to an EM system is a function of the target conductance and the EM system base frequency. For time domain EM systems that measure only in the off-time, there is a drop in the peak response of a target as the base frequency is lowered for all conductance values below the peak system

response. For example, the AeroTEM peak response occurs for a 10 S conductor in the early off-time and 100 S in the late off-time for a 150 Hz base frequency. Because base frequency and conductance form a linear relationship when considering the peak response of any EM system, a drop in base frequency of 50% will double the conductance at which an EM system shows its peak response. If the base frequency were lowered from 150 Hz to 30 Hz there would be a fivefold increase in conductance at which the peak response of an EM occurred.

However, in the search for highly conductive targets, such as pyrrhotite-related Ni-Cu-PGM deposits, a fivefold increase in conductance range is a high price to pay because the signal level to lower conductance targets is reduced by the same factor of five. For this reason, EM systems that operate with low base frequencies are not suitable for general exploration unless the target conductance is more than 100 S, or the target is covered by conductive overburden.

Despite the excellent progress that has been made in modeling software over the past two decades, there has been little work done on determining the optimum form of an EM system for mineral exploration. For example, the optimum configuration in terms of geometry, base frequency and so remain unknown. Many geophysicists would argue that there is no single ideal configuration, and that each system has its advantages and disadvantages. We disagree.

When it comes to detecting and discriminating high-conductance targets, it is necessary to measure the pure in-phase response of the target conductor. This measurement requires that the measured primary field from the transmitter be subtracted from the total measured response such that the secondary field from the target conductor can be determined. Because this secondary field is in-phase with the transmitter primary field, it must be made while the transmitter is turned on and the transmitter current is changing. The transmitted primary field is several orders of magnitude larger than the secondary field. AeroTEM uses a bucking coil to reduce the primary field at the receiver coils. The only practical way of removing the primary field is to maintain a rigid geometry between the transmitter, bucking and receiver coils. This is the main design consideration of the AeroTEM airframe and it is the only time domain airborne system to have this configuration.

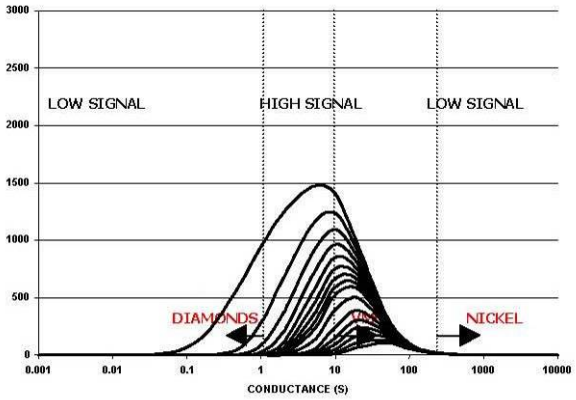

The off-time AeroTEM response for the 16 channel configuration.

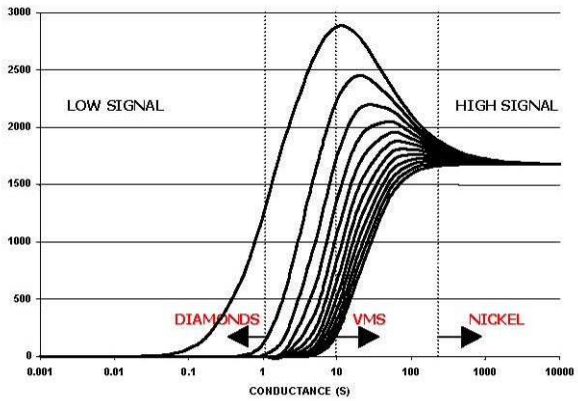

The on-time response assuming 100% removal of the measured primary field.

Figure 4. The off-time and on-time response nomogram of AeroTEM for a base frequency of 150 Hz. The on-time response is much stronger for higher conductance targets and this is why on-time measurements are more important than lower frequencies when considering high conductance targets in a resistive environment.

Advantage 3 – Multiple Receiver Coils

AeroTEM employs two receiver coil orientations. The Z-axis coil is oriented parallel to the transmitter coil and both are horizontal to the ground. This is known as a maximum coupled configuration and is optimal for detection. The X-axis coil is oriented at right angles to the transmitter coil and is oriented along the line-of-flight.

This is known as a minimum coupled configuration, and provides information on conductor orientation and thickness. These two coil configurations combined provide important information on the position, orientation, depth, and thickness of a conductor that cannot be matched by the traditional geometries of the HEM or fixed-wing systems. The responses are free from a system geometric effect and can be easily compared to model type curves in most cases. In other words, AeroTEM data is very easy to interpret. Consider, for example, the following modeled profile:

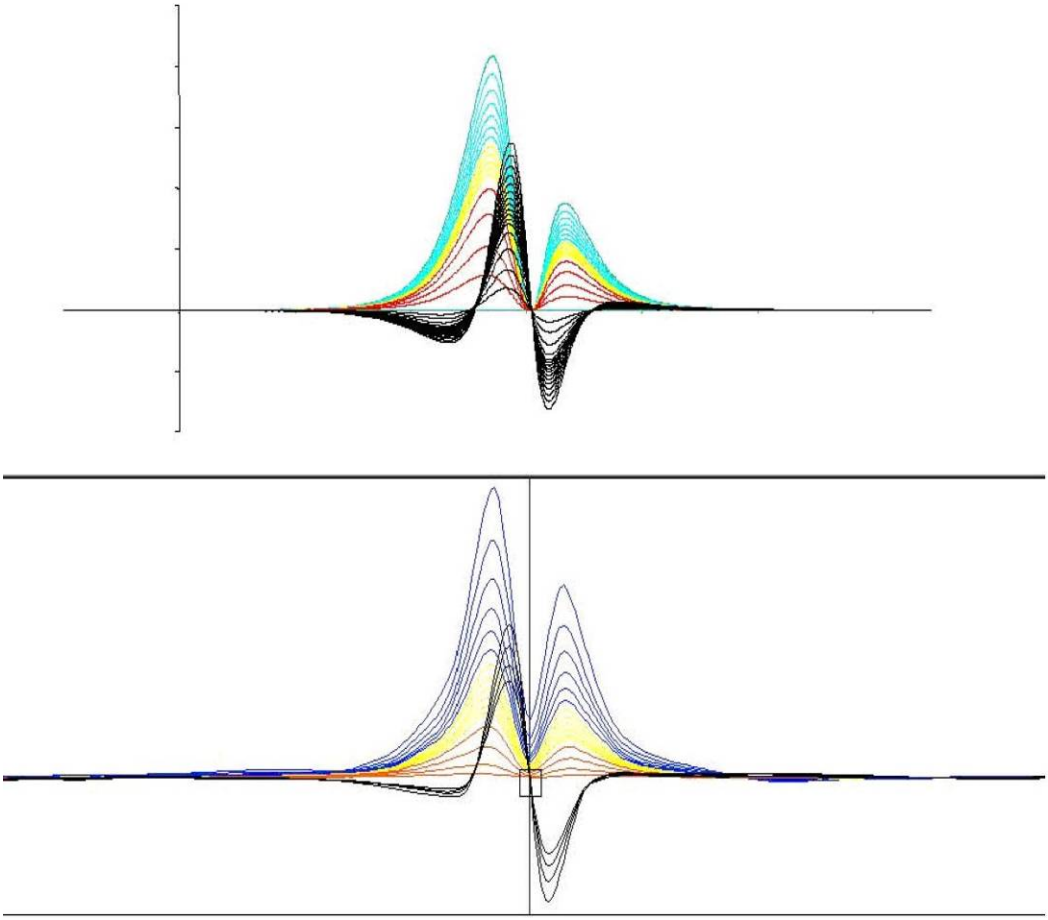

Figure 5. Measured (lower) and modeled (upper) AeroTEM responses are compared for a thin steeply dipping conductor. The response is characterized by two peaks in the Z-axis coil, and a cross-over in the X-axis coil that is centered between the two Z-axis peaks. The conductor dips toward the higher amplitude Z-axis peak. Using the X-axis cross-over is the only way of differentiating the Z-axis response from being two closely spaced conductors.

HEM versus AeroTEM

Traditional helicopter EM systems operate in the frequency domain and benefit from the fact that they use narrowband as opposed to wide-band transmitters. Thus all of the energy from the transmitter is concentrated in

a few discrete frequencies. This allows the systems to achieve excellent depth penetration (up to 100 m) from a transmitter of modest power. The Aeroquest Impulse system is one implementation of this technology.

The AeroTEM system uses a wide-band transmitter and delivers more power over a wide frequency range. This frequency range is then captured into 16 time channels, the early channels containing the high frequency information and the late time channels containing the low frequency information down to the system base frequency. Because frequency domain HEM systems employ two coil configurations (coplanar and coaxial) there are only a maximum of three comparable frequencies per configuration, compared to 16 AeroTEM off-time and 12 AeroTEM on-time channels.

Figure 6 shows a comparison between the Dighem HEM system (900 Hz and 7200 Hz coplanar) and AeroTEM (Zaxis) from surveys flown in Raglan, in search of highly conductive Ni-Cu-PGM sulphide. In general, the AeroTEM peaks are sharper and better defined, in part due to the greater S/N ratio of the AeroTEM system over HEM, and also due to the modestly filtered AeroTEM data compared to HEM. The base levels are also better defined in the AeroTEM data. AeroTEM filtering is limited to spike removal and a 5-point smoothing filter. Clients are also given copies of the raw, unfiltered data.

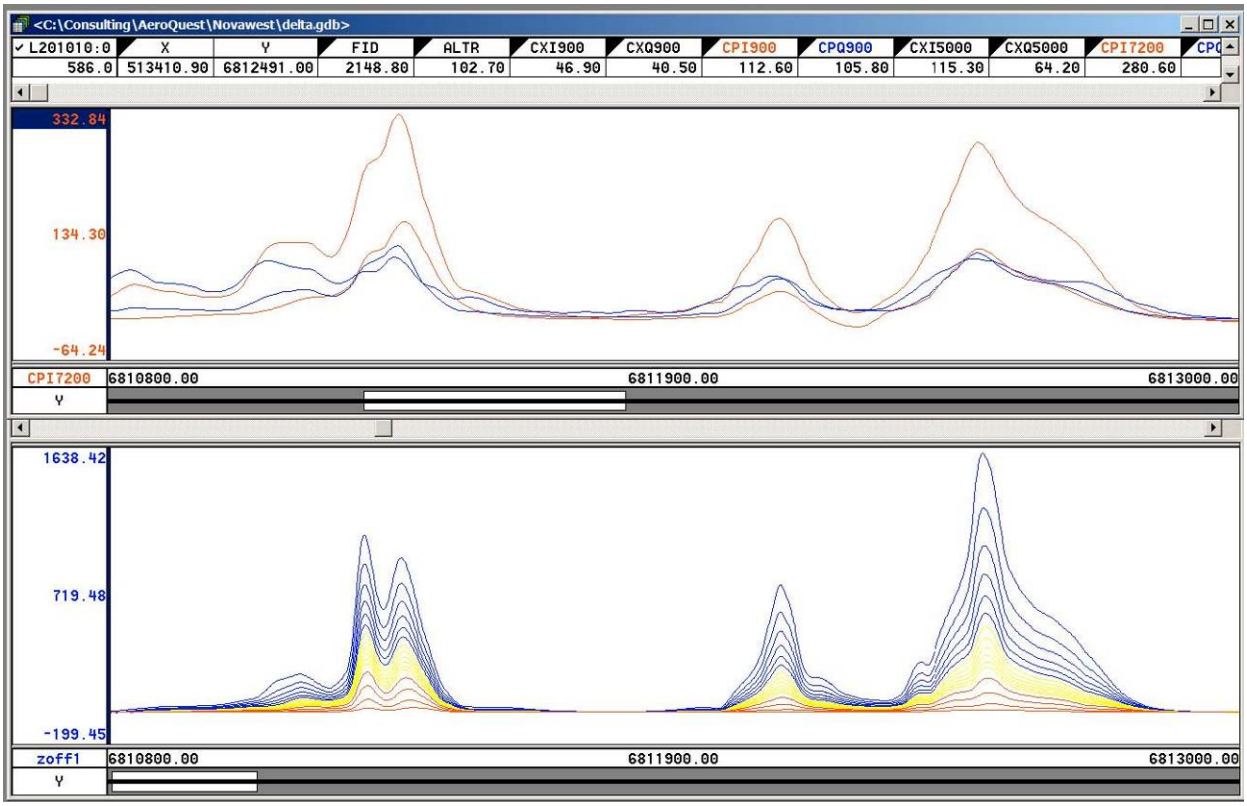

Figure 6. Comparison between Dighem HEM (upper) and AeroTEM (lower) surveys flown in the Raglan area. The AeroTEM responses appear to be more discrete, suggesting that the data is not as heavily filtered as the HEM data. The S/N advantage of AeroTEM over HEM is about 5:1.

Aeroquest Limited is grateful to the following companies for permission to publish some of the data from their respective surveys: Wolfden Resources, FNX Mining Company Inc, Canadian Royalties, Nova West Resources, Aurogin Resources, Spectrem Air. Permission does not imply an endorsement of the AeroTEM system by these companies.

APPENDIX 6: AEROTEM INSTRUMENTATION SPECIFICATION SHEET

AEROTEM Helicopter Electromagnetic System

System Characteristics

- Transmitter: Triangular Pulse Shape Base Frequency 150 Hz
- Tx On Time - 1,150 (150 Hz) µs
- Tx Off Time - 2,183 (150 Hz) µs
- Loop Diameter - 5 m
- Peak Current - 250 A
- Peak Moment - 38,800 NIA
- Typical Z Axis Noise at Survey Speed = 5 nT/s peak to peak
- Sling Weight: 270 Kg
- Length of Tow Cable: 40 m
- Bird Survey Height: 30 m nominal

Receiver

- Two Axis Receiver Coils (x, z) positioned at centre of transmitter loop
- Selectable Time Delay to start of first channel 21.3 , 42.7, or 64.0 ms

Display & Acquisition

- AERODAS Digital recording at 120 samples per decay curve at a maximum of 300 curves per second (27.778µs channel width)
- RMS Channel Widths: 52.9,132.3, 158.7, 158.7, 317.5, 634.9 µs
- Recording & Display Rate = 10 readings per second.
- On-board display - six channels Z-component and 1 X-component

System Considerations

Comparing a fixed-wing time domain transmitter with a typical moment of 500,000 NIA flying at an altitude of 120 m with a Helicopter TDEM at 30 m, notwithstanding the substantial moment loss in the airframe of the fixed wing, the same penetration by the lower flying helicopter system would only require a sixty-fourth of the moment. Clearly the AeroTEM system with nearly 40,000 NIA has more than sufficient moment. The airframe of the fixed wing presents a response to the towed bird, which requires dynamic compensation. This problem is non-existent for AeroTEM since transmitter and receiver positions are fixed. The AeroTEM system is completely portable, and can be assembled at the survey site within half a day.